# Towards a process-based understanding of Holocene polar climate change

Using glacier-fed lake sediments from Arctic Svalbard and Antarctic South Georgia

**Willem G.M. van der Bilt**


Dissertation for the degree of philosophiae doctor (PhD)

at the University of Bergen

2016

Dissertation date: May 3rd

Year: 2016

Title: Towards a process-based understanding of Holocene polar climate change

*Using glacier-fed lake sediments from Arctic Svalbard and Antarctic South Georgia*

Author: Willem G.M. van der Bilt

Print: AiT Bjerch AS / University of Bergen

*“Nature never disappoints you, no rejection” - Steve Coogan*

# Contents

## Scientific environment

Work for this thesis was mostly carried out at the Earth Science department of the University of Bergen, Norway, as well as Lamont-Doherty Earth Observatory (LDEO) of Columbia University, The United States of America. In addition, I spend time at the Research Laboratory for Archaeology & the History of Art (RHALA) at the University of Oxford and the University of Manchester in the United Kingdom, under the supervision of Dr. Christine Lane. My PhD program was financed through the Norwegian Research Council-funded Shifting Climate States of the Polar Regions (SHIFTS) project (grant no. 210004). Additional financial support was provided through the Meltzer fund, the Norwegian Research School in Climate Dynamics (ResClim), EU COST action ES0907 (INTIMATE), the Bjerknes Centre for Climate Research Group 6 (RG6), the EU INTERACT Transnational Access program (grant GLEESP), the Svalbard Science Forum (SSF) Arctic Field Grant program (RiS 6663) and the Open Access Publication fund at the University of Bergen (refs. 710029 588 & 533). Work was supervised by Prof. Jostein Bakke at the University of Bergen and Associate Research Professor William J. D`Andrea at LDEO.





# Acknowledgements

Time`s up and it has flown: the three years of my PhD have sped by. Moving to a new land, exploring the Arctic, living in New York and visiting faraway corners like Japan and Patagonia; it has been quite the ride. And let`s not forget the science: maybe masochistically, my research excites me as much as on the day I first walked into the Realfagbygget, thinking it was the university parking garage. But beyond exotic places and captivating science, the fond memories of my PhD have been shaped by the people around me. I count Mother Nature among that posse: thank you, for sparking curiosity and imagination, encouraging me to understand your mysteries. Some of these will always remain a mystery to me, like opening a beer bottle with a knife, but polar climate change is pretty much a closed case as this thesis will reveal. Anyway, as my parents and siblings surely remember, I was hooked on nature from a young age. Thank you for stimulating me to pursue this interest. Jostein, you have granted me an incredible amount of freedom over the years. That time you borrowed coring kit and raft to go explore eastern Greenland in a most disorganized fashion could easily have gone wrong. Thank you for your trust: surely, most PhD candidates praise their supervisors, but I actually mean it. Now that I am in a grateful mood, I might as well thank the marine boys, particularly Benny and Björn. We have had a lot of fun. I could (and probably have) spend weeks with you in Apollon. Drinks included, off course. Rick and Felix: distance typically weakens the bonds of friendship, but our LAT relationship has only grown stronger. You are my best friends and I think we should get hitched now that the law allows it. Gijs, our sauna debates and swimming discussions have been instrumental in pushing me over some crucial thresholds. You are one of the best listeners that I have known. Sander and Kalijn, thanks for habitually popping by in the midst of winter, year after year, to check our sanity in the cold dark North. Our skiing trips have been so much fun and together we have explored some amazing parts of Norway. Herr Werner, we have opened new analytical doors that will not be closed again. But most importantly, you are a very chilled out dude. I count myself lucky to have you as a friend. Anna, your presence really pimped my direct working environment. We have a good vibe going

in our office! Billy, we have lived some great memories. In spite of 2014`s Snowpocalypse and 2015`s Snowmageddon, my visits to Lamont were wonderful experiences. Thank you for introducing me to your fantastic family and the wonderful world of lipid biomarkers, and, let`s not forget, transporting me to a world of cheap ready-made corn dogs and chicken wings. Christine, thank you for showing me that kindness and ambition go well together. And I am sure that our minute glass shards will one day be identified. Jordan, your humour, warmth and honesty have always been a bright spot in my working days. Geo-bios, you have been part of the nucleus of my social life and offered a great deal of joy and mental support, including you, Jesus. Torgeir, our personality types could probability not be more different, yet we get along really well. I have many fond memories of our Iceland road trip and crazy field trips; may there be more to come. Øyvind, I have thoroughly enjoyed your devil`s advocate, good cop-bad cop routine over the past few years. This approach has motivated me to push my own limits on the South Georgia paper: thanks for bruising my ego. Anne and Wim, thankfully our paths still cross regularly. You have been instrumental in my choice to start a PhD and your support has greatly aided my fledgling academic career over the past years. To my colleagues of the SHIFTS team and the Quaternary Group in general: thank you for making me feel welcome in our corridor. To my colleagues from the INTIMATE network: it`s great bumping into you at conferences and enjoy a beer or ten. Or get lost taking the wrong Japanese bullet train. I would also like to express my gratitude to the administration of the geovitenskap department for helping me out with all the financial details, smoothing the ride. Meltzer fund, Cost-INTIMATE, ResClim, Bergen Open Access fund, SKD-Bjerknes, SSF and EU-INTERACT: thank you for helping me finance all those unforgettable research stays, conferences and field expeditions. They really are the icing on my PhD cake. Almost last, but by no means least: thank you David Bowie, Pink Floyd, Bruce Springsteen as well as George-Michael-Jackson and a handful of (other) guilty pleasures, which need not be mentioned, for providing the theme songs for my writing process. Finally and foremost, thank you Desiree: you really went out of your way to deal with the increasingly large shadow that this PhD cast on our private life. Being my sugar mama in between contracts, organizing memorable

getaways like our Faroese adventure or that sea-kayaking trip on Santorini, putting up with my increasingly un-emancipated stance on domestic responsibilities: the list of favours is endless. Trying to stay in science together is not easy, but I am confident that we will manage.

# Abstract

Earth`s polar regions are undergoing dramatic changes due to ongoing climate change as demonstrated by increasing temperatures, collapsing ice shelves, Arctic sea ice loss and rapid glacier retreat. Driving an accelerating rise in global sea level, this amplified regional response may have devastating global socio-economic consequences in the foreseeable future. Yet the causes and range of polar climate variability remain poorly understood as observational records are short and fragmentary, while climate proxy timeseries remain scarce and often lack resolution.

More detailed and longer paleoclimate archives are urgently needed to allow assessment of the full envelope of natural polar climate variability. This would allow us to contextualise ongoing warming and help improve policy scenarios, in effect using the past as the key to both present and future. Glaciers are sensitive recorders of climate variability as demonstrated by their response to ongoing global change. In addition to changes in size, this response is also captured by variations in glacial erosion in alpine glacier systems. The finest constituent of this process, known as glacial flour, is suspended in meltwater streams and may be deposited in downstream lakes. Hence, the bottom sediments of such glacier-fed lakes are continuous archives of past glacier activity and thus represent prime targets for paleoclimate studies.

In this thesis, the paleoclimatic potential of glacier-fed lake sediments is harnessed to improve our understanding of past polar climate change. To this end, sensitive sites on Arctic Svalbard and Antarctic South Georgia, in the pathways of major regional circulation patterns, were targeted. Emphasis is placed on the present Holocene interglacial as it is characterised by climatic boundary conditions that are similar to the present. A targeted multi-proxy approach, concentrating on geomorphological mapping, sediment fingerprinting, paleothermometry and advanced numerical techniques, was employed to enhance the potential of glacier-fed lakes as paleoclimate archives. Also, site-specific findings were contextualised through integration in a wider regional paleoclimate framework.

This thesis presents the first full Holocene records of glacier variability and summer temperature on Svalbard, in addition to the first continuous reconstruction of Late Holocene glacier Equilibrium Line Altitude (ELA) in the sub-Antarctic. The reported findings indicate a dynamic Holocene climate history of Svalbard, characterised by 1) pervasive Early Holocene glacial meltwater cooling, delaying the Hypsithermal until ± 7 ka BP and culminating in a glacier maximum, 2) a two-stage inception of the Neoglacial between ± 7-5 ka BP, driven by the strengthening influence of Arctic water and sea-ice against a backdrop of decreasing summer insolation and 3) a changeable Neoglacial from 4 ka BP onwards, characterised by a mean cold climate state that was perturbed by centennial-scale temperature excursions and glacial advances that were driven by the interaction between oceanic (AMOC), atmospheric (NAO) and solar forcing. This study shows that Late Holocene climate on South Georgia responded intricate transient phase-dependent interactions between regional circulation patterns (SWW, SAM and ENSO). In addition to these regional forcings, the reconstructed bi-polar expression of the Little Ice Age (LIA) and observed response to recent warming demonstrate the imprint of global forcing(s).

Notwithstanding limitations posed by e.g. closed-sum effects on proxy measurements as well as analytical and chronological uncertainties, this work advances our knowledge on Holocene polar climate variability, providing a reference to assess ongoing change. In addition to expanding the spatio-temporal coverage of high latitude proxy archives, future research should focus on 1) the integration of geomorphological mapping and sediment fingerprinting to constrain the signature of lake sedimentation, 2) the development of advanced ELA models in tandem with the application of paleothermometry to constrain the impact of atmosphere-driven shifts in hydroclimate and 3) the application of novel numerical tools to improve the robustness of glacier-fed lake-based paleoclimate studies. Prime examples include integration with model scenarios and instrumental calibration.

# Introduction

## Background

Humanity is confronted by rapidly shifting boundary conditions for its existence as global climate continues to change (Solomon, 2007). These shifts are particularly drastic in our planet`s high latitude regions, which demonstrate an amplified response to warming, particularly up North (Serreze and Barry, 2011). This polar amplification is most visibly expressed by a dramatic decline in Arctic sea ice over the past decades (Stroeve et al., 2007), while regional temperatures rose twice as fast as the global mean (Screen and Simmonds, 2010). In the antipodes, change is more equivocal and most evident around the Antarctic Peninsula, where glaciers retreat and summer temperatures rise (Cook et al., 2005; Mulvaney et al., 2012). Polar climate change may have dramatic ramifications around the world by driving a rise in global sea level: the vast majority of Earth`s land ice is locked away in high latitude land masses (Maurer, 2007). As almost two-thirds of the world`s major cities are found in lowland coastal areas (McGranahan et al., 2007), sea level rise could have devastating socio-economic consequences in the foreseeable future. Worryingly, recent studies suggest that the Greenland and West Antarctic Ice Sheets, respectively the world`s second and third most voluminous are losing mass (Shepherd et al., 2012; Shepherd and Wingham, 2007).

Yet, despite these severe global consequences, the causes of amplification and high-latitude climate change in general remain poorly understood on both hemispheres (Kennicutt et al., 2015; Miller et al., 2010). The reason for this is lacuna is twofold. First, the instrumental record is poorly constrained in space and time, providing us with a short and fragmentary time window into anthropogenic change. Secondly, to study the full range of polar climate dynamics, we ought to study geological paleoclimate archives that extend beyond instrumental timescales (Miller et al., 2010). Alas, such proxy timeseries remain scarce and far between (Marcott et al., 2013; Wanner et al., 2011). Furthermore, they often lack the resolution required to resolve rapid climate shifts, while covering short time intervals (Sundqvist et al.,

2014). Preferably, records should cover the entire present Holocene interglacial, to capture the full envelope of variability under boundary conditions similar to the present (Wanner, 2014a). Hence, new continuous high-resolution proxy archives could significantly improve our understanding of past polar climate variability, contextualizing current warming.

# High-latitude Holocene climate

## Millennial-scale variability

As posited in the background paragraph, our understanding of the Holocene climate evolution of Earth`s high latitudes remains poor. Yet, a growing body of evidence has recently shifted the paradigm of a stable Holocene (Alley and Ágústsdóttir, 2005; Bond et al., 2001; Grove, 1988), revealing a distinct gradual millennial-scale temperature evolution, driven by changes in orbital forcing (Bradley, 1999).

### *Arctic*

This signature is clearly expressed in the Northern Hemisphere, where the long-term evolution of Holocene proxy climate records typically follow a distinct pattern, in line with a gradual decrease in summer insolation (Wanner, 2014b; Wanner et al., 2008). An Early Holocene warmth plateau, the Hypsithermal, coincides with an insolation maximum, after which temperatures decrease through the Middle Holocene towards the Late Holocene, or Neoglacial because of the widespread reformation and growth of glaciers (Solomina et al., 2015), in sync with declining summer insolation (Renssen et al., 2005a). Additionally, pervasive 1500 year quasi-cycles have been reported in the North Atlantic region (Bond et al., 1997). The origin of these Bond cycles is still contested and attributed to either change in solar variability or ocean circulation (Bond et al., 2001; Came et al., 2007; Debret et al., 2007).

### *Antarctic*

In contrast, the Southern Hemisphere shows a more dampened response to orbital forcing throughout the Holocene (Wanner et al., 2008). Tracking changes in spring- instead of summer insolation due to the Southern Ocean`s thermal memory (Renssen

et al., 2005b), the climatic imprint of these changes bears resemblance to the Holocene evolution of Northern Hemisphere climate (Shevenell et al., 2011). However, this orbital signature is overprinted by variations in potent ocean-atmosphere-driven teleconnections, implicating shifts in dominant regional climate patterns like the Southern Westerlies Winds (SWW)(Lamy et al., 2001; Lamy et al., 2010; Van Daele et al., 2016).

## Bi-polar seesaw

The outlined dichotomy between the climate Holocene evolution of the Arctic and Antarctic appears to be a persistent feature of global climate, also leading to the notion of an inverse response between hemispheres. Known as the bi-polar seesaw (Broecker, 1998), this anti-phased climate response has been invoked during the last glacial and deglaciation, the entire Holocene, the Little Ice Age (LIA) as well as the 20th century (Barker et al., 2009; Broecker, 2000; Chylek et al., 2010; Ljung and Björck, 2007, Members, 2015 #782). Most studies claim a central role for a lagging redistribution of global heat via oceanic circulation pathways to explain this pattern (e.g. Stocker and Johnsen, 2003).

## Centennial-scale variability

Super-imposed on the outlined framework of millennial-scale high latitude Holocene climate change is a significant degree of centennial-scale variability (Abram et al., 2014; Mjell et al., 2015; Moreno et al., 2014; PAGES2K, 2013; Sarnthein et al., 2003; Shevenell et al., 2011; Wanner et al., 2011). Fluctuations include a number of marked high-amplitude events such as the well-known 8.2 ka cooling event, the Little Ice Age (LIA) and recent anthropogenic warming (Alley and Ágústsdóttir, 2005; Grove, 1988; Waters et al., 2016). Though incompletely understood due to the scarcity of evenly distributed continuous and well-dated climate records (Marcott et al., 2013; Sundqvist et al., 2014), a crude outline emerges from the literature. In the Arctic, centennial-scale Holocene climate seems to have been influenced by deglacial meltwater forcing, reorganizations of oceanic and atmospheric circulation, sea-ice feedbacks and changes in solar variability (Jennings et al., 2015; Jiang et al., 2015;

Kleiven et al., 2008; Mjell et al., 2015; Müller et al., 2012; Olsen et al., 2012; Risebrobakken et al., 2011; Screen and Simmonds, 2010; Thornalley et al., 2009). In contrast, transient and spatially heterogeneous interactions between SWW, the El Niño-Southern Oscillation (ENSO) cycle as well as the Southern Annular Mode (SAM) affected climate in the Antarctic, partly through modulation of low-latitude teleconnections (Abram et al., 2014; Ding et al., 2012; Fogt et al., 2011; Fogt and Bromwich, 2006). Also, the Pacific and Atlantic sectors of the Southern Ocean show a dichotomous climate response, known as the Antarctic di-pole (Yuan, 2004).

## Glacier-fed lakes as paleoenvironmental archives

At present, glaciers sensitively respond to climate change as demonstrated by their current retreat around the world (Pfeffer et al., 2014; WGMS, 1988-2011). Glacier variability is, however, not restricted to the present, but has changed Earth`s climate during the cycles of alternating glacial and interglacial epochs that characterized the last 2.59 million years of Earth`s history, the Quaternary. Compared to these dramatic oscillations, the degree of Holocene variability is modest, but as previously emphasized, by no means trivial. For example, glacial meltwater fluxes perturbed the Early Holocene North Atlantic, causing widespread cooling (McDermott et al., 2001), while extensive historical glacier advances during the Little Ice Age (LIA) eradicated farms throughout the Alps and Scandinavia (Bogen et al., 1989; Grove, 1987). Evidently, glaciers recorded Holocene climate shifts in the past and during the present. As will be explained in the next paragraph(s), glacier-fed lake sediments continuously record these changes, chronicling past climate variability. Consequently, these sediment archives represent continuous, high resolution and sensitive climate proxy timeseries that could improve our understanding of Holocene climate (Bakke and Paasche, 2014). Particularly so in Earth`s high latitude regions, where glacial lakes are ubiquitous (Carrivick and Tweed, 2013)

## Scientific rationale

Changes in glacier size result from shifts in the balance between accumulation and ablation (Oerlemans, 2005). This mass balance is governed by summer temperature and winter precipitation (Østrem and Liestøl, 1964). Consequently, changes in glacier size reflect a composite climate signal. In temperate glaciers, this signal may be continuously recorded over time by the sediment archives of downstream lakes through size-dependent glacial erosion (Dahl et al., 2003). At such settings, glacial erosion produces fine-grained (silty/clay) rock flour, which is suspended in meltwater streams that evacuate glaciers (*Fig. 1*) (Leemann and Niessen, 1994). As this sediment-laden water enters the low-energy environment of downstream lakes, flow speeds decrease and particles fall out of suspension (Liermann et al., 2012). Settling on the lake bottom, glacigenic sediments accumulate through time, continuously recording past glacier activity. Following from the above, sediment cores extracted from glacier-fed lakes rank among the best available climate proxy archives (Ashley, 1995; Carrivick and Tweed, 2013).

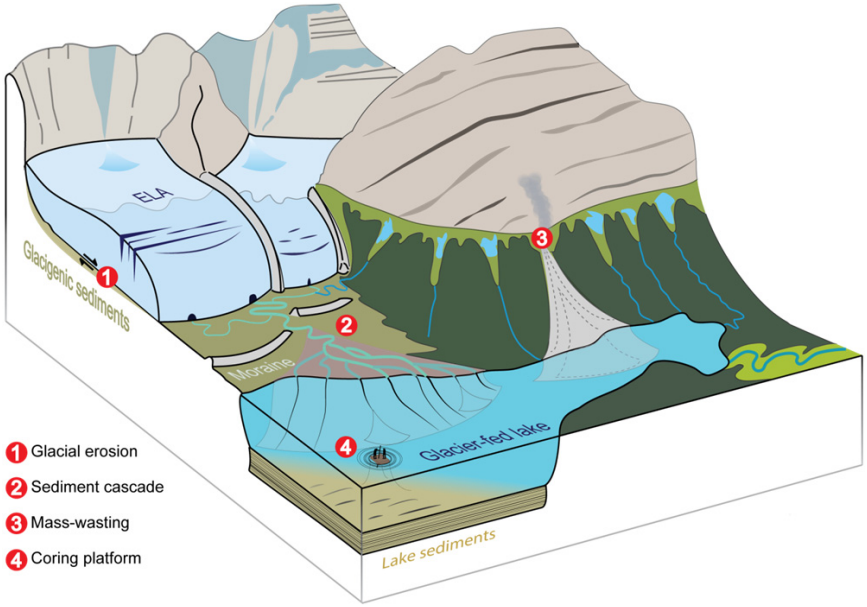


***Fig. 1**. Schematic block diagram, visualizing the rationale behind using glacier-fed lake sediments paleoenvironmental archives. Source: (Van der Bilt et al., in press)*

## Analytical approach

Though seemingly straightforward, accurately detecting and isolating a glacigenic signal from glacier-fed lake sediments requires a refined multi-disciplinary methodological toolbox. Fundamentally, this approach revolves around the defining physical characteristics of rock flour: fine-grained, poorly sorted and minerogenic (Leemann and Niessen, 1994). Following from this, purely glacigenic lake sediments are dense, comprising a tightly packed matrix of particles with a high specific weight (Bakke et al., 2005b). Consequently, bulk sediment density is commonly used as a diagnostic tool to detect glacier activity from glacier-fed lake sediments, with higher values signifying a larger glacier (McKay and Kaufman, 2009; Vasskog et al., 2012). Though still the backbone of many studies, sediment density measurements ought to be complemented by other methods for the sake of validation and replication.

A toolbox of additional physical, geochemical and environmental magnetic techniques is now routinely employed for this purpose (Bakke and Paasche, 2014). These encompass X-Ray Fluorescence (XRF) core scanning to qualitatively measure the concentrations of conservative minerogenic elements that may be indicative of glacial erosion (Bakke et al., 2009). But also magnetic susceptibility (MS) and remanence (e.g. SIRM and ARM), indicators of catchment-derived minerogenic input and mineral magnetic properties (mineralogy and grain size), respectively (Paasche et al., 2004; Thompson et al., 1975), are often applied in lake sediment-based glacier reconstructions (Matthews and Karlén, 1992; Snowball and Sandgren, 1996). Finally, grain size analysis is often applied to distinguish glacigenic sediments from other sediment sources in glacier-fed lake catchment that introduce noise to records (Støren et al., 2008; Vasskog et al., 2011). These include mass-wasting processes such as floods, slumps and avalanches that are typically characterized by a coarser grain-size distribution (*Fig. 1*) (Rubensdotter and Rosqvist, 2009).

Hence, the outlined multi-proxy toolbox is also indispensable for understanding non-glacial processes that affect glacier-fed lakes and their sediments (Jansson et al., 2005). Additional examples of this use include the investigation of mobile

geochemical element concentrations and magnetic indicators to identify the signature of shifting redox conditions (Croudace et al., 2006). If undetected, such shifts could lead to inaccurate interpretations, diluting the minerogenic imprint of glacigenic input or exacting a biological control on the mineral magnetic signature of sediments (Löwemark et al., 2011; Paasche et al., 2004).

Finally, the use of glacier-fed lakes as paleoclimate records also involves investigation beyond lacustrine sedimentary archives to understand catchment and in-lake processes that may impact lake sediments (Dahl et al., 2003). Typically, this entails a combination of pre-coring geomorphological mapping and geophysical surveying of investigated catchments and lakes, respectively. Mapping landforms provides insight into processes that affect the sediment cascade between glacier and lake (Carrivick et al., 2013). Most of these processes leave a sedimentological imprint that can be distinguished from glacigenic input, as previously mentioned. This is, however, not the case for older glacial deposits that may be reworked by erosive agents in the catchment (*Fig. 1*) (Ballantyne, 2002). The signature of such paraglacial modification may be indistinguishable from fresh glacial flour (Leonard, 1997; Rubensdotter and Rosqvist, 2009), compromising an accurate interpretation of the lacustrine sediment record. Progressing from catchment into lake basin, the bathymetry of investigated lakes is often surveyed using a range of geophysical techniques like sonar (echo sounder), radar (GPR) and seismology (CHIRP). Ensuing bathymetrical profiles and sediment thickness maps are vital to help identify suitable coring locations; flat and far from steep slopes and in- or outlets, minimizing disturbance, and underlain by an undisturbed sediment sequence.

## Numerical approach

The (ongoing) development of the outlined multi-proxy approach over the past few decades has resulted in large and complex datasets. Numerical methods are increasingly applied to adequately structure and mine these (Birks, 1998). Commonly applied techniques include normalization, cluster analysis and Rates of Change (RoC) analyses. Normalization is typically used to amplify the imprint of an environmental

signal. Normalizing minerogenic (glacigenic) elements against mobile (redox-sensitive) elements, for instance, to reduce the impact of discussed dilution effects on a minerogenic sediment signature (Kylander et al., 2011). Cluster analysis, a method derived from the field of paleo-ecology (Grimm, 1987), can be used to objectively subdivide sediment sequences into units with distinct characteristics (Bakke et al., 2013). RoC analysis can help detect abrupt transitions in sedimentology that may reflect the represent of `noisy` mass-wasting events (Støren et al., 2010). More intricate than the above techniques, and also increasingly applied to glacigenic lake sediments (Røthe et al., 2015; Vasskog et al., 2012), is Principal Component Analysis (PCA) (Hotelling, 1933). This ordination technique allows investigation both presence and strength of any shared signal between measured proxies, e.g. glacier variability, as well as detection of gradients of change (Sergeeva, 1983).

## Modelling techniques

Modelling techniques are also becoming commonplace, simulating relations between measured sediment parameters and other variables. Topical examples are mainly restricted to age-depth and Equilibrium Line Altitude (ELA) modelling, transforming sediment stratigraphies into timeseries and climate metrics, respectively.

### *Age-depth*

To be able to resolve detected sedimentary shifts in time, a high resolution measurement strategy should be matched by strong chronological control. Robust age-depth models are indispensable to do so. A first and crucial step is the procurement of sufficient high-quality dating samples. A range of different independent chronological methods is typically applied for this purpose, encompassing popular radiometric methods like $^{14}C$ and $^{210}Pb$ dating, but also non-radiometric tools such as tephrochronology and Paleomagnetic Secular Variations (PSV). Subsequent modelling fits these chronological markers together on a sediment core`s depth-scale through `classic` interpolation and regression or Bayesian Markov Monte Carlo (MCMC) simulation (Blaauw, 2010; Blaauw and Christen, 2011), depending on the goodness-of-fit. As with all models, age-depth relations are but

possible representations of reality. Thus, employing them to discuss proxy data through time deals just as much with chronological control as with uncertainty to avoid over-interpretation and allow detection of similarities as well as leads or lags.

### *ELA*

A glacier`s Equilibrium Line Altitude (ELA), where accumulation equals ablation (*Fig. 1*), is characterized by a statistically significant relationship between the primary controls on mass balance, summer temperature and winter precipitation (Østrem and Liestøl, 1964). This relationship, coined the Liestøl equation by Sissons (1979), enables the use of ELA as a climate metric, constraining the drivers of glacier variability. The integrated approach that derives a continuous record of past ELAs by calibrating lake sediment-based glacier variations against physical moraine-based evidence of past glacier size is frequently applied (Bakke et al., 2005a; Dahl and Nesje, 1996; Røthe et al., 2015). Models are key to **1**) calculate past ELAs using moraine, map or photographic tie-points to constrain former past glacier size and **2**) regress the lake sediment parameter that most accurately reflects past glacier activity against these tie-points (Bakke and Paasche, 2014; Osmaston, 2005). The latter are largely determined by ice distribution or hypsometry (Osmaston, 2005), determining the complexity of algorithms required to accurately approximate glacier behaviour.

## Setting

For this thesis, high-latitude glacier-fed lake sites were investigated on both hemispheres: in High Arctic Svalbard and sub-Antarctic South Georgia (*Figs. 2 and 3*). Both localities were selected due to their strategic location in the pathway of major regional circulation patterns, rendering local climate highly sensitive to changing conditions. Also, due to their rugged relief and high-latitude setting, glaciers and glacier-fed lakes are omnipresent on both islands.

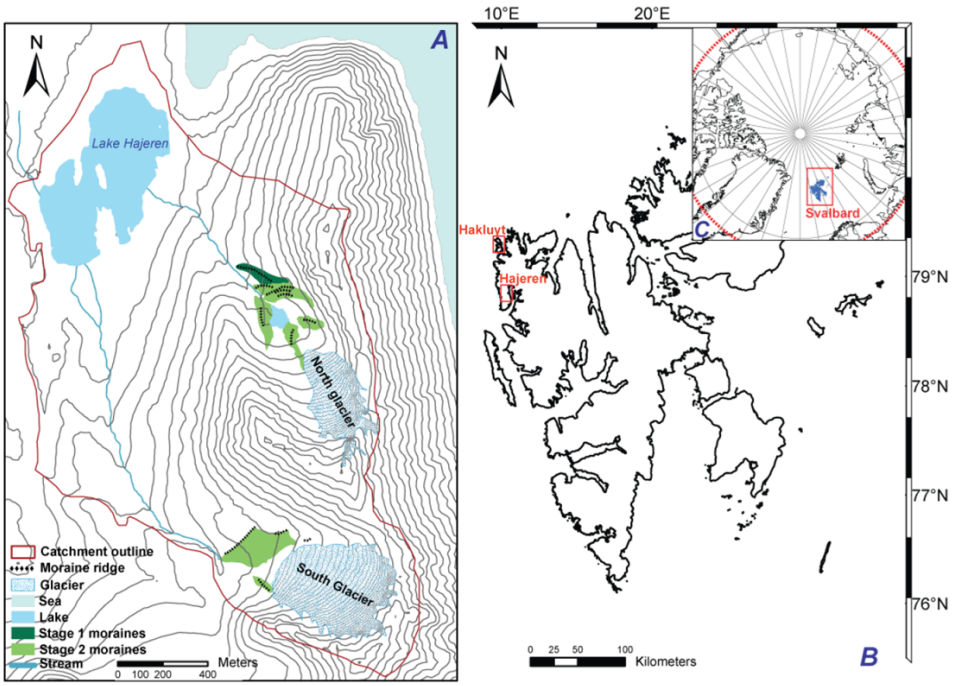


***Fig. 2**. A: a simple geomorphological map of the Hajeren catchment, outlined by a red line. North and South glaciers, their outlet streams and Lake Hajeren are shown B: close-up of the Svalbard archipelago, marking the Hajeren catchment with a red rectangle. C: North Pole view of Svalbard (blue) and the Arctic (red dashed line). Source: (van der Bilt et al., 2015)*

## Svalbard

The Svalbard archipelago sits at the changeable crossroads of warm Atlantic and cold Arctic waters of the West and East Spitsbergen currents, respectively (Rasmussen et al., 2014; Ślubowska-Woldengen et al., 2007; Werner et al., 2015; Werner et al., 2013). In combination with the proximity of the present-day average sea-ice limit (Benestad et al., 2002), this setting gives rise to a dynamic and sensitive local climate conditions (Müller et al., 2012). Instrumental records show that present-day climate can be characterized as polar maritime, with a mean temperature of -5 °C in combination with 427 mm of annual precipitation (Førland et al., 2011). Conditions have, however, been warming rapidly over the past three decades, repeatedly breaking records over the past decade (Nordli, 2010). This work reports on two glacier-fed lake sites on northwest Spitsbergen: Hajeren and Hakluyt (Fig. 2b). Lake

Hajeren (79.15°N, 11.31°E) is located on the Mitra peninsula and measures 0.23 km$^2$. At present, the lake is fed by two small cirque glaciers that have been in retreat for at least 80 years (*Fig. 2a*) (NPI, 1936, 2015). The catchment sits just above the local marine limit and is underlain by meta-sedimentary bedrock (Dallmann, 2015; Landvik et al., 2013). Lake Hakluyt (79.77°N, 10.74°E) sits on Amsterdam Island, west off northwest Spitsbergen (*Fig. 2b*). Presently fed by a glacier-turned-snow patch, this lake also sits above the reported marine limit (Salvigsen, 1979). Catchment bedrock mainly comprises migmatite and gneiss (NPI, 2015).

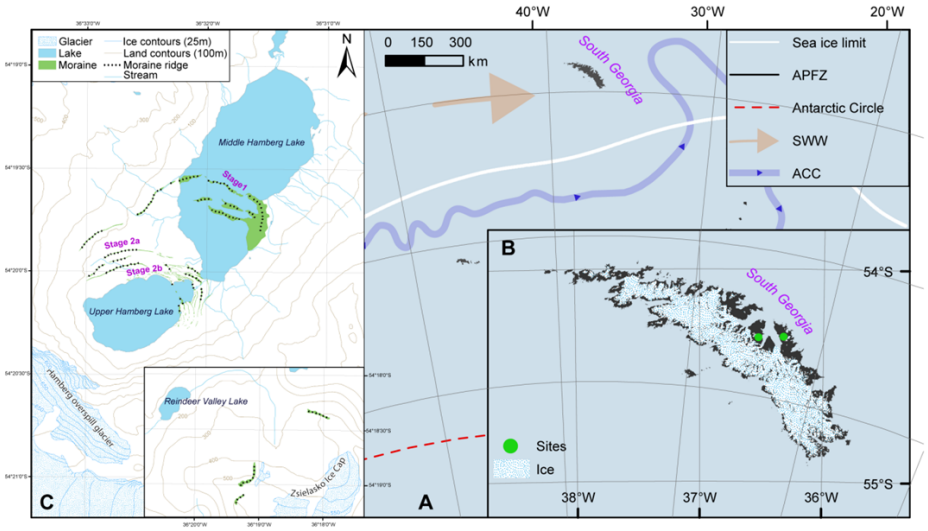


***Fig. 3**. A: overview of the Drake Passage sector of the Southern Ocean, showing major circulation patterns, i.e. the Antarctic Polar Front Zone (APFZ), the Southern Westerlies Winds (SWW) and the Antarctic Circumpolar Current (ACC), as well as the Antarctic Circle and winter sea-ice limit. B: Inset of South Georgia, indicating the island`s glacier coverage and the sites discussed in this paper. C: Simplified geomorphological map for the Hamberg and Reindeer Valley catchment, showing the overspill glacier and Szielasko Ice Cap. Source: (Van der Bilt et al., under review )*

## South Georgia

The island of South Georgia (± 54°S, 30°W) lies in the Drake Passage area of the Southern Ocean, midway between the Falkland Islands and the Antarctic Peninsula (*Figs. 3a and b*). Due to its location in the pathways of the core Southern Westerlies Winds (SWW) belt, the Southern Ocean`s main circulation system (Fogt et al., 2011),

and the coupled Antarctic Circumpolar Current (ACC), South Georgia is well-situated to record regional climate shifts (Rosqvist and Schuber, 2003). Present-day climate is cool and maritime, with a mean temperature of 1.9 °C and 1450 mm of annual precipitation (Trouet and Van Oldenborgh, 2013). At present, about half of South Georgia is ice-covered (Smith, 1960), though most glaciers have retreated over the past decades (Cook et al., 2010). In this thesis, two glacier-fed lakes in the Cumberland Bay area are examined (*Fig. 3c*): the Middle Hamberg and Reindeer Valley lakes. The Middle Hamberg Lake (54.21°S, 36.33°W) covers 1.29 $km^2$ and is part of a chain of glacial lakes. All are fed by the up-valley Hamberg overspill glacier, a tributary of the larger Hamberg glacier system (Clapperton et al., 1989). The Reindeer Valley Lake (54.14°S, 36.20°W) sits across Cumberland Bay, measures 0.16 $km^2$ and is fed by the Szielasko Ice Cap. Maps and satellite data confirm that both ice bodies retreating over the past decades (DOS, 1958; Pfeffer et al., 2014; USGS and NASA, 2000). Both Reindeer and Hamberg catchment are underlain by shales (Macdonald et al., 1987; Stone, 1980).

# Objectives

The main goal of this thesis is generating the high-resolution (centennial-scale) climate proxy timeseries required to expand our knowledge of Holocene high-latitude climate. Doing so allows capturing the full range of natural variability under present climatic boundary conditions, contextualizing ongoing warming. To this end, sediment archives from glacier-fed lakes, prime paleoclimate archives (Carrivick and Tweed, 2013), were selected on strategically located Arctic Svalbard and sub-Antarctic South Georgia. In addition, specific objectives have been identified, aimed at enhancing the paleoclimate potential of glacier-fed lake sediments:

*Explore the potential of numerical techniques to improve:*

- Modelling the relationship between glacier ELA and lacustrine glacigenic input

- Quantification and propagation of analytical and chronological uncertainty

- Validation and replication of a detected glacigenic signal

*Assess the impact of non-glacial processes on glacier-fed lake sediments through*:

- Geomorphological mapping

- Sediment fingerprinting

*Contextualise site-specific findings in a regional paleoclimate framework to:*

- Improve our understanding of polar climate dynamics

- Understand the forcings behind past glacier variability

*Constrain the climatic signature of past glacier change*

- Employing alkenone-based paleothermometry

# Thesis outline

The main body of this thesis consists of 5 papers, reviewing the application of glacier-fed lake sediments as paleoenvironmental archives (*paper 1*), examining the potential of geomorphological mapping to gain a process-based understanding of sedimentation in glacier-fed lakes (*paper 2*), reconstructing the Holocene history of glacier activity in the glacier-fed catchment of Lake Hajeren on Arctic northwest Spitsbergen (*paper 3*), using quantitative alkenone-based paleothermometry to understand the signature of Holocene climate shifts on northwest Spitsbergen (*paper 4*) and, finally, presenting a continuous reconstruction of glacier Equilibrium Line Altitude (ELA) over the past millennium on sub-Antarctic South Georgia (*paper 5*).

**Paper 1: Glacier-fed lakes as paleoenvironmental archives**

This paper reiterates the prior introduction to the use of glacier-fed lake sediments as paleoenvironmental archives in more generalist terms for non-specialists. After explaining the physical mechanisms that record a climate sensitive sediment signal, the multi-proxy toolbox, applied to subsequently fingerprint this signature, is discussed. Special attention is given to the use of advanced dating methods, which enable researchers to resolve climate shifts in ever greater detail. Novel numerical techniques, increasingly used to validate sediment-based glacier signals, quantify as well as propagate uncertainty and decompose their climate signature, are also explicated. Like the conclusions section of this thesis, paper 1 concludes with a brief outlook on promising new research avenues.

**Paper 2: Mapping sediment–landform assemblages to constrain lacustrine sedimentation in a glacier-fed lake catchment in northwest Spitsbergen**

This paper seeks to improve the robustness of glacigenic signals detected from glacier-fed lake sediments by constraining the contribution of non-glacial processes. These may overprint the meltwater-driven rock flour signal that records glacier activity, thereby introducing noise. Also, reworking of older glacigenic sediments may leave a sedimentological imprint that is indistinguishable from freshly eroded

glacial flour. For this purpose, a combined approach of remote sensing and ground-truthing is employed to map sediment sources in the catchment of Lake Hajeren on northwest Spitsbergen. By linking these to surface processes, their contribution to the sediment cascade between glacier and lake (sediments) is constrained.

**Paper 3: Reconstruction of glacier variability from lake sediments reveals dynamic Holocene climate in Svalbard**

This paper presents the first record of glacier variability on High Arctic northwest Spitsbergen that covers the entire Holocene, using sediments from glacier-fed Lake Hajeren. 26 dated radiocarbon samples and Paleomagnetic Secular Variation (PSV) correlation provide unprecedented control. The analytical multi-proxy toolbox outlined in the introduction, combined with regression, normalization and ordination techniques, allowed robust fingerprinting of glacier activity on centennial timescales, whilst also constraining non-glacial controls on lacustrine sedimentation.

**Paper 4: Alkenone-based reconstructions reveal four-phase Holocene temperature evolution for High Arctic Svalbard**

This work seeks to fingerprint the signature of Holocene climate shifts on northwest Svalbard, using quantitative paleothermometry. For this purpose, the established biomarker-based UK37 index was calculated on sediments from the Hajeren and Hakluyt lakes. By analysing sample UK37 isomer distributions, the phylogenetic signature of alkenone producers could be fingerprinted. This, in turn, enabled selecting a UK37 calibration, transforming measurements into paleotemperature estimates. The ensuing records represent the first quantitative terrestrial summer temperature reconstructions from the High Arctic that cover the entire Holocene.

**Paper 5: South Georgia glacier fluctuations during the past millennium reveal medieval retreat and inter-hemispheric Little Ice Age**

This paper presents the first continuous reconstruction of glacier Equilibrium Line (ELA) over the past millennium from sub-Antarctic South Georgia. Whilst covering well-known historical climate events like LIA, this period has not been previously

targeted by similar studies. Two glacier-fed sites were investigated to assess the representativeness of recorded glacier signals, the Middle Hamberg and Reindeer Valley lakes. To this end, a novel Bayesian approach was applied (Werner and Tingley, 2015), finding greatest similarity between both records within the prescribed uncertainty range of generated age-depth models. The lake sediment signal was also calibrated against known past ice front positions by employing a novel model that accounts for non-linear glacier responses, transforming relative glacier activity to quantitative ELA estimates.

# References cited in Introduction section

Abram, N.J., Mulvaney, R., Vimeux, F., Phipps, S.J., Turner, J., England, M.H., 2014. Evolution of the Southern Annular Mode during the past millennium. Nature Clim. Change 4, 564-569.
Alley, R.B., Ágústsdóttir, A.M., 2005. The 8k event: cause and consequences of a major Holocene abrupt climate change. Quaternary Science Reviews 24, 1123-1149.
Ashley, G., 1995. Glaciolacustrine environments. Glacial Environments 1, 417-444.
Bakke, J., Dahl, S.O., Paasche, Ø., Løvlie, R., Nesje, A., 2005a. Glacier fluctuations, equilibrium-line altitudes and palaeoclimate in Lyngen, northern Norway, during the Lateglacial and Holocene. The Holocene 15, 518-540.
Bakke, J., Lie, Ø., Heegaard, E., Dokken, T., Haug, G.H., Birks, H.H., Dulski, P., Nilsen, T., 2009. Rapid oceanic and atmospheric changes during the Younger Dryas cold period. Nature Geoscience 2, 202-205.
Bakke, J., Nesje, A., Dahl, S.O., 2005b. Utilizing physical sediment variability in glacier-fed lakes for continuous glacier reconstructions during the Holocene, northern Folgefonna, western Norway. The Holocene 15, 161-176.
Bakke, J., Paasche, Ø., 2014. Sediment Core and Glacial Environment Reconstruction, Encyclopedia of Snow, Ice and Glaciers. Springer, pp. 979-984.
Bakke, J., Trachsel, M., Kvisvik, B.C., Nesje, A., Lyså, A., 2013. Numerical analyses of a multi-proxy data set from a distal glacier-fed lake, Sørsendalsvatn, western Norway. Quaternary Science Reviews 73, 182-195.
Ballantyne, C.K., 2002. Paraglacial geomorphology. Quaternary Science Reviews 21, 1935-2017.
Barker, S., Diz, P., Vautravers, M.J., Pike, J., Knorr, G., Hall, I.R., Broecker, W.S., 2009. Interhemispheric Atlantic seesaw response during the last deglaciation. Nature 457, 1097-1102.
Benestad, R., Hanssen-Bauer, I., Skaugen, T., Førland, E., 2002. Associations between sea-ice and the local climate on Svalbard. Oslo: Norwegian Meteorological Institute Report, 1-7.
Birks, H., 1998. DG Frey and ES Deevey Review 1: Numerical tools in palaeolimnology–Progress, potentialities, and problems. Journal of Paleolimnology 20, 307-332.
Blaauw, M., 2010. Methods and code for 'classical' age-modelling of radiocarbon sequences. Quaternary Geochronology 5, 512-518.
Blaauw, M., Christen, J.A., 2011. Flexible paleoclimate age-depth models using an autoregressive gamma process. Bayesian Analysis 6, 457-474.
Bogen, J., Wold, B., Østrem, G., 1989. Historic glacier variations in Scandinavia, Glacier fluctuations and climatic change. Springer, pp. 109-128.
Bond, G., Kromer, B., Beer, J., Muscheler, R., Evans, M.N., Showers, W., Hoffmann, S., Lotti-Bond, R., Hajdas, I., Bonani, G., 2001. Persistent solar influence on North Atlantic climate during the Holocene. Science 294, 2130-2136.
Bond, G., Showers, W., Cheseby, M., Lotti, R., Almasi, P., Priore, P., Cullen, H., Hajdas, I., Bonani, G., 1997. A pervasive millennial-scale cycle in North Atlantic Holocene and glacial climates. science 278, 1257-1266.
Bradley, R.S., 1999. Paleoclimatology: reconstructing climates of the Quaternary. Academic Press.
Broecker, W.S., 1998. Paleocean circulation during the last deglaciation: a bipolar seesaw? Paleoceanography 13, 119-121.
Broecker, W.S., 2000. Was a change in thermohaline circulation responsible for the Little Ice Age? Proceedings of the National Academy of Sciences 97, 1339-1342.

Came, R.E., Oppo, D.W., McManus, J.F., 2007. Amplitude and timing of temperature and salinity variability in the subpolar North Atlantic over the past 10 ky. Geology 35, 315-318.
Carrivick, J.L., Geilhausen, M., Warburton, J., Dickson, N.E., Carver, S.J., Evans, A.J., Brown, L.E., 2013. Contemporary geomorphological activity throughout the proglacial area of an alpine catchment. Geomorphology 188, 83-95.
Carrivick, J.L., Tweed, F.S., 2013. Proglacial lakes: character, behaviour and geological importance. Quaternary Science Reviews 78, 34-52.
Chylek, P., Folland, C.K., Lesins, G., Dubey, M.K., 2010. Twentieth century bipolar seesaw of the Arctic and Antarctic surface air temperatures. Geophysical Research Letters 37, L08703.
Clapperton, C.M., Sugden, D.E., Birnie, J., Wilson, M.J., 1989. Late-glacial and Holocene glacier fluctuations and environmental change on South Georgia, Southern Ocean. Quaternary Research 31, 210-228.
Cook, A., Fox, A., Vaughan, D., Ferrigno, J., 2005. Retreating glacier fronts on the Antarctic Peninsula over the past half-century. Science 308, 541-544.
Cook, A.J., Poncet, S., Cooper, A.P.R., Herbert, D., Christie, D., 2010. Glacier retreat on South Georgia and implications for the spread of rats. Antarctic Science 22, 255-263.
Croudace, I.W., Rindby, A., Rothwell, R.G., 2006. ITRAX: description and evaluation of a new multi-function X-ray core scanner. SPECIAL PUBLICATION-GEOLOGICAL SOCIETY OF LONDON 267, 51.
Dahl, S.O., Bakke, J., Lie, Ø., Nesje, A., 2003. Reconstruction of former glacier equilibrium-line altitudes based on proglacial sites: an evaluation of approaches and selection of sites. Quaternary Science Reviews 22, 275-287.
Dahl, S.O., Nesje, A., 1996. A new approach to calculating Holocene winter precipitation by combining glacier equilibrium-line altitudes and pine-tree limits: a case stud from Hardangerjokulen, central southern Norway. The Holocene 6, 381-398.
Dallmann, W.K.E., 2015. Geoscience Atlas of Svalbard. Norwegian Polar Institute Tromsø.
Debret, M., Bout-Roumazeilles, V., Grousset, F., Desmet, M., McManus, J.F., Massei, N., Sebag, D., Petit, J.-R., Copard, Y., Trentesaux, A., 2007. The origin of the 1500-year climate cycles in Holocene North-Atlantic records. Climate of the Past Discussions 3, 679-692.
Ding, Q., Steig, E.J., Battisti, D.S., Wallace, J.M., 2012. Influence of the tropics on the Southern Annular Mode. Journal of Climate 25, 6330-6348.
DOS, 1958. Falkland Island Dependencies, South Georgia. Directorate of Overseas Surveys, London.
Fogt, R., Bromwich, D., Hines, K., 2011. Understanding the SAM influence on the South Pacific ENSO teleconnection. Climate Dynamics 36, 1555-1576.
Fogt, R.L., Bromwich, D.H., 2006. Decadal variability of the ENSO teleconnection to the high-latitude South Pacific governed by coupling with the Southern Annular Mode*. Journal of Climate 19, 979-997.
Førland, E.J., Benestad, R., Hanssen-Bauer, I., Haugen, J.E., Skaugen, T.E., 2011. Temperature and precipitation development at Svalbard 1900–2100. Advances in Meteorology 2011, 1-14.
Grimm, E.C., 1987. CONISS: a FORTRAN 77 program for stratigraphically constrained cluster analysis by the method of incremental sum of squares. Computers & Geosciences 13, 13-35.
Grove, J., 1987. Glacier fluctuations and hazards. Geographical journal, 351-367.
Grove, J., 1988. The Little Ice Age, 498. Methuen, New York.
Hotelling, H., 1933. Analysis of a complex of statistical variables into principal components. Journal of educational psychology 24, 417.

Jansson, P., Rosqvist, G., Schneider, T., 2005. Glacier fluctuations, suspended sediment flux and glacio-lacustrine sediments. Geografiska Annaler: Series A, Physical Geography 87, 37-50.
Jennings, A., Andrews, J., Pearce, C., Wilson, L., Ólafsdóttir, S., 2015. Detrital carbonate peaks on the Labrador shelf, a 13–7 ka template for freshwater forcing from the Hudson Strait outlet of the Laurentide Ice Sheet into the subpolar gyre. Quaternary Science Reviews 107, 62-80.
Jiang, H., Muscheler, R., Björck, S., Seidenkrantz, M.-S., Olsen, J., Sha, L., Sjolte, J., Eiríksson, J., Ran, L., Knudsen, K.-L., 2015. Solar forcing of Holocene summer sea-surface temperatures in the northern North Atlantic. Geology 43, 203-206.
Kennicutt, M., Chown, S., Cassano, J., Liggett, D., Peck, L., Massom, R., Rintoul, S., Storey, J., Vaughan, D., Wilson, T., 2015. A roadmap for Antarctic and Southern Ocean science for the next two decades and beyond. Antarctic Science 27, 3-18.
Kleiven, H.K.F., Kissel, C., Laj, C., Ninnemann, U.S., Richter, T.O., Cortijo, E., 2008. Reduced North Atlantic deep water coeval with the glacial Lake Agassiz freshwater outburst. Science 319, 60-64.
Kylander, M.E., Ampel, L., Wohlfarth, B., Veres, D., 2011. High-resolution X-ray fluorescence core scanning analysis of Les Echets (France) sedimentary sequence: new insights from chemical proxies. Journal of Quaternary Science 26, 109-117.
Lamy, F., Hebbeln, D., Röhl, U., Wefer, G., 2001. Holocene rainfall variability in southern Chile: a marine record of latitudinal shifts of the Southern Westerlies. Earth and Planetary Science Letters 185, 369-382.
Lamy, F., Kilian, R., Arz, H.W., Francois, J.-P., Kaiser, J., Prange, M., Steinke, T., 2010. Holocene changes in the position and intensity of the southern westerly wind belt. Nature Geoscience 3, 695-699.
Landvik, J.Y., Brook, E.J., Gualtieri, L., Linge, H., Raisbeck, G., Salvigsen, O., Yiou, F., 2013. 10Be exposure age constraints on the Late Weichselian ice-sheet geometry and dynamics in inter-ice-stream areas, western Svalbard. Boreas 42, 43-56.
Leemann, A., Niessen, F., 1994. Varve formation and the climatic record in an Alpine proglacial lake: calibrating annually-laminated sediments against hydrological and meteorological data. The Holocene 4, 1-8.
Leonard, E.M., 1997. The relationship between glacial activity and sediment production: evidence from a 4450-year varve record of neoglacial sedimentation in Hector Lake, Alberta, Canada. Journal of Paleolimnology 17, 319-330.
Liermann, S., Beylich, A.A., van Welden, A., 2012. Contemporary suspended sediment transfer and accumulation processes in the small proglacial Sætrevatnet sub-catchment, Bødalen, western Norway. Geomorphology 167–168, 91-101.
Ljung, K., Björck, S., 2007. Holocene climate and vegetation dynamics on Nightingale Island, South Atlantic—an apparent interglacial bipolar seesaw in action? Quaternary Science Reviews 26, 3150-3166.
Löwemark, L., Chen, H.-F., Yang, T.-N., Kylander, M., Yu, E.-F., Hsu, Y.-W., Lee, T.-Q., Song, S.-R., Jarvis, S., 2011. Normalizing XRF-scanner data: A cautionary note on the interpretation of high-resolution records from organic-rich lakes. Journal of Asian Earth Sciences 40, 1250-1256.
Macdonald, D., Storey, B., Thomson, J., 1987. South Georgia. BAS GEOMAP Series, Sheet 1, Scale 1: 250000, Geological map and supplementary text. British Antarctic Survey.
Marcott, S.A., Shakun, J.D., Clark, P.U., Mix, A.C., 2013. A reconstruction of regional and global temperature for the past 11,300 years. science 339, 1198-1201.

Matthews, J.A., Karlén, W., 1992. Asynchronous neoglaciation and Holocene climatic change reconstructed from Norwegian glaciolacustrine sedimentary sequences. Geology 20, 991-994.
Maurer, J., 2007. Atlas of the Cryosphere. National Snow and Ice Data Center.(26 January 2012.
McDermott, F., Mattey, D.P., Hawkesworth, C., 2001. Centennial-Scale Holocene Climate Variability Revealed by a High-Resolution Speleothem δ18O Record from SW Ireland. Science 294, 1328-1331.
McGranahan, G., Balk, D., Anderson, B., 2007. The rising tide: assessing the risks of climate change and human settlements in low elevation coastal zones. Environment and urbanization 19, 17-37.
McKay, N.P., Kaufman, D.S., 2009. Holocene climate and glacier variability at Hallet and Greyling Lakes, Chugach Mountains, south-central Alaska. Journal of Paleolimnology 41, 143-159.
Miller, G.H., Alley, R.B., Brigham-Grette, J., Fitzpatrick, J.J., Polyak, L., Serreze, M.C., White, J.W.C., 2010. Arctic amplification: can the past constrain the future? Quaternary Science Reviews 29, 1779-1790.
Mjell, T.L., Ninnemann, U.S., Eldevik, T., Kleiven, H.K.F., 2015. Holocene Multidecadal-to-Millennial Scale Variations in Iceland-Scotland Overflow and Their Relationship to Climate. Paleoceanography.
Moreno, P.I., Vilanova, I., Villa-Martínez, R., Garreaud, R., Rojas, M., De Pol-Holz, R., 2014. Southern Annular Mode-like changes in southwestern Patagonia at centennial timescales over the last three millennia. Nature communications 5.
Mulvaney, R., Abram, N.J., Hindmarsh, R.C., Arrowsmith, C., Fleet, L., Triest, J., Sime, L.C., Alemany, O., Foord, S., 2012. Recent Antarctic Peninsula warming relative to Holocene climate and ice-shelf history. Nature 489, 141-144.
Müller, J., Werner, K., Stein, R., Fahl, K., Moros, M., Jansen, E., 2012. Holocene cooling culminates in sea ice oscillations in Fram Strait. Quaternary Science Reviews 47, 1-14.
Nordli, Ø., 2010. The Svalbard airport temperature series. Bulletin of Geography. Physical Geography Series, 5-25.
NPI, 1936. s36_2066, in: dpi, s. (Ed.). NPI, Svalbard.
NPI, 2015. Svalbardkartet.
Oerlemans, J., 2005. Extracting a Climate Signal from 169 Glacier Records. Science 308, 675-677.
Olsen, J., Anderson, N.J., Knudsen, M.F., 2012. Variability of the North Atlantic Oscillation over the past 5,200 years. Nature Geoscience 5, 808-812.
Osmaston, H., 2005. Estimates of glacier equilibrium line altitudes by the Area× Altitude, the Area× Altitude Balance Ratio and the Area× Altitude Balance Index methods and their validation. Quaternary International 138, 22-31.
Paasche, Ø., Løvlie, R., Dahl, S.O., Bakke, J., Nesje, A., 2004. Bacterial magnetite in lake sediments: late glacial to Holocene climate and sedimentary changes in northern Norway. Earth and Planetary Science Letters 223, 319-333.
PAGES2K, 2013. Continental-scale temperature variability during the past two millennia. Nature Geoscience 6, 339-346.
Pfeffer, W.T., Arendt, A.A., Bliss, A., Bolch, T., Cogley, J.G., Gardner, A.S., Hagen, J.-O., Hock, R., Kaser, G., Kienholz, C., 2014. The Randolph Glacier Inventory: a globally complete inventory of glaciers. Journal of Glaciology 60, 537-552.
Rasmussen, T.L., Thomsen, E., Skirbekk, K., Ślubowska-Woldengen, M., Klitgaard Kristensen, D., Koç, N., 2014. Spatial and temporal distribution of Holocene temperature

maxima in the northern Nordic seas: interplay of Atlantic-, Arctic-and polar water masses. Quaternary Science Reviews 92, 280-291.
Renssen, H., Goosse, H., Fichefet, T., Brovkin, V., Driesschaert, E., Wolk, F., 2005a. Simulating the Holocene climate evolution at northern high latitudes using a coupled atmosphere-sea ice-ocean-vegetation model. Climate Dynamics 24, 23-43.
Renssen, H., Goosse, H., Fichefet, T., Masson-Delmotte, V., Koç, N., 2005b. Holocene climate evolution in the high-latitude Southern Hemisphere simulated by a coupled atmosphere-sea ice-ocean-vegetation model. The Holocene 15, 951-964.
Risebrobakken, B., Dokken, T., Smedsrud, L.H., Andersson, C., Jansen, E., Moros, M., Ivanova, E.V., 2011. Early Holocene temperature variability in the Nordic Seas: The role of oceanic heat advection versus changes in orbital forcing. Paleoceanography 26.
Rosqvist, G.C., Schuber, P., 2003. Millennial-scale climate changes on south Georgia, southern ocean. Quaternary Research 59, 470-475.
Rubensdotter, L., Rosqvist, G., 2009. Influence of geomorphological setting, fluvial-, glaciofluvial-and mass-movement processes on sedimentation in alpine lakes. The Holocene 19, 665-678.
Røthe, T.O., Bakke, J., Vasskog, K., Gjerde, M., D'Andrea, W.J., Bradley, R.S., 2015. Arctic Holocene glacier fluctuations reconstructed from lake sediments at Mitrahalvøya, Spitsbergen. Quaternary Science Reviews 109, 111-125.
Salvigsen, O., 1979. The last deglaciation of Svalbard. Boreas 8, 229-231.
Sarnthein, M., Kreveld, S., Erlenkeuser, H., Grootes, P., Kucera, M., Pflaumann, U., Schulz, M., 2003. Centennial-to-millennial-scale periodicities of Holocene climate and sediment injections off the western Barents shelf, 75 N. Boreas 32, 447-461.
Screen, J.A., Simmonds, I., 2010. The central role of diminishing sea ice in recent Arctic temperature amplification. Nature 464, 1334-1337.
Sergeeva, L., 1983. Trace element associations as indicators of sediment accumulation in lakes, in: Meriläinen, J., Huttunen, P., Battarbee, R.W. (Eds.), Paleolimnology. Springer Netherlands, pp. 81-84.
Serreze, M.C., Barry, R.G., 2011. Processes and impacts of Arctic amplification: A research synthesis. Global and Planetary Change 77, 85-96.
Shepherd, A., Ivins, E.R., A, G., Barletta, V.R., Bentley, M.J., Bettadpur, S., Briggs, K.H., Bromwich, D.H., Forsberg, R., Galin, N., Horwath, M., Jacobs, S., Joughin, I., King, M.A., Lenaerts, J.T.M., Li, J., Ligtenberg, S.R.M., Luckman, A., Luthcke, S.B., McMillan, M., Meister, R., Milne, G., Mouginot, J., Muir, A., Nicolas, J.P., Paden, J., Payne, A.J., Pritchard, H., Rignot, E., Rott, H., Sørensen, L.S., Scambos, T.A., Scheuchl, B., Schrama, E.J.O., Smith, B., Sundal, A.V., van Angelen, J.H., van de Berg, W.J., van den Broeke, M.R., Vaughan, D.G., Velicogna, I., Wahr, J., Whitehouse, P.L., Wingham, D.J., Yi, D., Young, D., Zwally, H.J., 2012. A Reconciled Estimate of Ice-Sheet Mass Balance. Science 338, 1183-1189.
Shepherd, A., Wingham, D., 2007. Recent sea-level contributions of the Antarctic and Greenland ice sheets. science 315, 1529-1532.
Shevenell, A., Ingalls, A., Domack, E., Kelly, C., 2011. Holocene Southern Ocean surface temperature variability west of the Antarctic Peninsula. Nature 470, 250-254.
Sissons, J., 1979. Palaeoclimatic inferences from former glaciers in Scotland and the Lake District.
Ślubowska-Woldengen, M., Rasmussen, T.L., Koç, N., Klitgaard-Kristensen, D., Nilsen, F., Solheim, A., 2007. Advection of Atlantic Water to the western and northern Svalbard shelf since 17,500 calyr BP. Quaternary Science Reviews 26, 463-478.
Smith, J., 1960. Glacier problems in South Georgia. Journal of Glaciology 3, 707-714.

Snowball, I., Sandgren, P., 1996. Lake sediment studies of Holocene glacial activity in the Kårsa valley, northern Sweden: contrasts in interpretation. The Holocene 6, 367-372.
Solomina, O.N., Bradley, R.S., Hodgson, D.A., Ivy-Ochs, S., Jomelli, V., Mackintosh, A.N., Nesje, A., Owen, L.A., Wanner, H., Wiles, G.C., 2015. Holocene glacier fluctuations. Quaternary Science Reviews 111, 9-34.
Solomon, S., 2007. Climate change 2007-the physical science basis: Working group I contribution to the fourth assessment report of the IPCC. Cambridge University Press.
Stocker, T.F., Johnsen, S.J., 2003. A minimum thermodynamic model for the bipolar seesaw. Paleoceanography 18.
Stone, P., 1980. The geology of South Georgia: IV. Barff Peninsula and Royal Bay areas. British Antarctic Survey, Cambridge.
Stroeve, J., Holland, M.M., Meier, W., Scambos, T., Serreze, M., 2007. Arctic sea ice decline: Faster than forecast. Geophysical research letters 34.
Støren, E.N., Dahl, S.O., Lie, Ø., 2008. Separation of late-Holocene episodic paraglacial events and glacier fluctuations in eastern Jotunheimen, central southern Norway. The Holocene 18, 1179-1191.
Støren, E.N., Dahl, S.O., Nesje, A., Paasche, Ø., 2010. Identifying the sedimentary imprint of high-frequency Holocene river floods in lake sediments: development and application of a new method. Quaternary Science Reviews 29, 3021-3033.
Sundqvist, H., Kaufman, D., McKay, N., Balascio, N., Briner, J., Cwynar, L., Sejrup, H., Seppä, H., Subetto, D., Andrews, J., 2014. Arctic Holocene proxy climate database–new approaches to assessing geochronological accuracy and encoding climate variables. Climate of the Past Discussions 10, 1-63.
Thompson, R., Battarbee, R.W., O'Sullivan, P.E., Oldfield, F., 1975. Magnetic susceptibility of lake sediments. Limnology and Oceanography 20, 687-698.
Thornalley, D.J.R., Elderfield, H., McCave, I.N., 2009. Holocene oscillations in temperature and salinity of the surface subpolar North Atlantic. Nature 457, 711-714.
Trouet, V., Van Oldenborgh, G.J., 2013. KNMI Climate Explorer: a web-based research tool for high-resolution paleoclimatology. Tree-Ring Research 69, 3-13.
USGS, NASA, 2000. Landsat Global Land Survey, in: Esri (Ed.).
Van Daele, M., Bertrand, S., Meyer, I., Moernaut, J., Vandoorne, W., Siani, G., Tanghe, N., Ghazoui, Z., Pino, M., Urrutia, R., 2016. Late Quaternary evolution of Lago Castor (Chile, 45.6° S): Timing of the deglaciation in northern Patagonia and evolution of the southern westerlies during the last 17 kyr. Quaternary Science Reviews 133, 130-146.
Van der Bilt, W.G., Bakke, J., Vasskog, K., Røthe, T., Støren, E.N., in press. Glacier-fed lakes as paleoenvironmental archives Geology Today.
van der Bilt, W.G.M., Bakke, J., Vasskog, K., D'Andrea, W.J., Bradley, R.S., Ólafsdóttir, S., 2015. Reconstruction of glacier variability from lake sediments reveals dynamic Holocene climate in Svalbard. Quaternary Science Reviews 126, 201-218.
Van der Bilt, W.G.M., Bakke, J., Werner, J.P., Paasche, Ø., Rosqvist, G., Vatle, S.S., under review South Georgia glacier fluctuations during the past millennium reveal medieval retreat and interhemispheric Little Ice Age Quaternary Science Reviews.
Vasskog, K., Nesje, A., Støren, E.N., Waldmann, N., Chapron, E., Ariztegui, D., 2011. A Holocene record of snow-avalanche and flood activity reconstructed from a lacustrine sedimentary sequence in Oldevatnet, western Norway. The Holocene, 0959683610391316.
Vasskog, K., Paasche, Ø., Nesje, A., Boyle, J.F., Birks, H.J.B., 2012. A new approach for reconstructing glacier variability based on lake sediments recording input from more than one glacier. Quaternary Research 77, 192-204.
Wanner, H., 2014a. Holocene Climate. Global Environmental Change, 55-59.
Wanner, H., 2014b. Holocene Climate, Global Environmental Change. Springer, pp. 55-59.

Wanner, H., Beer, J., Bütikofer, J., Crowley, T.J., Cubasch, U., Flückiger, J., Goosse, H., Grosjean, M., Joos, F., Kaplan, J.O., 2008. Mid-to Late Holocene climate change: an overview. Quaternary Science Reviews 27, 1791-1828.
Wanner, H., Solomina, O., Grosjean, M., Ritz, S.P., Jetel, M., 2011. Structure and origin of Holocene cold events. Quaternary Science Reviews 30, 3109-3123.
Waters, C.N., Zalasiewicz, J., Summerhayes, C., Barnosky, A.D., Poirier, C., Gałuszka, A., Cearreta, A., Edgeworth, M., Ellis, E.C., Ellis, M., 2016. The Anthropocene is functionally and stratigraphically distinct from the Holocene. Science 351, aad2622.
Werner, J.P., Tingley, M.P., 2015. Technical Note: Probabilistically constraining proxy age–depth models within a Bayesian hierarchical reconstruction model. Climate of the Past 11, 533-545.
Werner, K., Müller, J., Husum, K., Spielhagen, R.F., Kandiano, E.S., Polyak, L., 2015. Holocene sea subsurface and surface water masses in the Fram Strait–Comparisons of temperature and sea-ice reconstructions. Quaternary Science Reviews.
Werner, K., Spielhagen, R.F., Bauch, D., Hass, H.C., Kandiano, E., 2013. Atlantic Water advection versus sea-ice advances in the eastern Fram Strait during the last 9 ka: Multiproxy evidence for a two-phase Holocene. Paleoceanography 28, 283-295.
WGMS, 1988-2011. Glacier Mass Balance Bulletin (GMBB), Biennial, Zurich.
Yuan, X., 2004. ENSO-related impacts on Antarctic sea ice: a synthesis of phenomenon and mechanisms. Antarctic Science 16, 415-425.
Østrem, G., Liestøl, O., 1964. Glaciological investigations in Norway 1963. Norsk Geografisk Tidsskrift 18, 281-340.

# List of publications

**Paper 1**: Van der Bilt, W.G., Bakke, J., Vasskog, K., Røthe, T., Støren, E.N., in press. Glacier-fed lakes as paleoenvironmental archives. Geology Today.

**Paper 2**: van der Bilt, W.G.M., Bakke, J., Balascio, N.L., 2015. Mapping sediment–landform assemblages to constrain lacustrine sedimentation in a glacier-fed lake catchment in northwest Spitsbergen. Journal of Maps, 1-9.

**Paper 3**: van der Bilt, W.G.M., Bakke, J., Vasskog, K., D'Andrea, W.J., Bradley, R.S., Ólafsdóttir, S., 2015. Reconstruction of glacier variability from lake sediments reveals dynamic Holocene climate in Svalbard. Quaternary Science Reviews 126, 201-218.

**Paper 4**: van der Bilt, W.G.M., William J. D`Andrea, Jostein Bakke, Johannes P. Werner and Marthe Gjerde, *Prepared for submission to Quaternary Science Reviews.* Alkenone-based reconstructions reveal four-phase Holocene temperature evolution for High Arctic Svalbard

**Paper 5**: van der Bilt, W.G.M., Bakke, J., Werner, J.P., Paasche, Ø., Rosqvist, G., Vatle, S.S., *under review*. South Georgia glacier fluctuations during the past millennium reveal medieval retreat and inter-hemispheric Little Ice Age, Quaternary Science Reviews.

II

# Paper 2: Mapping sediment-landform assemblages to constrain lacustrine sedimentation in a glacier-fed lake catchment in northwest Spitsbergen

Willem G.M. van der Bilt[a b] , Jostein Bakke[a b] & Nicholas L. Balascio[c]

[a] Department of Earth Science, University of Bergen, Allégaten 41, 5020, Bergen, Norway

[b] Bjerknes Centre for Climate Research, Allégaten 55, 5007, Bergen, Norway

[c] Lamont-Doherty Earth Observatory, Columbia University, Palisades, 10964, New York, USA

*Key words: Spitsbergen; mapping; sediment transport; glacier-fed lake; paraglacial modification*

## Abstract

Changes in the deposition of fine-grained rock-flour in glacier-fed lakes reflect glacier variability. This meltwater-driven signal is, however, often overprinted by other processes. To constrain the signature of lacustrine sedimentation, we mapped the catchment of glacier-fed Lake Hajeren in northwest Spitsbergen, identifying sediment sources and linking them to surface processes. To this end, we employed a combined approach of aerial image interpretation and field mapping. Our map comprises sediment-landform assemblages commonly found in pro-, peri- and paraglacial landsystems on Spitsbergen, including weathered moraines outboard Little Ice Age limits. Based on the presented map, we argue that mass-wasting does not directly impact lake sedimentation. Also, due to the scarcity of fines in historical

glacial deposits, we suggest that modified glacigenic sediments only briefly affect a recorded glacier signal, following retreat. These findings highlight the value of geomorphological maps as tools to constrain catchment processes, improving the interpretation of lake sediment records.

## Introduction

Glaciers are highly sensitive to climate change as demonstrated by their rapid retreat in response to current warming (WGMS, 1988-2011). Apart from geomorphological evidence, changes in glacier size are continuously recorded by variations in erosion rates and the flux of fine-grained (1-63 μm) minerogenic rock flour into distal glacier-fed lakes (Karlén, 1981; Leemann & Niessen, 1994). As such, sedimentary archives extracted from these lakes are widely used proxies of past climate variability (Bakke et al., 2010; Guyard, Chapron, St-Onge, & Labrie, 2013; McKay & Kaufman, 2009).

However, sedimentation in glacier-fed lakes is frequently affected by other sediment sources that leave a similar imprint in the lacustrine sediment record (Rubensdotter & Rosqvist, 2009; Vasskog et al., 2011). These commonly include reworked glacigenic sediments that have been modified by non-glacial processes (Ballantyne, 2002; Dahl, Bakke, Lie, & Nesje, 2003). In addition to such paraglacial modification (Church & Ryder, 1972), mass-wasting could overprint the signature of a glacier signal (Vasskog et al., 2011). The impact of these processes should be understood to ensure an accurate reconstruction of a glacier variability (Jansson, Rosqvist, & Schneider, 2005; Rubensdotter & Rosqvist, 2009).

Here, we present a 1:8000 scale geomorphological map of the glaciarized catchment of lake Hajeren in northwest Spitsbergen (79°15'N: 11°31'E) (Figures 1 and 2), based on aerial photographs and ground-truthing. Mapping enables us to identify sediment sources and transport mechanisms that may affect the lacustrine sediment record (Carrivick & Tweed, 2013). We aim to assess the relationship between the morphology of mapped landforms and their genesis to gain a process-based understanding of sediment transport in the catchment. This information will help

validate the robustness of a separately published glacier activity reconstruction, based on sediments from Lake Hajeren (van der Bilt et al., 2015).

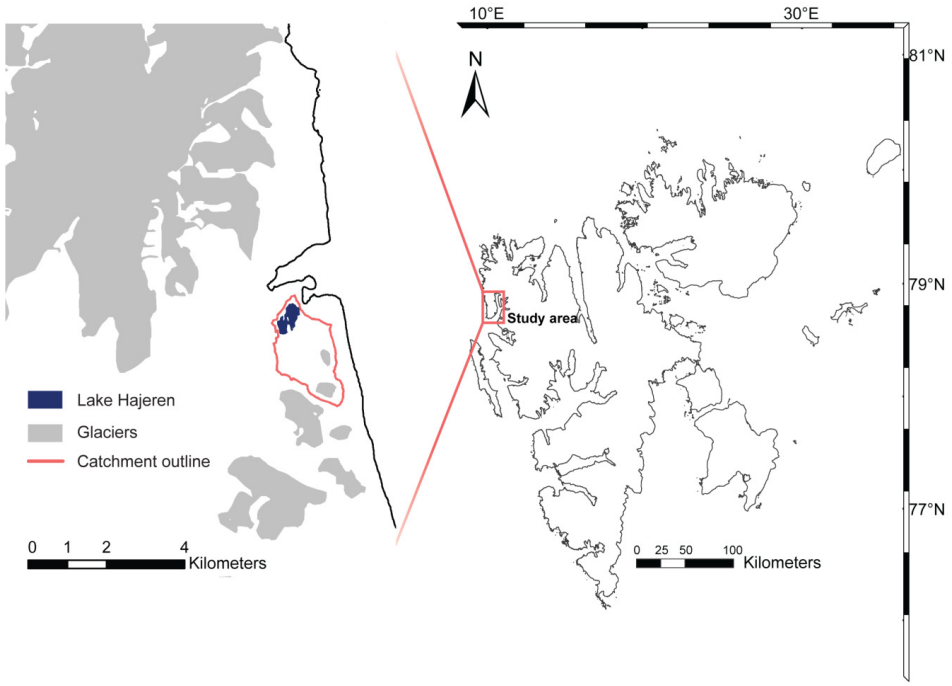


*Fig. 1. Map showing the Svalbard archipelago and an inset of the study area in the Hajeren catchment. Lake Hajeren is indicated in blue in the left panel, while present-day glacier extent is shown in grey (NPI, 2015).*

## Study site

The 2.96 km$^2$ Hajeren watershed, mapped for this study, is located on the Mitra peninsula in northwest Spitsbergen (79°15'N: 11°31'E) (Figures 1 and *2*).The catchment is unvegetated and covered by unconsolidated sediments and Grenvillian age schist bedrock belonging to the Signehamna formation (Krasilščikov, 1975; Ohta et al., 2002). The Mean Annual Air Temperature (MAAT) is approximately -5 °C (Førland, Benestad, Hanssen-Bauer, Haugen, & Skaugen, 2012) and the area falls within the zone of continuous permafrost (Nelson, Anisimov, & Shiklomanov, 2002). At present, two small glaciers occupy cirques in the Southeast sector of the Hajeren

catchment, the North Glacier (0.08 $km^2$) and South Glacier (0.17 $km^2$). Both glaciers drain into Lake Hajeren in the northwest sector of the catchment. Aerial photographs show the glaciers of the Hajeren catchment reached a historical maximum during the early 20th century culmination of the Little Ice Age (LIA) (NPI, 1936), like most Svalbard glaciers (Glasser & Hambrey, 2014; Hagen, Melvold, Pinglot, & Dowdeswell, 2003; Salvigsen & Høgvard, 2006). Also, documented front positions show that the North and South glaciers have been retreating since (NPI, 2015).

# Map compilation

## Mapping methods

The presented map was compiled using a combination of aerial image interpretation and field mapping. The former was carried out using a 195.8 megapixel aerial photograph from the Norwegian Polar Institute (NPI) with a 40-50 cm ground sampling distance, taken with a Microsoft Vexcel UltraCam-Xp in July 2009 (NPI, 2009). This image was provided in a digital .tiff format and was neither ortho- nor georectified. Also, the image was not supplied with a set of Rational Polynomial Coefficients (RPCs) and could therefore not be readily orthorectified (Faste Aas, pers. Comm.). Instead, to put the file into a known coordinate system, it was georeferenced, establishing tie-points with GIS data of the 2009 outline of lakes and glaciers as well as a 20m Digital Elevation Model (DEM), all provided by the NPI (NPI, 2013, 2014). This projection was later verified against field-logged Ground Control Points (GCPs), recorded with a handheld GPS at easily identifiable features.

The 2009 aerial photograph was geo-rectified using the georeferencing toolbar in ESRI ArcMap 10.2, applying a 1st order polynomial transformation. To this end, we selected 18 control points on polygons of Lake Hajeren and both North and South Glaciers from 2009 (NPI, 2014), projected to UTM zone 33N on the WGS84 ellipsoid. .

Next, to correct for distortive effects of catchment relief, we selected additional summit control points on a 20m resolution Digital Elevation Model (DEM) of

Svalbard. We then draped the rectified aerial photograph over the 20m DEM in ArcScene 10.2 to highlight topographical features (Figure 2). We subsequently used this projection for a preliminary survey of the sediment cascade between glaciers and lake, identifying sediment sources that may affect the lacustrine sediment record.

Mapping was mostly carried out during a 2-day field survey on 5 and 6 September 2014. As the study area falls outside existing Differential GPS (DGPS) networks, we used a regular Garmin GPSMAP 62S with an indicated 5m accuracy. Even though the outlined pre-fieldwork survey enabled us to target our field effort, some sections could not be mapped on site. These solely concerned high-lying steep terrain above 250 m a.s.l., either covered by bedrock, weathered material, the upper reaches of talus cones or glacier ice. These easily identifiable units were mapped using the discussed georectified 2009 aerial photograph. As outlined, this projection was ground-truthed prior to mapping, using GPS-logged GPCs of mapped and photographed features (Figure 4). Based on the correspondence between these datasets, we argue that remaining projection errors fall within the uncertainty of the GPS device.

## Map production

The presented map was produced in ArcMap 10.2 and Adobe Illustrator CS6. First, GPS tracks and waypoints of field-logged landforms were imported into ArcMap 10.2, converting the former to points and the latter to polylines or polygons. Information on glacier and lake extent was taken from a NPI GIS database (NPI, 2014). To delineate the Hajeren catchment, we applied the hydrology toolset in the ArcGIS 10.2 spatial analyst toolbox. Aerial-mapped landforms were traced using the freehand construction tool on ArcMap 10.2`s editor toolbar. For this purpose, shadowed sections of the image were first processed using the shadows and highlights adjustment in Adobe Photoshop CS6. To warrant compatibility with other regional maps, features were drawn following the standardized symbology of the Geological Survey of Norway (NGU)(Bergstrøm, Reite, Sveian, & Olsen, 2001).In the text, we occasionally deviate from this generalized scheme to provide more specific morphological details. The ensuing map was displayed on an A3 format data

frame and overlain by a 100m kilometre-rounded UTM grid, using a 1:8000 reference scale and then exported to Adobe illustrator CS6 for formatting.

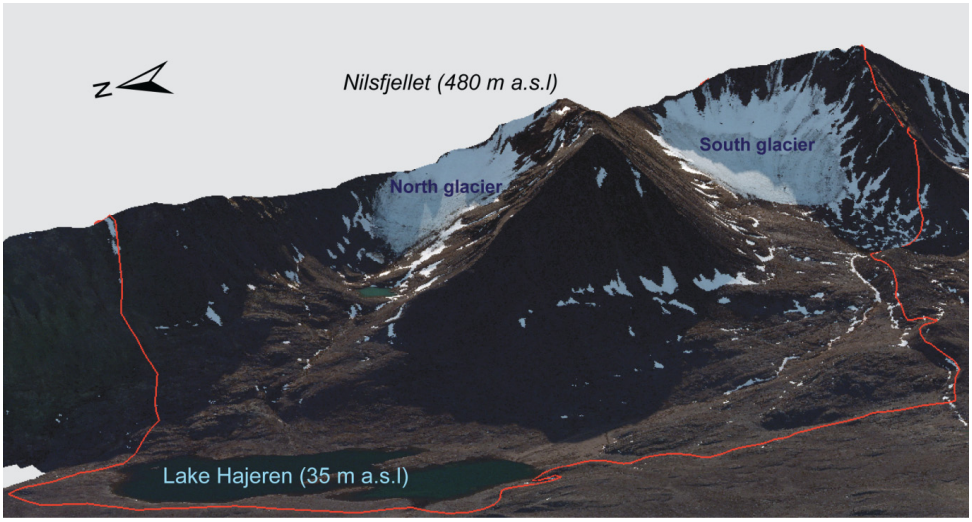


*Fig. 2. Oblique view of the Hajeren catchment towards the west (NPI, 2009, 2013). North as well as South glaciers are indicated and the catchment outline is delineated by a red line.*

## Mapped sediment-landform assemblages

In total, we identified 29 separate landforms and features on the presented map. The catchment is dominated by expanses of highly weathered material, concentrated around Lake Hajeren. These often appear modified by periglacial processes as demonstrated by the presence of polygonal ground, solifluction lobes and frost-shattered surfaces. Glacier forelands are predominantly covered by tills and (marginal) moraine deposits with frequent occurrences of large boulders and kettle holes. Fan-shaped mass movement deposits are located on the steeper mountain sides and often associated with rock glaciers. Glaciofluvial deposits are found in forelands and valley floors as floodplains (Sandurs). Lacustrine deposits are concentrated around Lake Hajeren as well as a small lake found in front of the North glacier. Catchment hydrology, which plays a vital role sediment transport, as well as weathered surfaces and exposed bedrock surfaces are also indicated on our map. Following e.g. Evans, Twigg, and Orton (2010), we categorized the surficial geology

of the catchment into sediment-landform assemblages to allow discussion of their genesis and their role in the catchment sediment cascade ("discussion").

## Till and moraines

Marginal moraines are found fronting both North and South glaciers and were grouped into Stage 1 and 2 deposits. However, stage 1 deposits were solely observed at the North Glacier, while Stage 2 deposits are most prominent here (Figure 3).

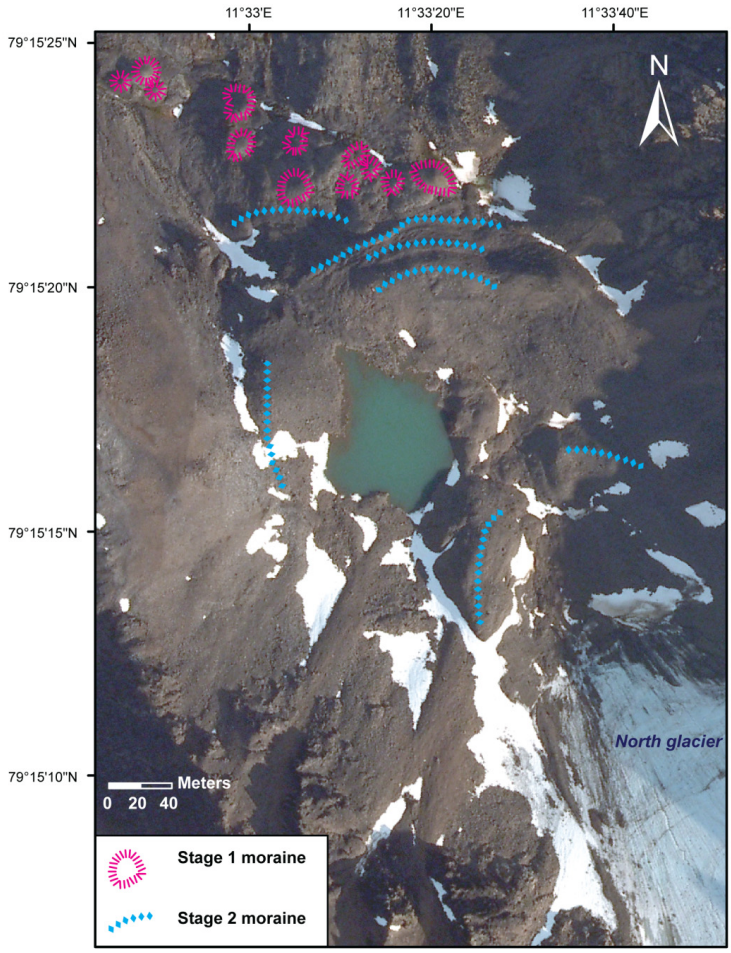


***Fig. 3**. A close-up of the foreland of the North glacier, showing the discussed Stage 1 and 2 moraine deposits, with an aerial image in the background (NPI, 2009).*

### *North Glacier*

Stage 1 moraines were deposited as a complex of mounds. In total, we discerned 12 westward facing 10-20 m high mounds, mainly comprising boulders (Figure 3). Extensive frost-shattering and lichen-coverage indicates heavy weathering. The most distal of these lies approximately 140 meters in front of Stage 2 deposits. Also, both deposits intersect at around 177 m a.s.l. (Figure 4(A)). Stage 2 moraines in front of the North glacier comprise a moraine-mound complex (Glasser & Hambrey, 2014; Hambrey, Huddart, Bennett, & Glasser, 1997), consisting of marginal composite ridges that are transversely aligned with the glacier front and not uniformly pronounced. The outer 50 m of the system is characterized by small-scale ridges with ±1 m high crests (Figure 4(B)). The inner part is composed of 3 large-scale 40 m high ridges that are strewn with frequent large boulders. The gravelly material of the innermost ridge is draped with silt and appears recently exposed. Fresh deposits, inboard the North Glacier`s Stage 2 moraines, comprise a series of near conical mounds, oriented parallel to the glacier front. Based on large amounts of supraglacial debris in combination with abundant unconsolidated material and the presence of kettle holes, we interpreted these as ice-cored moraines (mapped as `till`). Finally, a pair of fairly symmetrical rounded ridges was identified along both sides of the glacier. These were interpreted as lateral moraines, smoothed by material delivered from the slopes surrounding the glacier.

### *South Glacier*

The foreland of the South Glacier is delineated by an undulating boulder-strewn Stage 2 moraine ridge (Figure 4(C)). Additionally, a pronounced 30 m high lateral moraine flanks the South side of the glacier. A ridge of bouldery diamict, interpreted as a frontal moraine, is nudging the massive lateral moraine complex of adjacent Karlbreen. The foreland itself is covered by ±2 m high mounds of bouldery diamict. Based on the high concentration of supra-glacial debris on the glacier front, we suggest these are ablation moraines, following the definition of Bennett and Glasser (2009). In general, moraines outboard of the present South glacier are much less pronounced than those seen at the North Glacier (Figure 4(C)).

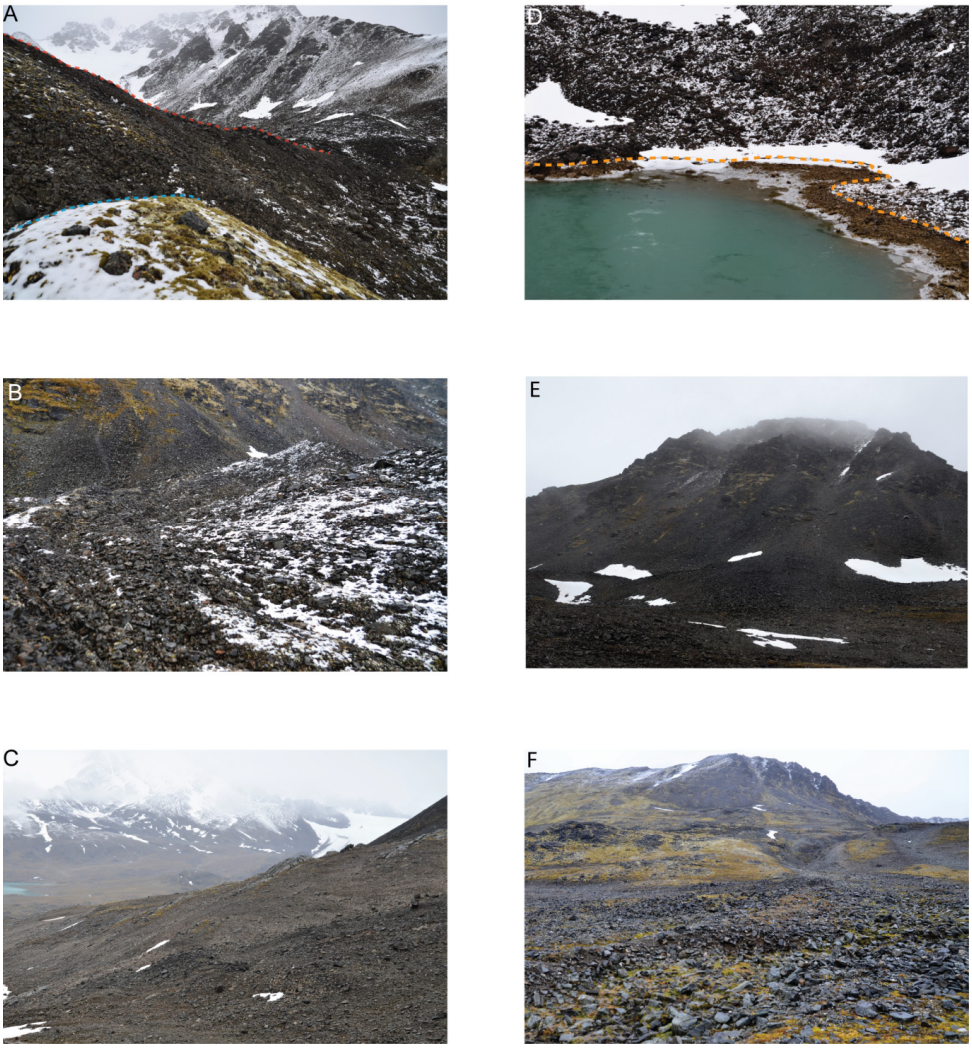


***Fig. 4**. Field pictures of A) the contact between Stage 1(blue) and 2 (red) deposits at the North glaciers (facing east), B) composite ridges on Stage 2 moraines in front of North glacier (facing North), C) Stage 2 moraines of the South glacier (view towards the northwest), D) ice-contact lake fronting the North glaciers with exposed shorelines indicated by the yellow dashed line (facing south), E) snow-covered rock glacier termini and associated talus fans (view towards the northeast) and F) in-active outwash plain draining the North Glacier (facing east).*

## Lacustrine deposits

In the field, old lake shorelines, marked by sets of pebbly pavement features, were identified ± 1.5 m above contemporary water level at Hajeren. These run parallel to the present-day shore and can be discerned around most of the lake`s perimeter. Their presence is accentuated by visible differences in vegetation cover and the degree of weathering. Areas between former and present shore were mapped as lacustrine deposits. Along the southwest of Lake Hajeren, we mapped a bouldery spillway which drains the lake. The elevation of this presently dry outlet corresponds to that of the set of old shorelines. Finally, a 600 m2 proglacial lake sits between the North Glacier and its Stage 2 moraines (Figure 4(D)). Based on the interpretation of the surrounding terrain as ice-cored deposits, this lake is described as an ice-contact lake after Ashley (1995). Silt-draped exposed shorelines suggest a recent drop in water level.

## Periglacial features

Large swaths of mapped weathered surfaces in the Hajeren catchment are covered by periglacial features, mostly patterned ground features. These predominantly consist of contiguous sorted polygons with an average diameter of ± 1 m. Frost-shattering of weathered bouldery deposits is mainly restricted to deposits of former (in-active) meltwater channels (c.f. “glaciofluvial deposits”). Solifluction lobes are restricted to a moderately gentle (16.5°) exposed southwest facing slope in the southern part of the watershed. Here, 10-30 m wide lobes group together in sheets along a stepped profile on the well-vegetated soil that characterize the area. We also classify the rock-glaciers of the Hajeren watershed as periglacial features due to their previously acknowledged association with upslope colluvium (Barsch, 1977; Johnson, 1974). Rock-glaciers in the Hajeren catchment share a set of morphological characteristics. Fronts terminate around the 225 m contour line, are approximately 15 m high and originate from individual talus cones (Figure 4(E)). As such, only termini are mapped as rock glaciers. Moreover, all termini were snow covered both on aerial photographs and in the field (Figure 4(E)). Judging by steep snouts and unvegetated instable

surfaces, we assume that these rock glaciers are active (Martin & Whalley, 1987). This is also supported by the fact that the mapped area falls well within the zone of continuous permafrost (Nelson, Anisimov, & Shiklomanov, 2002). Surface material is dominated by open angular boulder-sized debris while snow is concentrated in voids (Martin & Whalley, 1987). Finally, all mapped rock glaciers have a south-westerly aspect to the leeside of prevailing easterly winds (Beine, Argentini, Maurizi, Mastrantonio, & Viola, 2001).

## Slope deposits

The stratigraphy of slope deposits could not be investigated in full detail during our field survey. Hence, we were not able to distinguish between processes of downslope wasting with certainty and grouped these deposits on our map as mass-movement deposits. Slope deposits are mostly found below steep rock fall areas where periglacial processes such as frost wedging may detach bedrock. Here, colluvium accumulates near the rock fall shadow and mantles concave slopes in lobate shaped talus sheets. All mapped fans terminate far from the shores of Lake Hajeren. Often, these fans comprise fining upward sequences with a downslope concentration of large boulders known as out-runners (Blikra & Nemec, 1998). In general, the surface of slope deposits appears fresh compared to surrounding deposits, suggesting regular activation. This notion is supported by the previously mentioned large supply of supraglacial debris as both glaciers are flanked by colluvial fans. Based on their consistent co-occurrence (Figure 4(E)), we suggest that talus cones extend into downslope rock glaciers following Ballantyne (2002).

## Glaciofluvial deposits

In the Hajeren catchment, glaciofluvial deposits are concentrated in the foreland of the South Glacier and on the valley floor. At both glaciers, these glacial and pro-glacial systems are connected by high-gradient channels that cross the steep terrain between cirques and valley floor. Here, meltwater has carved 20m deep ravines into the erosive marbles found in the upper part of the catchment (> 140 m a.s.l.). Moreover, the channel coming from the South Glacier has cut a glaciofluvial scarp

into the moraine complex of Karlbreen, bordering the Hajeren watershed to the west. At the South Glacier, outwash emerges from a single supra-glacial channel that has incised a laterally constrained (± 30 m wide) ice-proximal fan into the adjacent till deposits. In contrast, no outwash emerges in the foreland of the North Glacier. From both cirques, Sandurs radiate out onto the valley floor towards the shores of Lake Hajeren. The southernmost plain is particularly extensive, with a width of 130 m at its distal end. Up-valley, it develops into a valley Sandur, hemmed in by mountainsides. Cross-cutting relations are apparent at its southern edge, where fluvial erosion cut into severely frost-shattered weathered deposits with traces of currently in-active meltwater channels. Similar channel deposits are found adjacent to the previously discussed Stage 1 mounds in front of the North Glacier. The gently sloping surface (2.75°) of the southern Sandur is covered by an alternation of gravelly bars and both active as well as in-active pebbly braided meltwater channels. The Sandur in the northern part of the catchment is smaller and characterized by coarser material (pebbles-boulders), suggesting a high energy level during deposition. Active meltwater channels appear over-dimensioned in relation to present flow. This is also attested by a minor inactive outwash plain that branches off from the main Sandur (Figure 4(F)). These deposits are frost-shattered and lichen-covered, indicating prolonged inactivity (Figure 4(F)).

## Discussion

Following the identification of sediment-landform assemblages, we will use the ensuing geomorphological map to assess sediment delivery to Lake Hajeren. As previously stressed, a process-based understanding of landforms is critical to understand the signature of lacustrine sedimentation in glacier-fed sites (Carrivick & Tweed, 2013; Dahl et al., 2003). In the case of Lake Hajeren, this insight will help evaluate the robustness of the separately published glacier activity reconstruction, based on the lacustrine sediment record (van der Bilt et al., 2015).

The observed difference in the degree of weathering between Stage 1 and Stage 2 moraines suggests that glacial erosion has repeatedly affected sedimentation in the

catchment. Based on the discussed 1936 aerial photograph (NPI, 1936), as well as a similar relation to the present ice extent as nearby glacier systems (Evans, Strzelecki, Milledge, & Orton, 2012; Hambrey et al., 2005; Hodson et al., 1998; Røthe et al., 2015), Stage 2 moraines are assumed to have been deposited during the LIA Although chronological control is lacking, a high degree of weathering and deposition outboard of Stage 2 deposits indicates that the Stage 1 moraines at the North Glacier represent a Holocene glacier maximum that predates the LIA. Based on a minimum age of 6.7 ka BP for an ice-cored moraine fronting adjacent Karlbreen (Røthe et al., 2015), we propose an Early Holocene age.

The combination of composite ridges and ice-cored moraines, observed at Stage 2 deposits fronting the North Glacier, often indicate glacial deformation of permafrozen material on Svalbard (Boulton, Van der Meer, Beets, Hart, & Ruegg, 1999; Etzelmüller & Hagen, 2005). Based on this landsystem signature, we infer erosive polythermal basal conditions for the North Glacier with temperate ice and a frozen snout as described for Spitsbergen glaciers by e.g. Evans et al. (2012) and Hambrey et al. (2005). The observed composite ridges are grouped in small- and large-scale features. We suggest that the former are the result of seasonal glacier fluctuations whereas the latter reflect persistent glacier advances following Bennett and Glasser (2009). Based on the dominance of supraglacial meltwater drainage (Hodson et al., 1998) and a lack of glacigenic sediments (Fitzsimons, 2003), we tentatively infer a non-erosive cold-based regime for the South Glacier. Though geomorphological evidence is lacking, we cannot exclude the possibility of a regime shift due to recent thinning as reported by Björnsson et al. (1996). To conclude, we argue that only the North Glacier is capable of producing significant amounts of glacigenic sediments through glacial erosion.

Large areas of the catchment were mapped as periglacial deposits, mainly comprising patterned ground, particularly around Lake Hajeren. Patterned ground exclusively consists of polygonal ground, suggesting formation by lateral squeezing and confinement of rock material as suggested by Kessler and Werner (2003). In contrast, more dynamic periglacial features (i.e. solifluction lobes and rock glaciers) are

concentrated in steeper sections of the catchment, particularly in the forelands of both glaciers. The same is true for associated slope deposits ("slope deposits"). We argue that the combination of comparatively stable features around the lake and dynamic deposits in steeper sections shields the lacustrine record against mass-wasting processes.

Our map demonstrates that glacifluvial drainage couples glacial, pro-glacial and lacustrine environments in the catchment. We therefore argue that glaciofluvial transport is the dominant sediment delivery pathway to Lake Hajeren. In addition to the transfer of glacial and pro-glacial sediments, streams also act as agents of erosion, cutting through bedrock in the steep transition between foreland and Sandur of the North Glacier`s debris cascade (Benn & Evans, 2014).

Moreover, meltwater streams rework older glacigenic deposits in the catchment. Near the South Glacier, for example, meltwater incises diamict deposits. The potential for paraglacial reworking is particularly great for the fresh (post)-LIA sediments stored in the Stage 2 foreland of the erosive North Glacier. However, fine-grained reworked deposits, which may leave a similar imprint in the lacustrine sediment record as fresh glacial flour (Jansson et al., 2005; Rubensdotter & Rosqvist, 2009), are scarce in the catchment ("till and moraines"). As both glaciers were more active in the recent past (NPI, 1936), this observation favours a rapid exhaustion of fine-grained glacigenic sources, in line with the findings of Harbor and Warburton (1993) for similar small catchments. Still, we cannot rule out that postglacial processes, like melt-out of the ice-cored moraines near the North Glacier, may remobilize glacigenic sediments on longer timescales as suggested by Etzelmüller and Hagen (2005). However, following Leonard (1997), we argue that the sediment record of Lake Hajeren is mainly affected by paraglacial modification during transition phases subsequent to retreat or advance.

The observed presence of in-active and over-dimensioned meltwater channels and Sandur sections, in combination with raised old lake shorelines, is indicative of past hydrological change. Previous monitoring studies in glaciarized catchments have demonstrated a strong correlation between glacier melt and run-off (Leemann &

Niessen, 1994; Liermann, Beylich, & van Welden, 2012). Based on the large degree of past glacier activity, indicated by Stage 1 and 2 moraines, we tentatively attribute these inferred episodic discharge changes to glacier variability. Nevertheless, we cannot exclude the possibility that these features result from channel migration as suggested by Williams and Rust (1969), redepositing glacifluvial deposits in the process. Moreover, fill/drain cycles of ephemeral lakes similar to the ice-contact lake fronting the North glacier, may have contributed to run-off pulses, in addition to trapping glacial flour (Carrivick & Tweed, 2013).

## Conclusions

The presented map enables us to gain a process-based understanding of sedimentation in the Hajeren catchment. This, in turn, helps constrain the impact of mass-wasting and paraglacial modification on the lacustrine sediment record, validating the findings of van der Bilt et al. (2015). In summary, we identify glaciofluvial transport as the dominant sediment delivery pathway in the catchment, coupling lake Hajeren and the catchment`s main depositional zones in the forelands of North and South glaciers. Most observed landform-assemblages are solely found in these areas, as shown on our map. In contrast, the area around Lake Hajeren is covered by gently sloping expanses of weathered material, minimizing the impact of mass-wasting on the lacustrine sediment record. Based on its discussed landsystem signature, we claim that the North Glacier is the dominant producer of glacigenic sediments in the catchment. However, due to an observed lack of fines, we propose a short paraglacial period, characteristic for comparable small catchments (Harbor & Warburton, 1993). Following Leonard (1997), we argue that paraglacial modification only affects the lacustrine record briefly after glacier retreats or advances. In conclusion, his study underlines the value of geomorphological mapping as a tool to constrain lacustrine sedimentation. Similar exercises could therefore contribute to the robustness of attendant lake sediment studies.

## Software

Mapping was carried out using ESRI ArcMap 10.2. In addition to the editor, we used both georeferencing and spatial analyst toolbars. The resulting map was edited using Adobe illustrator CS6.

## Acknowledgments

This work was supported by the Norwegian Research Council Arctic Field Grant, awarded to WGMB, NLB and JB. We would like to thank Raymond Bradley, William D`Andrea, Greg de Wet, Sædís Ólafsdóttir, Marthe Gjerde and Torgeir Røthe for their assistance in the field. Finally, WGMB would like to express his gratitude for Harald Faste Aas at the NPI for providing aerial photographs of the study area.

## Map design

For the presented map, we used symbology, colour coding as well as fonts (points) provided by the Norwegian Geological Survey (NGU) as the study area is part of Norway (Bergstrøm et al., 2001). By doing so, we hope to increase compatibility with available maps. Projected base layers such as contours, glacier extent, lakes and sea, in addition to the aerial photograph used for mapping (NPI, 2009), have been provided by the Norwegian Polar Institute (NPI, 2015). We have drawn our map on an A3-sized data frame, using a 1:8000 scale, so that smaller and closely spaced features remain visible on print. In order to emphasize glacier shape and relief, we interpolated 5m contours for the discussed North and South glaciers, using the 20m Digital Elevation Model (DEM) provided by the Norwegian Polar Institute (NPI, 2013). Using the same DEM, we defined the boundary of the studied catchment, applying the fill, calculate flow direction and basin commands from ESRI`s hydrology tools. Mapped features have either been drawn using GPS tracks taken in the field or the aerial photograph mentioned before. To this end, we used the freehand and polygon tools from ArcMap`s editing toolbar to create (point)-lines and polygons, respectively. Different features have been organized in ArcMap in group

layers: points, lines and polygons. Finally, graticules at are shown on the map of our study measure 1 $km^2$.

## References

Ashley, G. (1995). Glaciolacustrine environments. Glacial Environments, 1, 417-444.
Bakke, J., Dahl, S. O., Paasche, Ø., Riis Simonsen, J., Kvisvik, B., Bakke, K., & Nesje, A. (2010). A complete record of Holocene glacier variability at Austre Okstindbreen, northern Norway: an integrated approach. Quaternary Science Reviews, 29(9), 1246-1262.
Ballantyne, C. K. (2002). Paraglacial geomorphology. Quaternary Science Reviews, 21(18), 1935-2017.
Barsch, D. (1977). Nature and importance of mass-wasting by rock glaciers in alpine permafrost environments. Earth Surface Processes, 2(2-3), 231-245.
Beine, H., Argentini, S., Maurizi, A., Mastrantonio, G., & Viola, A. (2001). The local wind field at Ny-Å lesund and the Zeppelin mountain at Svalbard. Meteorology and Atmospheric Physics, 78(1-2), 107-113.
Benn, D., & Evans, D. J. (2014). Glaciers and glaciation: Routledge.
Bennett, M. M., & Glasser, N. F. (2009). Glacial geology: ice sheets and landforms: John Wiley & Sons.
Bergstrøm, B., Reite, A., Sveian, H., & Olsen, L. (2001). Feltrutiner, kartleggingsprinsipper og standarder for kvartærgeologisk kartlegging-løsmassekartlegging ved NGU. Norges geologiske undersokelse Internal Report 2001.018.
Björnsson, H., Gjessing, Y., Hamran, S.-E., Hagen, J. O., Liestøl, O., Pálsson, F., & Erlingsson, B. (1996). The thermal regime of sub-polar glaciers mapped by multi-frequency radio-echo sounding. Journal of Glaciology, 42(140), 23-32.
Blikra, L. H., & Nemec, W. (1998). Postglacial colluvium in western Norway: depositional processes, facies and palaeoclimatic record. Sedimentology, 45(5), 909-960.
Boulton, G., Van der Meer, J., Beets, D., Hart, J., & Ruegg, G. (1999). The sedimentary and structural evolution of a recent push moraine complex: Holmstrømbreen, Spitsbergen. Quaternary Science Reviews, 18(3), 339-371.
Carrivick, J. L., & Tweed, F. S. (2013). Proglacial lakes: character, behaviour and geological importance. Quaternary Science Reviews, 78(0), 34-52. doi: http://dx.doi.org/10.1016/j.quascirev.2013.07.028
Church, M., & Ryder, J. M. (1972). Paraglacial sedimentation: a consideration of fluvial processes conditioned by glaciation. Geological Society of America Bulletin, 83(10), 3059-3072.
Dahl, S. O., Bakke, J., Lie, Ø., & Nesje, A. (2003). Reconstruction of former glacier equilibrium-line altitudes based on proglacial sites: an evaluation of approaches and selection of sites. Quaternary Science Reviews, 22(2), 275-287.
Etzelmüller, B., & Hagen, J. O. (2005). Glacier-permafrost interaction in Arctic and alpine mountain environments with examples from southern Norway and Svalbard. Geological Society, London, Special Publications, 242(1), 11-27.
Evans, D. J. A., Strzelecki, M., Milledge, D. G., & Orton, C. (2012). Hørbyebreen polythermal glacial landsystem, Svalbard. Journal of Maps, 8(2), 146-156. doi: 10.1080/17445647.2012.680776
Evans, D. J. A., Twigg, D. R., & Orton, C. (2010). Satujökull glacial landsystem, Iceland. Journal of Maps, 6(1), 639-650. doi: 10.4113/jom.2010.1129

Fitzsimons, S. J. (2003). Ice-marginal terrestrial landsystems: polar continental glacier margins. Glacial Landsystems. Arnold, London, 89-110.
Glasser, N., & Hambrey, M. J. (2014). Ice-marginal terrestrial landsystems: Svalbard polythermal glaciers. In D. Evans (Ed.), Glacial Landsystems (pp. 24). Florence, KY, USA: Taylor & Francis.
Guyard, H., Chapron, E., St-Onge, G., & Labrie, J. (2013). Late-Holocene NAO and ocean forcing on high-altitude proglacial sedimentation (Lake Bramant, Western French Alps). The Holocene.
Hambrey, M. J., Huddart, D., Bennett, M. M., & Glasser, N. F. (1997). Genesis of 'hummocky moraines' by thrusting in glacier ice: evidence from Svalbard and Britain. Journal of the Geological Society, 154(4), 623-632.
Hambrey, M. J., Murray, T., Glasser, N. F., Hubbard, A., Hubbard, B., Stuart, G., . . .
Kohler, J. (2005). Structure and changing dynamics of a polythermal valley glacier on a centennial timescale: Midre Lovénbreen, Svalbard. Journal of Geophysical Research: Earth Surface (2003–2012), 110(F1).
Harbor, J., & Warburton, J. (1993). Relative rates of glacial and nonglacial erosion in alpine environments. Arctic and Alpine Research, 1-7.
Hodson, A., Gurnell, A., Tranter, M., Bogen, J., Hagen, J. O., & Clark, M. (1998). Suspended sediment yield and transfer processes in a small High-Arctic glacier basin, Svalbard. Hydrological Processes, 12(1), 73-86.
Jansson, P., Rosqvist, G., & Schneider, T. (2005). Glacier fluctuations, suspended sediment flux and glacio-lacustrine sediments. Geografiska Annaler: Series A, Physical Geography, 87(1), 37-50.
Johnson, P. G. (1974). Mass movement of ablation complexes and their relationship to rock glaciers. Geografiska Annaler. Series A. Physical Geography, 93-101.
Karlén, W. (1981). Lacustrine Sediment Studies. A Technique to Obtain a Continous Record of Holocene Glacier Variations. Geografiska Annaler. Series A. Physical Geography, 273-281.
Kessler, M., & Werner, B. (2003). Self-organization of sorted patterned ground. science, 299(5605), 380-383.
Leemann, A., & Niessen, F. (1994). Varve formation and the climatic record in an Alpine proglacial lake: calibrating annually-laminated sediments against hydrological and meteorological data. The Holocene, 4(1), 1-8.
Leonard, E. M. (1997). The relationship between glacial activity and sediment production: evidence from a 4450-year varve record of neoglacial sedimentation in Hector Lake, Alberta, Canada. Journal of Paleolimnology, 17(3), 319-330.
Liermann, S., Beylich, A. A., & van Welden, A. (2012). Contemporary suspended sediment transfer and accumulation processes in the small proglacial Sætrevatnet sub-catchment, Bødalen, western Norway. Geomorphology, 167–168(0), 91-101. doi: http://dx.doi.org/10.1016/j.geomorph.2012.03.035
Martin, H. E., & Whalley, W. B. (1987). Rock glaciers part 1: rock glacier morphology: classification and distribution. Progress in Physical Geography, 11(2), 260-282.
McKay, N. P., & Kaufman, D. S. (2009). Holocene climate and glacier variability at Hallet and Greyling Lakes, Chugach Mountains, south-central Alaska. Journal of Paleolimnology, 41(1), 143-159.
Nelson, F., Anisimov, O., & Shiklomanov, N. I. (2002). Climate change and hazard zonation in the circum-Arctic permafrost regions. Natural Hazards, 26(3), 203-225.
NPI. (1936). s36_2066. In s. dpi (Ed.). Svalbard: NPI.
NPI. (2009). Aerial photograph, ID: 13822/730. In 13822 (Ed.), (Vol. 310 mb): Norwegian Polar Institute

NPI. (2013). S100 terrengmodell Svalbard 20*20 m.
NPI (Cartographer). (2014). Kartdata Svalbard 1:100 000 (S100 Kartdata).
NPI. (2015). Svalbardkartet. 2014, from (www.npolar.no/svalbardkartet
Rubensdotter, L., & Rosqvist, G. (2009). Influence of geomorphological setting, fluvial-, glaciofluvial-and mass-movement processes on sedimentation in alpine lakes. The Holocene, 19(4), 665-678.
Røthe, T. O., Bakke, J., Vasskog, K., Gjerde, M., D'Andrea, W. J., & Bradley, R. S. (2015). Arctic Holocene glacier fluctuations reconstructed from lake sediments at Mitrahalvøya, Spitsbergen. Quaternary Science Reviews, 109(0), 111-125. doi: http://dx.doi.org/10.1016/j.quascirev.2014.11.017
van der Bilt, W. G. M., Bakke, J., Vasskog, K., D'Andrea, W. J., Bradley, R. S., & Ólafsdóttir, S. (2015). Reconstruction of glacier variability from lake sediments reveals dynamic Holocene climate in Svalbard. Quaternary Science Reviews, 126, 201-218. doi: http://dx.doi.org/10.1016/j.quascirev.2015.09.003
Vasskog, K., Nesje, A., Støren, E. N., Waldmann, N., Chapron, E., & Ariztegui, D. (2011). A Holocene record of snow-avalanche and flood activity reconstructed from a lacustrine sedimentary sequence in Oldevatnet, western Norway. The Holocene, 0959683610391316.
WGMS. (1988-2011). Glacier Mass Balance Bulletin (GMBB). Retrieved 25.09.2014 http://www.wgms.ch/gmbb.html
Williams, P. F., & Rust, B. R. (1969). The sedimentology of a braided river. Journal of Sedimentary Research, 39(2).

III

# Paper 3: Reconstruction of glacier variability from lake sediments reveals dynamic Holocene climate in Svalbard

Willem G.M. van der Bilt[a b] , Jostein Bakke[a b,] Kristian Vasskog[b c], William J. D`Andrea[d], Raymond S. Bradley [e], Sædis Ólafsdóttir[a b]

[a] Department of Earth Science, University of Bergen, Allégaten 41, 5007, Bergen, Norway

[b] Bjerknes Centre for Climate Research, Allégaten 55, 5020, Bergen, Norway

[c] Uni Climate, Uni Research, Allégaten 55, 5007 Bergen, Norway

[d] Lamont-Doherty Earth Observatory, Columbia University, Palisades, NY 10964, USA

[e] Department of Geosciences, University of Massachusetts, Amherst, MA 01003, USA

*Keywords: Holocene climate, Svalbard, glacier activity, lake sediments, numerical analyses*

## Abstract

The Arctic is warming faster than anywhere else on Earth. Holocene proxy time-series are increasingly used to put this amplified response in perspective by understanding Arctic climate processes beyond the instrumental period. However,

available datasets are scarce, unevenly distributed and often of coarse resolution. Glaciers are sensitive recorders of climate shifts and variations in rock-flour production transfer this signal to the lacustrine sediment archives of downstream lakes. Here, we present the first full Holocene record of continuous glacier variability on Svalbard from glacier-fed Lake Hajeren. This reconstruction is based on an undisturbed lake sediment core that covers the entire Holocene and resolves variability on centennial scales owing to 26 dating points. A toolbox of physical, geochemical (XRF) and magnetic proxies in combination with multivariate statistics has allowed us to fingerprint glacier activity in addition to other processes affecting the sediment record.

Evidence from variations in sediment density, validated by changes in Ti concentrations, reveal glaciers remained present in the catchment following deglaciation prior to 11 300 cal BP, culminating in a Holocene maximum between 9.5-9.6 ka cal BP. Correspondence with freshwater pulses from Hudson Strait suggests that Early Holocene glacier advances were driven by the melting Laurentide Ice Sheet (LIS). We find that glaciers disappeared from the catchment between 7.4-6.7 ka cal BP, following a late Hypsithermal. Glacier reformation around 4250 cal BP marks the onset of the Neoglacial, supporting previous findings. Next, between 3380-3230 cal BP, we find evidence for a previously unreported centennial-scale glacier advance. Both events are concurrent with well-documented episodes of North Atlantic cooling. We argue that brief forcing created suitable conditions for glaciers to reform in the catchment against a background of gradual orbital cooling. These findings highlight the climate-sensitivity of the small glaciers studied, which rapidly responded to climate shifts. The start of prolonged Neoglacial glacier activity commenced during the Little Ice Age (LIA) around 700 cal BP, in agreement with reported advances from other glaciers on Svalbard. In conclusion, this study proposes a three-stage Holocene climate history of Svalbard, successively driven by LIS meltwater pulses, episodic Atlantic cooling and declining summer insolation.

## Introduction

Instrumental observations suggest that the Arctic has been changing faster than any other region on the Northern hemisphere over the past decades (Serreze and Barry, 2011). This amplified response has consistently been simulated by climate models for a future with increased atmospheric greenhouse gas concentrations (Pithan and Mauritsen, 2014). But though albedo and temperature feedbacks have been suggested (Screen and Simmonds, 2010), the drivers of Arctic climate variability have yet to be fully constrained (Miller et al., 2010). It is important to improve our understanding of forcing mechanisms, as the Arctic has a disproportionately large influence on global climate (McGuire et al., 2006; Solomon, 2007). As the paradigm of a stable Holocene climate has shifted (Bond et al., 2001; Overpeck et al., 1997), Holocene proxy time-series are increasingly considered as potential analogues for future climate, and may help assess the range of natural Arctic climate variability (McKay and Kaufman, 2014; Wanner et al., 2011).

However, Arctic climate proxy datasets are scarce and unevenly distributed (Wanner et al., 2011). Moreover, records often cover only parts of the Holocene and lack robust chronological control (Sundqvist et al., 2014). Continuous, well-dated and high-resolution archives are required to resolve the temporal and spatial signature of Holocene Arctic climate variability. Glaciers are ubiquitous in the Arctic and rapidly respond to shifts in summer temperature and winter precipitation (Oerlemans, 2005; Østrem and Liestøl, 1964). This sensitive response to climate change is captured by variations in minerogenic rock-flour production and may be recorded in lacustrine sediment archives of downstream glacier-fed lakes (Karlén, 1976; Karlén, 1981). Monitoring data demonstrate that variations in the flux of minerogenic sediments into glacier-fed lakes provide a robust high-resolution record of glacier activity and size (Leemann and Niessen, 1994a; Liermann et al., 2012; Roland and Haakensen, 1985). The signature of rock-flour in lacustrine sediments therefore serves as a climate proxy that has been widely applied (Bakke et al., 2010; McKay and Kaufman, 2009; Rosqvist and Schuber, 2003; Simonneau et al., 2014). Indeed, sediment records from glacier-fed lakes are rated among the best continuous high-resolution terrestrial proxy

archives available (Ashley, 1995; Carrivick and Tweed, 2013). Here, the conceptual model described above has been further developed into a multi-proxy approach that integrates physical (Bakke et al., 2005), magnetic (Paasche et al., 2007) and geochemical tools (Bakke et al., 2009), in combination with numerical techniques (Bakke et al., 2013; Vasskog et al., 2012).

We present a sediment record from the glacier-fed Lake Hajeren in northwest Spitsbergen that encompasses the entire Holocene. This region sits at the crossroads of Arctic and Atlantic water masses and is therefore sensitive to climate shifts (Rasmussen et al., 2014; Werner et al., 2013). Nonetheless, the coverage of high-resolution terrestrial climate proxy records in the area is sparse. The main goal of this study is to provide a reconstruction of Holocene glacier activity that will improve our understanding of centennial-scale Arctic climate variability. To this end, we apply a multi-proxy toolbox to ensure rigor in our interpretations. The methods also enable us to detect other catchment and lake processes that leave an imprint in the lake sediment record. Accurate detection of sediments reflecting glacier activity requires a full understanding of these processes, which include, but are not limited to, paraglacial redeposition (Ballantyne, 2002), mass wasting (Vasskog et al., 2011), lake stratification (Leemann and Niessen, 1994a; Richards et al., 2012) and redox processes (Lamoureux and Gilbert, 2004). Moreover, to ensure the chronological robustness required to resolve centennial climate variability (Sundqvist et al., 2014), we have used a combination of radiocarbon dating and Paleomagnetic Secular Variations (PSV). Finally, we integrate this study into a regional paleoclimatic context by comparing our site-specific findings to other high-resolution proxy records from the Arctic sector of the North-Atlantic.

## Setting

Hajeren, the distal glacier-fed lake investigated in this study, measures 0.23 $km^2$ and is located on the Mitrahalvøya Peninsula in Northwest Spitsbergen (79°15'33.47"N 11°31'4.25"E) (Fig. 1). Bathymetric profiling reveals two basins with a maximum

depth of 19.5 m (Fig. 2). The lake`s surface elevation is 35 m a.s.l., placing Hajeren slightly above the local marine limit reported by Landvik et al. (2013) (32 m a.s.l.).

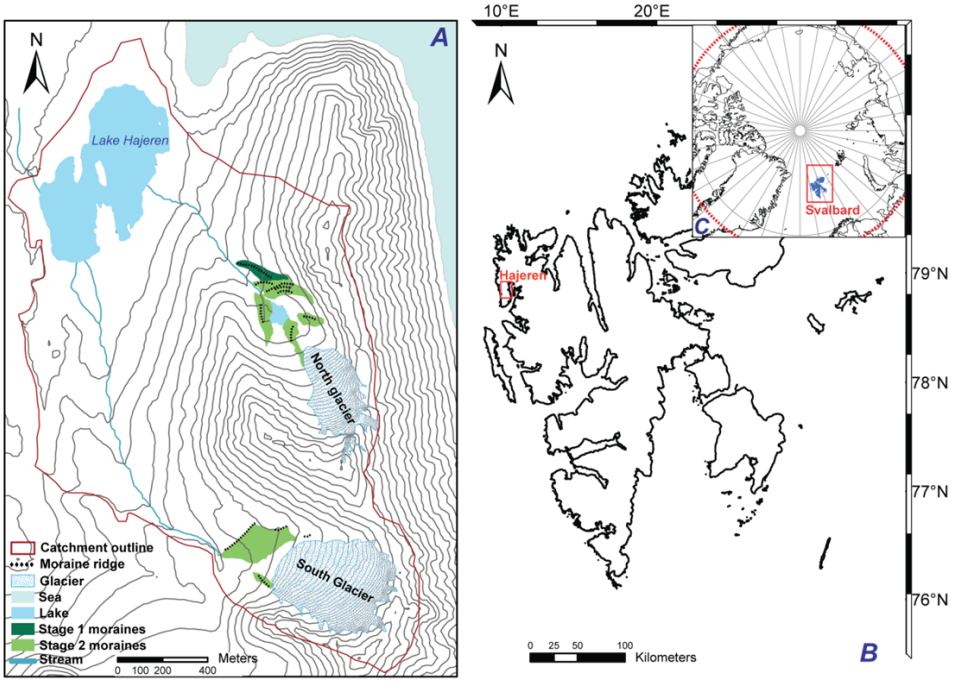


***Fig.1**. A: a simplified 25m contour geomorphological map of the Hajeren catchment, outlined by a red line. Both North and South glaciers, their outlet streams and lake Hajeren are displayed. B: close-up of the Svalbard archipelago, marking the Hajeren catchment with a red rectangle. C: North Pole view map of Svalbard (blue) and the Arctic (delimited by the red dashed line).*

The catchment of Lake Hajeren covers 2.96 $km^2$ of which 0.25 $km^2$ is presently glacier-covered. Two northwest-facing non-surging cirque glaciers drain into the lake (Fig. 1), which will henceforth be referred to as North and South glaciers. Based on field observations (Van der Bilt et al., 2015), the North Glacier (0.8 $km^2$) is believed to be polythermal, while the South Glacier (0.17 $km^2$) may have turned cold-based due to recent thinning. Based on documented past glacier front positions (NPI, 2015) and a lack of geomorphic evidence (e.g. tectonised sediments and looped moraines), we argue that both glaciers are not surging. Also, using a historical aerial photographs (NPI, 1936), both have been retreating for at least 78 years and likely since the Little

Ice Age (LIA). This period of favourable conditions for glacier growth commenced after 1.3 ka cal BP and culminated on Svalbard during the 19th century (Salvigsen and Høgvard, 2006). Lake Hajeren is drained by an ephemeral spillway, enhancing its capacity to retain glacigenic suspended load (Dahl et al., 2003).

The glacial geomorphology of the catchment is characterized by two sets of terminal moraine deposits that are indicated as stages 1 and 2 in Fig. 1. Based on aerial photographs from 1936 (NPI, 1936), Stage 2 moraines were deposited during the culmination of the Little Ice Age (LIA) in the 19th century. The more distal Stage 1 moraines are exclusively found in front of the more erosive polythermal North glacier and comprise a complex of mounds (Van der Bilt et al., 2015). Their weathered appearance and position outside Stage 2 moraine deposits suggests that they were possibly deposited during a pre-LIA glacier maximum, in agreement with findings from nearby catchments (Reusche et al., 2014; Røthe et al., 2015).

Bedrock geology comprises Proterozoic protoliths of the Krossfjorden group that were metamorphosed during the Grenvillian orogeny (Dallmann, 2015). Local bedrock predominantly consists of NNW-SSE trending Signehamna formation schists that are horizontally overlain by marble belonging to the Generalfjellet formation in southern Mitrahalvøya (Krasilščikov, 1975).

Climate in Spitsbergen is influenced by the West and East Spitsbergen currents (Rasmussen et al., 2014). The former transports warm and saline Atlantic waters Northward (Aagaard-Sørensen et al., 2014), while the latter brings in cold water from the Arctic Ocean (Loeng, 1991). The interplay between these distinctly different water masses create a climate that is highly sensitive to shifting oceanic and atmospheric conditions (Rasmussen et al., 2014) as well as changes in sea ice extent (Benestad et al., 2002; Müller et al., 2012). At present, Northwest Spitsbergen has a maritime polar climate with an average annual temperature of -5°C and 427 mm of annual precipitation measured at nearby Ny Ålesund for the 1980-2010 period (Førland et al., 2012). Temperatures have been recorded since 1898 and reveal highly variable, but generally warming conditions during the 20th century (Nordli et al.,

2014). Moreover, the last 30 years are characterized by continuous warming with the warmest years on record occurring during the past decade (Nordli, 2010).

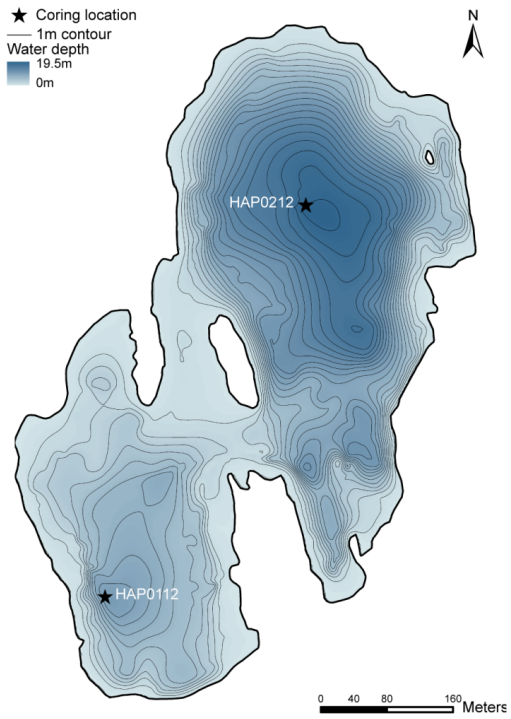


***Fig.2.*** *Bathymetry of Lake Hajeren with 1m contour lines, showing two sub-basins. Coring locations of cores HAP0112 and HAP0212 are indicated.*

# Material & Methods

## Coring and mapping

In August 2012, a seismic survey was carried out on Lake Hajeren, using a Malå Ground Penetrating Radar (GPR) system fitted with a 50 Mhz antenna. Post-processing of these data using the RadExplorer software package revealed a fairly homogeneous distribution of soft sediments over two sub-basins henceforth referred to as North and South basins, with water depths of 13 and 19.5 m, respectively (Fig. 2 and 3). Following the seismic survey, sediment cores were extracted close to the deepest spots in each basin (Fig. 3). Figure 2 demonstrates that the lake bottom

surrounding both coring sites is flat, reducing the risk of post-depositional sediment disturbance like slumping (Dahl et al., 2003). Two cores, HAP0112 and HAP0212, were extracted from a coring platform, using a modified Nesje piston corer (Nesje, 1992) fitted with 110 mm diameter tubing (Fig. 3). Coring was followed by geomorphological mapping during the summer of 2014. Landform-sediment assemblages in the catchment have subsequently been mapped at in detail (Van der Bilt et al., 2015), complimenting aerial photograph evidence (NPI, 1936, 2009).

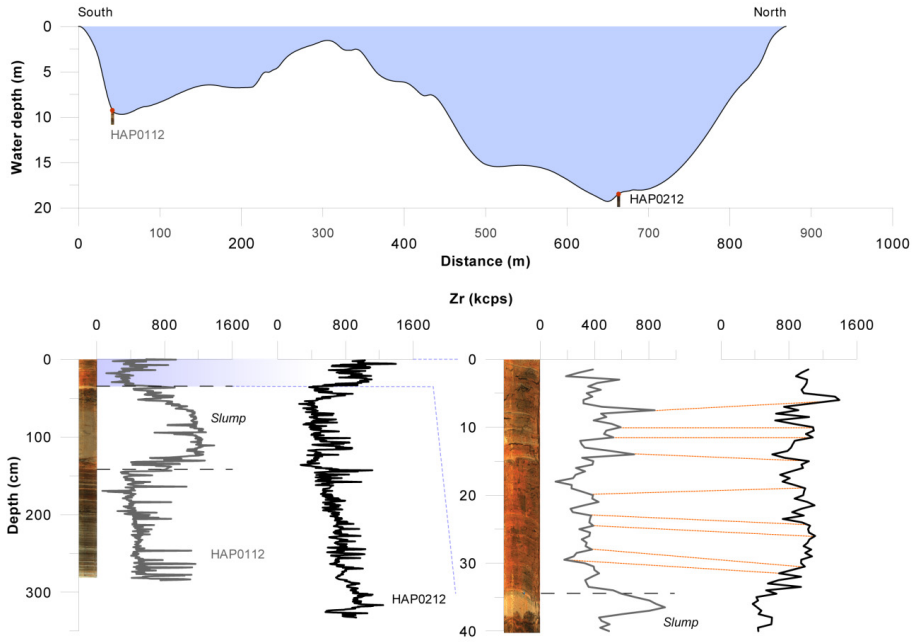


***Fig.3**. Transect through both South and North basins of Lake Hajeren. Coring locations of HAP0112 and HAP0212 are indicated. The upper 40 cm of both cores have been correlated using Zr count rates.*

## Analyses

We reconstructed glacier activity in the Hajeren catchment using a combination of geomorphological mapping, lake coring, and laboratory analyses of the lake sediments. The latter encompass a toolbox of physical, geochemical and magnetic proxies, developed to detect a glacier signal in distal glacier-fed lakes (Bakke et al., 2013; Røthe et al., 2015; Wittmeier et al., 2015). A robust chronology was

established using Accelerator Mass Spectrometry (AMS) radiocarbon dating of terrestrial macrofossils and Paleomagnetic Secular Variations (PSV).

### *Lithostratigraphy*

Before describing their lithological characteristics, the extracted piston cores were split. Sediments from core HAP0112, extracted adjacent to a steep slope in the South basin, were found to be disturbed between 35 and 125 cm core depth (Fig. 3). As such, the 332 cm long undisturbed core HAP0212 from the North basin of Lake Hajeren was selected as master core (Fig. 3 and 4). Moderate correspondence with the undisturbed upper 35 cm of HAP0112, using Zr counts, suggests that the sedimentary signal from HAP0212 is representative (Fig. 3). To measure sediment Dry Bulk Density (DBD), indicative for the influx of suspended rock-flour (Karlén, 1976) and a proxy for glacier activity (Bakke et al., 2005),0.5 cm3 of sediment was extracted every 0.5 cm (n = 618). The bottom 20 cm of HAP0212 comprises a pebbly diamict and could therefore not be sampled. Samples were subsequently dried overnight at 105 °C and weighted for DBD and Water Content (WC) following Menounos (1997). To measure organic content, the same samples were subsequently transferred to crucibles and ignited at 550 °C for Loss-On-Ignition (LOI) in a muffle furnace (Heiri et al., 2001).

### *Magnetic properties*

Mineral magnetic properties are commonly used as indicators of glacially-derived minerogenic matter in the sedimentary record of glacier-fed lakes (Matthews and Karlén, 1992; Snowball and Sandgren, 1996). For this study, we measured surface Magnetic Susceptibility (MS) and (bulk) Anhysteric Remanent Magnetization ((X)ARM) on HAP0212. Surface MS was measured continuously at 1 cm resolution with a Bartington MS3 meter equipped with a MS2E surface sensor. ARM was first measured on extracted u-channels at 1 cm intervals in a 2G superconducting rock magnetometer at Oregon State University by applying a 0.1 mT Direct Current (DC) field followed by a 10 mT Alternating Current (AC) field. To allow for a more detailed investigation of the variable upper core half, we also measured bulk ARM (XARM) on 6 cm3 discrete samples extracted at 0.5 cm intervals (n = 327). To this

end, we imposed identical DC and AC field strengths in a 2G Alternating Field (AF) degausser.

### *Geochemistry*

X-Ray Fluorescence (XRF) count rates detect changes in lithogenic influx and have been used to infer changes in glacier mass turnover (Bakke et al., 2009). Accordingly, the geochemistry of HAP0212 was semi-quantitatively mapped using an XRF core scanner (Croudace et al., 2006).Elemental profiles were obtained at 200 µm resolution from the split cores by a Cox Analytical Systems ITRAX scanner at the department of Earth Science in Bergen. To acquire the highest sensitivity for heavier lithogenic elements, scans were performed using a Molybdenum (Mo) tube (Boës et al., 2011). The cores were covered with foil to prevent sediments from drying out and protect the detector of the instrument after Tjallingii et al. (2007). To prevent interannual variability from obscuring the centennial-scale climate signal studied here (Birks, 1998), measurements were smoothed using a 25-point moving average and subsequently resampled at 0.5 cm resolution.

***Table 1**. Overview of radiocarbon samples from core HAP0212. 1 indicate designated outliers*

| Core | Lab nr. | Material | mg C | Depth (cm) | $^{14}$C age (BP) | Min. age (cal BP) | Max. age (cal BP) | Mean (cal BP) |
|---|---|---|---|---|---|---|---|---|
| HAP0212 1-2 | Poz-57711 | Plant macrofossil | 0.5 | 8.5 | 175 ± 25 | 137 | 223 | 171 |
| HAP0212 1-2 | Poz-57712 | Plant macrofossil | 0.4 | 16.5 | 350 ± 40 | 313 | 493 | 388 |
| HAP0212 1-2 | LuS 10735 | Plant macrofossil | 0.19 | 35 | 800 ± 60 | 658 | 802 | 738 |
| HAP0212 1-2 | LuS 10736 | Plant macrofossil | 0.3 | 53.5 | 1470 ± 50 | 1293 | 1418 | 1417 |
| HAP0212 1-2 | LuS 10737 | Plant macrofossil | 0.22 | 60 | 1935 ± 60 | 1722 | 2000 | 1798 |
| HAP0212 1-2 | Poz-57713 | Plant macrofossil | 0.3 | 73.5 | 2200 ± 50 | 2109 | 2339 | 2210 |
| HAP0212 1-2 | Poz-57714 | Plant macrofossil | 0.5 | 81.5 | 2305 ± 35 | 2301 | 2360 | 2337 |
| HAP0212 1-2 | LuS 10738 | Plant macrofossil | 0.42 | 89.5 | 2500 ± 50 | 2426 | 2743 | 2563 |
| HAP0212 1-2 | LuS 10739 | Plant macrofossil | 0.44 | 116 | 3175 ± 50 | 3322 | 3484 | 3393 |
| HAP0212 1-2 | LuS 10740 | Plant macrofossil | 0.36 | 123 | 3355 ± 50 | 3461 | 3699 | 3609 |
| HAP0212 1-2 | LuS 10741 | Plant macrofossil | 0.36 | 127 | 3480 ± 50 | 3633 | 3879 | 3737 |
| HAP0212 1-2 | Poz-57715 | Plant macrofossil | 0.4 | 155 | 4070 ± 40 | 4436 | 4649 | 4595 |
| HAP0212 1-2 | LuS 10742 | Plant macrofossil | 0.48 | 160 | 4230 ± 50 | 4611 | 4767 | 4782 |
| HAP0212 1-2 | Poz-57716 | Plant macrofossil | 0.8 | 163 | 4370 ± 35 | 4856 | 4984 | 4895 |
| HAP0212 2-2 | Poz-60452 | Plant macrofossil | 0.6 | 167 | 4425 ± 35 | 4872 | 5069 | 5030 |
| HAP0212 2-2 | Poz-60453 | Plant macrofossil | 0.7 | 172.5 | 4480 ± 35 | 5035 | 5291 | 5217 |
| HAP0212 2-2 | Poz-60454 | Plant macrofossil | 0.6 | 177.5 | 4720 ± 40 | 5324 | 5416 | 5411 |
| HAP0212 2-2 | Poz-60455 | Plant macrofossil | | 191.5 | 5200 ± 35 | 5903 | 6004 | 5965 |
| HAP0212 2-2 | Poz-60456 | Plant macrofossil | 0.4 | 201.5 | 5770 ± 50 | 6446 | 6672 | 6591 |
| HAP0212 2-2 | LuS 10866 | Plant macrofossil | 0.4 | 231.5 | 7305 ± 50 | 8004 | 8200 | 8185 |
| HAP0212 2-2 | LuS 10867 | Plant macrofossil | 0.3 | 248.5 | 9565 ± 55 | 10715 [1] | 11109 [1] | 10912 [1] |
| HAP0212 2-2 | LuS 10868 | Plant macrofossil | 0.2 | 265.5 | 16580 ± 180 | * | * | * |
| HAP0212 2-2 | LuS 10869 | Plant macrofossil | 0.4 | 269.5 | 9750 ± 55 | 11082 | 11254 | 11118 |
| HAP0212 2-2 | LuS 10870 | Plant macrofossil | 0.3 | 317 | 25100 ± 300 | * | * | * |

## *Chronology*

We used two independent chronological methods to construct an age-depth model for core HAP0212: radiocarbon dating and Paleomagnetic Secular Variation (PSV) correlation. 24 terrestrial plant macrofossil samples were extracted at frequent intervals by wet-sieving sediments using a 125 μm mesh, transferred to sterile vials and submitted for AMS radiocarbon dating (Table 1). Samples with a dry weight equal or less than 2 mg (n = 13) were sent to the Lund University Radiocarbon Dating Laboratory (LuS). Larger samples (n = 12) were processed by the Poznan Radiocarbon Laboratory (Poz). PSV describe the directional and intensity changes of Earth`s magnetic field and enables chronological synchronization between records

(Thompson and Turner, 1979). To improve chronological accuracy, we used a PSV-derived chronology for core sections below 231.5 cm depth, characterized by the infrequent and scarce occurrence of datable macrofossils (table 1). Declination, inclination and intensity component records were measured on core HAP0212 at 1 cm resolution, using a 2G superconducting rock magnetometer at Oregon State University. Tie-points were then generated by synchronizing HAP0212 inclination and declination features to those of the well-dated MD99-2269 marine core from the Icelandic shelf (Ólafsdóttir et al., 2013; Stoner et al., 2007).

### *Grain size*

As glacial meltwater is characterized by an abundance of suspended silt and clay grains (1-63 μm) (Leemann and Niessen, 1994a), we analysed the grain-size distribution of selected minerogenic intervals. 8-12 gr of sediment were extracted every 1 cm for the intervals between 39.5-47.5 (1), 110.5-115.5 (2) and 137.5-144.5 (3) cm core depth (n = 36). The same was done between 30.5 and 34.5 cm (n = 5), the onset of a period of sustained minerogenic sedimentation and documented LIA glacier activity ("setting") To dissolve organic matter, sediment samples were stirred for 2 days in a 5% H2O2 aqueous solution before being sieved through a 63 μm mesh. The dried residue was then disaggregated in a 0.005% Calgon solution (Jones et al., 1988) and analysed in a Micromeritics Sedigraph 5100 equipped with a Mastertech 5.1 automatic sampler. We employed the GRADISTAT grain size statistics package by Blott and Pye (2001) to process Sedigraph measurements using the geometric Folk and Ward method (Folk and Ward, 1957).

### *Statistics*

Statistical analyses are increasingly applied on lake sediment records to improve our understanding of multi-proxy datasets (Birks, 1998; Koinig et al., 2003). Here, we applied cluster analysis on the HAP0212 dataset to objectively categorize the record into different units, while normalization against LOI was used to account for dilution effects in the geochemical data. Finally, ordination was performed using Principal Component Analysis (PCA) in order to investigate variability shared between proxies.

**Cluster analysis**

Lake sediment records are commonly categorized into stratigraphical units using subjective methods such as visual inspection. Here, cluster analysis was applied to objectively categorize the HAP0212 record into different units. Following Bakke et al. (2013), we used the constrained incremental sum of squares clustering (CONISS) algorithm (Grimm, 1987) in the Tilia software package (Grimm, 2011). The independently measured parameters ARM, DBD and MS were selected for cluster analysis. Dissimilarity was then calculated using Euclidean distance and expressed using total mean square values. We took a total sum of squares cut-off value of 1.25 to subdivide the record.

**Normalization**

Elemental profiles measured by XRF core scanner are affected by physical sediment properties (Croudace et al., 2006) and should therefore be cautiously interpreted. For this study, we used normalization to address impacts of the commonly described closed-sum effect (Rollison, 1993), which concerns dilution of the XRF signal by organic matter. This may obscure relative changes in elemental abundances and could therefore overprint sources of environmental variability in our data that are unrelated to changing organic content.

We first applied multiple criteria for the selection of XRF elemental profiles in our analysis. Only elements with high sensitivity to the Mo tubing fitted during measurement were included according to Cox Analytical Systems specifications. This selection excludes lighter elements that are known to be sensitive to scattering and absorption of X-rays by water, such as Al and Si (Tjallingii et al., 2007). Moreover, elements with low count rates, here defined as having a mean < 100 kilocounts per second (kcps), were omitted following Striberger et al. (2011). Finally, we excluded elements with a low signal-to-noise ratio (SNR), defined as the ratio of mean $\mu$ over standard deviation $\sigma$ after Montgomery (2008), equal or less than 2.

Different approaches that aim to resolve the closed-sum effect on scanning XRF data through normalization have been proposed. For example, Thomson et al. (2006) and Löwemark et al. (2011) suggest normalizing against conservative Al. Kylander et al.

(2011), on the other hand, normalize their data against the ratio of incoming plus coherent scattering, which responds to shifts in organic content. Here we adopted a variation of the latter approach, normalizing conservative elements against our separately measured LOI record. Normalizing against LOI enables us to isolate environmental variability not related to changes in organic content of the sediments. This step is expected to amplify the subtle shifts in minerogenic input characteristic for changes in the mass turnover rate of small glaciers like those in the study area (Leonard, 1985).

**Ordination**

Ordination techniques have been increasingly employed to understand gradients of environmental variation in lake sediment core data since the 1980s (Sergeeva, 1983). Following Vasskog et al. (2012) ,we carried out Principal Component Analysis (PCA) (Hotelling, 1933) on our multi-proxy dataset to assess whether variables show a shared response to glacigenic sedimentation. To this end, we used version 5 of the CANOCO software by Ter Braak (1988). Assessed variables were transformed prior to PCA to reduce the asymmetry of their distribution and increase linearity (Legendre and Birks, 2012), following CANOCO suggestions. Non-linearity between variables reduces the common variability detected by PCA and renders the ordination axes dependent (Šmilauer and Lepš, 2014). To emphasize correlations in the ordination diagram, variables were respectively centered and standardized before analysis, following the recommendations of Šmilauer and Lepš (2014). Based on the previously described criteria, 9 variables were included in the PCA on a shared 1-cm sampling resolution (n = 250): elemental count rates of K, Ti, Fe, Rb and Zr in addition to the physical parameters DBD and LOI as well as magnetic properties ARM and MS.

# Results

## Lithostratigraphy

The lithostratigraphy of core HAP0212 is shown in figures 4 and 5. By means of cluster analysis, the upper 320 cm of the record were objectively categorized into four units (1-4). The bottom 20 cm of HAP0212 (unit 5) was too coarse-grained and uneven for sampling or scanning and is therefore also excluded from cluster analysis. We could not extract material for basal dating from both units 4 and 5 in the absence of macrofossils.

### *Unit 5 (332 - 320 cm)*

Unit 5 encompasses the bottom 12 cm of core HAP0212 and comprises two sub-units, 5a and 5b. 5a (332-323.5 cm) is a diamict that consists of sub-angular pebble-sized clasts with no apparent orientation, embedded in a matrix of grey silty clay with a 2.5Y 6/2 Munsell chart value (Munsell and Color, 2000). The embedded clasts all consist of mica schist, similar to the Signehamna formation bedrock found in the Hajeren watershed (Ohta et al., 2002). The angular open work fine gravels of sub-unit 5b (320-323.5 cm) are poorly sorted and fine upwards. The transition into unit 4 is abrupt along a truncated surface.

### *Unit 4 (320 - 272 cm)*

Unit 4 consists of massive grey (2.5Y 7/2) sandy silts with high DBD values that average 1.55g/cm3 (Fig. 4). We measured undrained shear strength of 126 kPa in duplicate at 300 cm core depth using a fall cone test after Tanaka et al. (2012), suggesting compaction. Dewatering structures are also visible at selected intervals. In its entirety, unit 4 is faintly stratified, as the silty fining-upwards sediments are regularly interspersed with sandier intervals.

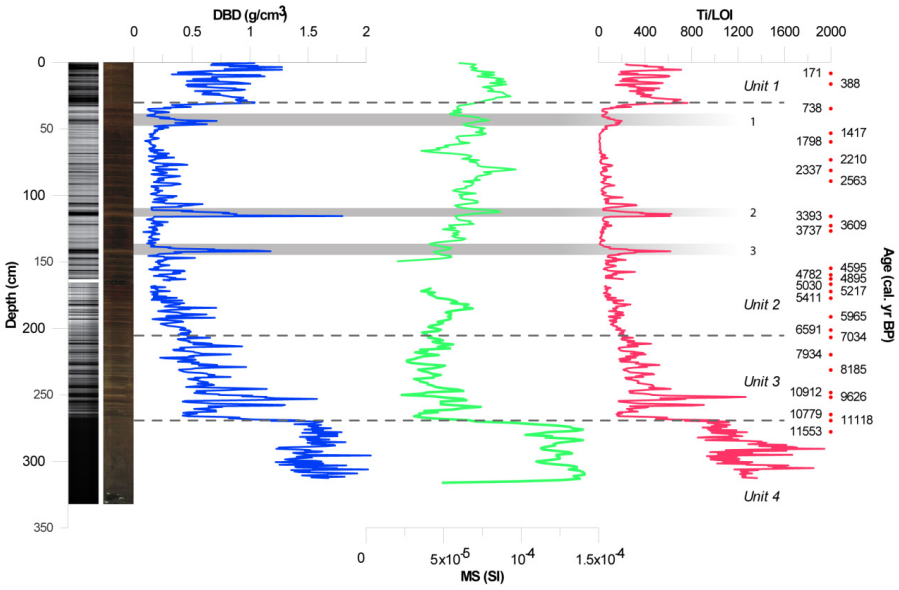


***Fig. 4**. Minerogenic (glacigenic) indicators DBD and Ti/LOI as well as MS from core HAP0212, plotted on depth-scale at 0.5 cm resolution. The 4 main units, determined by cluster analysis are delimited with dashed lines. Intervals 1, 2 and 3 are emphasized by shaded bars. Optical (RGB) and radiograph grayscale images are displayed on the left, while the core depths (red bullets) and calibrated ages of dated samples are shown on the right.*

### *Unit 3 (272 - 203 cm)*

Figure 4 shows that the physical characteristics of units 3 and 4 differ significantly. The faint laminations in the upper part of unit 4 become more apparent in unit 3 due to more distinct variations in minerogenic content reflected by LOI and DBD curves (Fig. 4 and 5). The lower 10 cm of unit 3 consist of dark brown (7.5YR 4/3) organic-rich sediments and show a marked prolonged spike in LOI with maximum values of 10.5 % (Fig. 5). In general, unit 3 is characterized by gradual but distinct alternations between grey (10YR 8/1) minerogenic (LOI ≈ 1.5 – 5 %) and relatively organic-rich dark brown (7.5YR 6/3) intervals (LOI ≈ 5 -11 %). DBD values peak around 251 cm depth (Fig. 4). Towards the upper boundary, unit 3 grades into dark brown gyttja with a consistently higher organic content.

### *Unit 2 (203 - 30.5 cm)*

Unit 2 is characterized by a prolonged increase in LOI values as shown in figure 5. This rise in organic content is asymmetrically shaped with a slow build-up from ≈ 5% towards ≈ 28% peak at 69 cm depth followed by a rapid decline towards unit 1. Low DBD values suggest minimal minerogenic and/or high organic sedimentation throughout most of unit 2. This trend is interrupted by intervals 1, 2 and 3, as shown in figure 5.

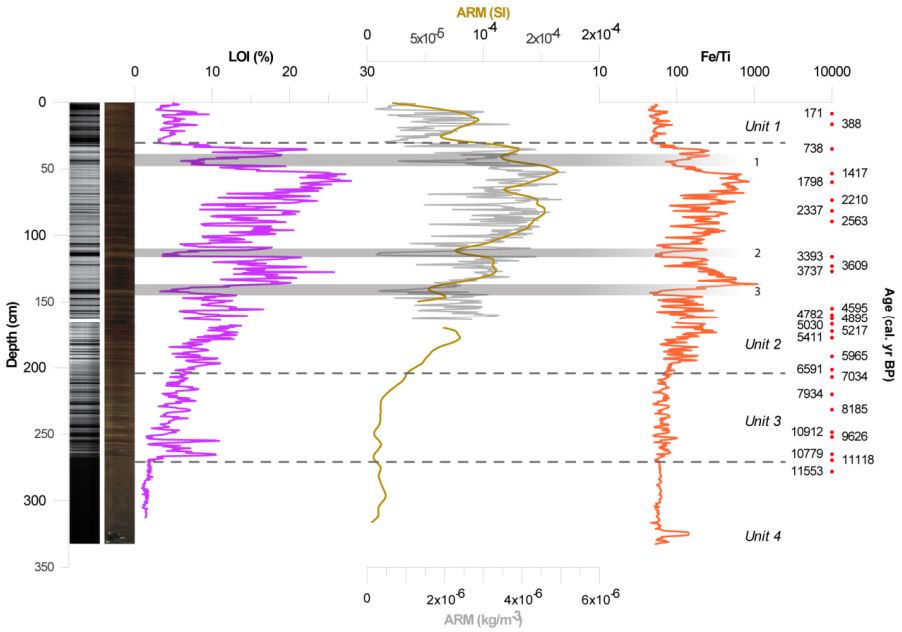


***Fig. 5**. LOI and ARM, scanned ARM (brown), XARM (grey), and Fe/Ti (orange) from core HAP0212, plotted on depth-scale at 0.5 cm resolution on depth-scale. The 4 main units, determined by cluster analysis ("cluster analysis") are delimited with dashed lines. Intervals I, 2 and 3 are emphasized by shaded bars. Optical (RGB) and radiograph grayscale images are displayed on the left, while core depths (red bullets) and calibrated ages of dated radiocarbon samples (blue) as well as PSV tie-points (red) are shown on the right.*

The organic-rich sections (LOI > 10%) are coloured dark brown (7.5YR 2.5/1), whereas intervals 1, 2 and 3 are yellowish grey (10YR 7/3). The sediments of unit 2 are laminated throughout, but layer properties differ substantially between organic-

rich and minerogenic intervals. The former comprise millimetre-scale couplets, while laminae in the latter are substantially wider. Figure 4 demonstrates that DBD values change rapidly towards the boundary with unit 1, marking a shift towards increasingly minerogenic lacustrine sedimentation.

### *Unit 1 (30.5 - 0 cm)*

The upper unit of core HAP0212 covers the first period of prolonged minerogenic sedimentation since unit 3. Sediments comprises grey (10YR 7/1-2) silty clays, comparable to those found in unit 3. Moreover, the grayscale image shows that unit 1 also exhibits the centimetre-scale laminations found in unit 3 and intervals 1, 2 and 3 in unit 2. After spiking at the onset of unit 1, DBD values gradually increase towards the top and peak around 4 cm depth at 1.27 g/cm3. This value is similar to those observed in unit 3 as well as intervals 1, 2 and 3 as shown by figure 4.

## Age-depth model

The HAP0212 age-depth model was generated using the Clam 2.2 package (Blaauw, 2010), run in the open-source R environment version 3.0.1 (RCoreTeam, 2014). Included radiocarbon ages (n = 21) were calibrated using the IntCal13 terrestrial calibration curve for the Northern Hemisphere (Reimer et al., 2013). Based on outlined signs of reworking and a dynamic sedimentology (“unit 4”), sections unit 4 that are older than 11480 cal BP were excluded from our age-depth model. This basal age was generated through synchronization of the Hajeren PSV record with that of the well-dated master curve from core MD99-2269 (Ólafsdóttir et al., 2013; Stoner et al., 2007). Due to the outlined scarcity of macrofossils and conflicting ages (table 1), PSV ties were used to constrain our model below 231.5 cm core depth. In total, we admitted 5 points with ages of 7019, 8115, 9639, 10718 and 11480 cal BP (Fig. 6). To account for uncertainties, we applied a ± 100 years uncertainty envelope after Larsen et al. (2012). Based on the PSV chronology, radiocarbon dates LuS 10867 and LuS868 (table 1) were designated as an outlier. The final age-depth model was generated using default smooth spline interpolation, producing the highest goodness-of-fit (11.44) (Fig. 6). Ages were interpolated at the common 0.5 cm resolution of our

proxy data using 10000 iterations, as recommended by Blaauw (2010). The resulting age-depth model has an average down-core sample resolution R of 21.91 years, with an average dating sample frequency f of 421.56 years (Sundqvist et al., 2014).

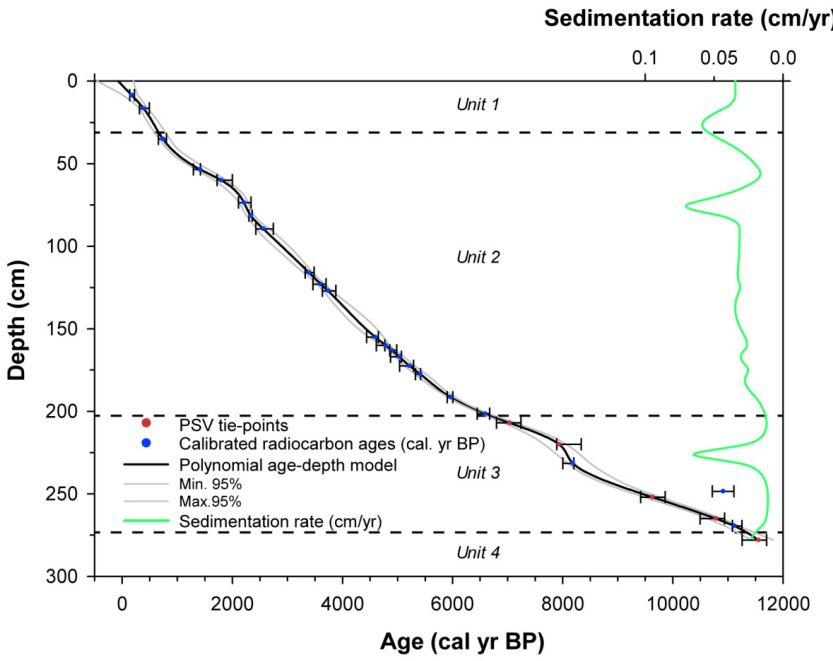


***Fig. 6**. Age-depth model constructed for core HAP0212, applying polynomial regression on the radiocarbon dates listed in table 1, indicated by blue dotes. Calibrated age uncertainties are expressed by asymmetrical error bars, while 95% confidence limits are marked by grey lines. Reconstructed sedimentation rates are displayed on the right.*

## Grain size

Clay and silt (1-63 μm) fractions from the previously described minerogenic intervals 1, 2 and 3 were analysed to help identify their depositional signature (Fig. 7). Additionally, grain size analysis was performed on reference sediments, deposited during the onset of a period of documented glacier activity ("setting). As can be seen in figure 7, minerogenic intervals 1, 2 and 3 are dominated by the fine silt and clay fractions. A similar development can be observed for the onset of prolonged late Holocene minerogenic sedimentation in Hajeren at the top of unit 2. Coarser fractions, which often characterize mass-wasting events (Rubensdotter and Rosqvist,

2009; Vasskog et al., 2011), are under-represented in intervals 1, 2 and 3. The grain size distribution profiles also indicate weak bimodality for the discussed intervals with peaks in the (very) fine silt fractions. Finally, figure 7 shows that distribution patterns from the latter intervals correspond to those seen for the minerogenic reference sediments of LIA age that border unit 1.

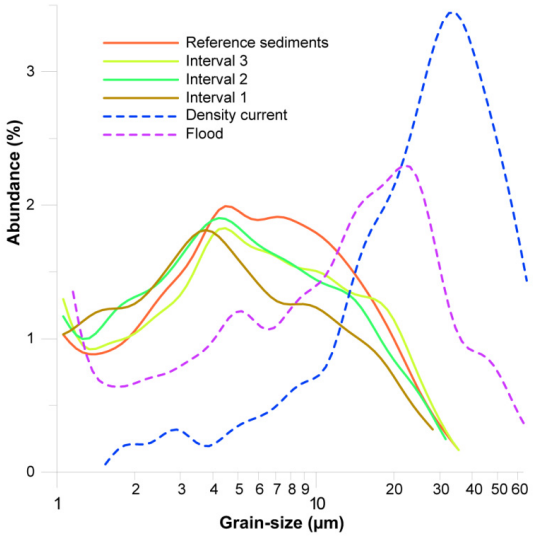


***Fig. 7.*** *Grain size distribution data (0-63 µm) plotted on a semi logarithmic scale for minerogenic intervals 1, 2 and 3, compared to LIA sediments (red) as well as common mass-wasting events density currents and floods (dashed) from Vasskog et al. (2011).*

## Magnetic properties

MS and ARM were measured on HAP0212 to track glacier-derived minerogenic sedimentation in Hajeren following Snowball and Sandgren (1996) and Matthews and Karlén (1992). Figures 4 and 5 show down-core variations in (X)ARM and MS. MS values are highest in the coarse sediments of unit 4 (Fig. 4). Average MS values of unit 4 are 56% higher than those of unit 1, which has the second-highest MS values of HAP0212. Based on the MS measurements, unit 4 appears distinctly different from the other units. It is also apparent that MS and DBD visually correlate in the minerogenic units 1 and 4. This relationship is less visible in unit 3 and poor in unit 2 as demonstrated by a Spearman`s rho (ϱ) of 0.316 (n = 130). MS values show a

similar asymmetric increase towards the top of unit 2 as observed in the LOI record. Figure 5 demonstrates this pattern is more pronounced in the ARM record of unit 2. A ϱ of 0.67 (n = 256) between LOI and discrete ARM measurements on unit 2 (XARM) affirms the strength of this correlation. However, as with the previously described LOI record, the build-up of ARM through unit 2 is disrupted by intervals 1, 2 and 3. Following Paasche et al. (2004), XARM was plotted against LOI to investigate the relationship between the two variables through unit 2 in closer detail (Fig. 8). Units 1 and 2 form distinct populations, characterized by different relationships between LOI and ARM as underlined by disparate regression coefficients. Though R2 values attest to a fairly scattered sample distribution, the trends show that LOI and XARM exhibit a positive relationship with an inflection around 5-10% LOI. XARM and LOI increase congruously throughout unit 2 and high values of both parameters co-occur. However, this relation is, however, markedly different for the low LOI values of minerogenic unit 1. Here, XARM values are an order of magnitude lower. Figure 8 shows that LOI and XARM combinations from intervals 1, 2 and 3 notably group with those of unit 1.

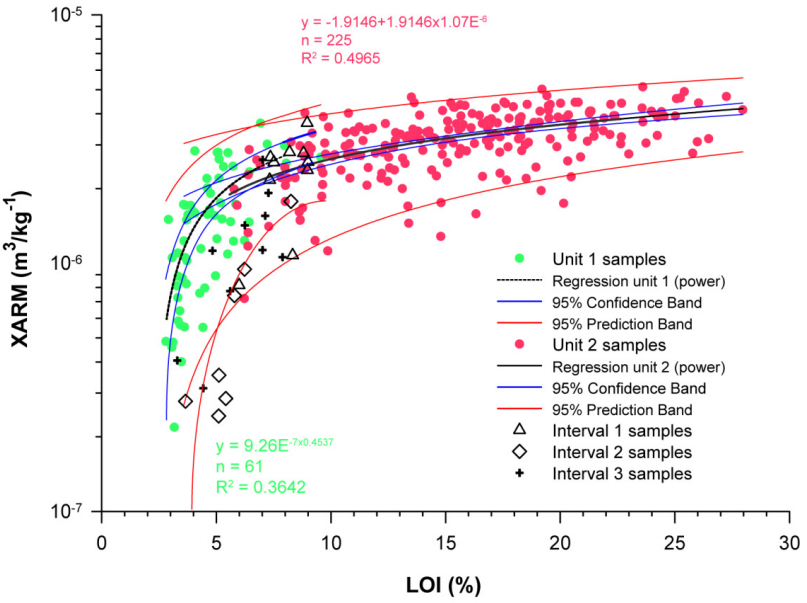


***Fig. 8**. XARM plotted against LOI on a semi logarithmic scale for samples from units 1 (green), 2 (pink) and minerogenic intervals 1, 2 and 3 (symbols) (n = 327). Regression coefficients emphasize that both groups exhibit different relationship between LOI and XARM. 95% predication and confidence limits are marked by red and blue lines, respectively.*

## Geochemistry

Following the previously described selection criteria ("normalization"), we included elemental count rates of K, Ti, Fe, Rb and Zr in our study to detect changes in lithogenic influx and glacier mass turnover (Bakke et al., 2010; Guyard et al., 2013; Kylander et al., 2011; Vasskog et al., 2012). We used the frequently applied Fe/Ti ratio (Croudace et al., 2006; Cuven et al., 2010; Thomson et al., 2006) to assess the impact of redox diagenesis on the Hajeren record. Figure 5 demonstrates that Fe/Ti ratios are low and vary little throughout unit 4 and, to a lesser extent, units 1 and 3. Unit 2, on the other hand, displays a notably higher degree of variability while average Fe/Ti ratios are an order of magnitude larger. Fe/Ti mimics LOI throughout units 1, 2 and 3 as attested by a $\varrho$ of 0.81 (n = 533). ARM values also capture Fe/Ti variability, as expected based on the relation between organic content and XARM show in figure 8. This correlation is strongest for the 0.5 cm XARM record ($\varrho$ = 0.55,

n = 324). As with LOI and ARM, the higher and more variable Fe/Ti ratios of unit 2 also display a similar asymmetrical increase towards maximum values between 50 and 60 cm core depth. This build-up is also interrupted in the Fe/Ti record during intervals 1, 2 and 3 where values are lowest.

We used conservative Titanium (Ti) to detect changes in lithogenic influx and glacier mass turnover following Bakke et al. (2009). Ti elemental count rates were normalized against LOI ("normalization") to address the closed-sum effect (Rollison, 1993) and isolate variability not related to changes in sediment organic content. Figure 4 indicates that down-core Ti/LOI variability bears great resemblance to the previously described DBD record as demonstrated by a Spearman`s rho ($\varrho$) of 0.944 (n = 616). Values peak in the course-grained sandy silts of unit 4 and are generally high in the minerogenic silty clays of units 1 and 3. Ti/LOI ratios gradually decrease from the latter unit towards low background values of organic-rich unit 2. As can be seen in figure 4, the minerogenic intervals 1, 2 and 3 also show up as marked features in the Ti/LOI record. As with DBD, intervals 2 and 3 are particularly pronounced with values similar to the minerogenic sediments of unit 1. Like DBD, Ti/LOI values are highly variably throughout unit 1. After levelling off after the onset of minerogenic sedimentation, average values decline while displaying a high degree of variability before peaking again around 4 cm depth.

## Ordination

To detect common environmental variability in our dataset and help assess whether proxies show a shared response to glacier activity, we carried out PCA following Vasskog et al. (2012) and Bakke et al. (2013). Figure 9 shows the ensuing ordination diagram with the 9 selected geochemical, physical and magnetic variables. Post-analysis transformation included scaling sample scores using a 0.4 factor, suggested by CANOCO, to further highlight inter-variable correlations. Here, we plotted sample scores along the first two ordination axes (PC1 and PC2) which together capture 84.5 % of variation in core HAP0212. PC1 is most significant and explains 70.5 % of all variation, signifying strong shared variability between the measured proxies in

Hajeren. As demonstrated by figure 9, ordination underlines the robustness of the performed cluster analysis as samples from individual units group together. Samples from the silty clay of units 1 and 3 plot close to PC1 in the lower left quarter of the ordination diagram and are associated with detrital indicators Rb, Zr, Ti and K as well as DBD. Scores for the minerogenic intervals 1, 2 and 3 group near those from units 1 and 3. Samples from the coarse-grained and compacted unit 4 also plot near the DBD vector. Moreover, the distinctness of unit 4 is reflected by the PCA by a relatively strong loading on PC2 and grouping of samples close to the MS vector. Unit 2 samples plot on a gradient along PC1 between the groups of units 1 and 3 towards the correlated variables ARM, LOI and Fe. In general, PC1 covers a gradient of variability between minerogenic indicators (DBD, Rb, Zr, Ti and K) and variables that co-vary with LOI (Fe and ARM).

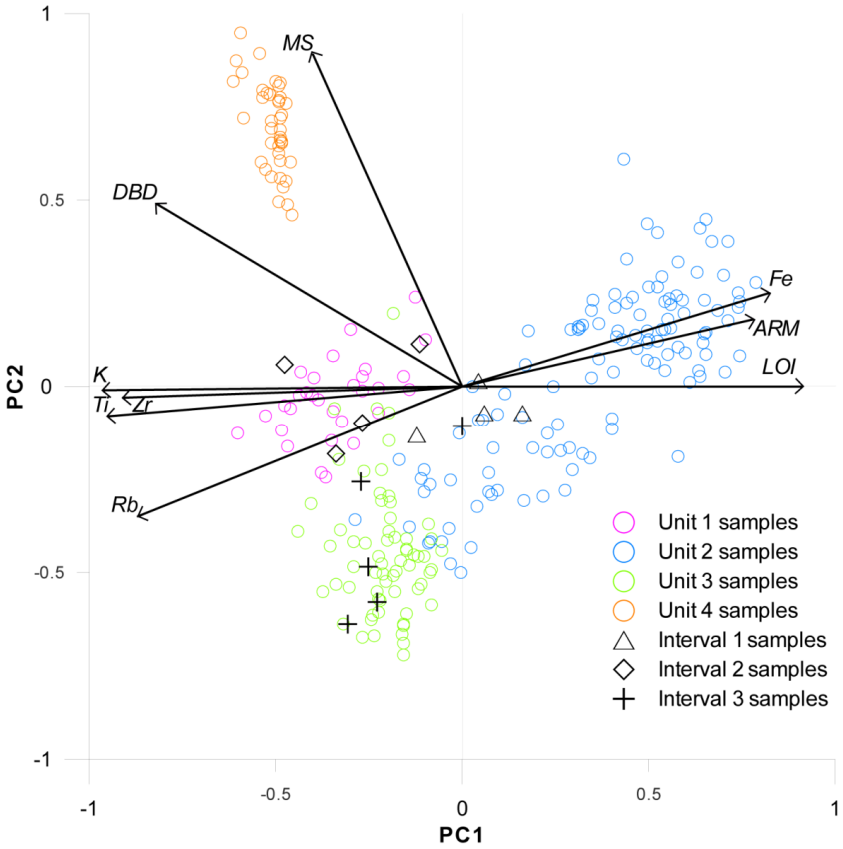

***Fig. 9**. An ordination diagram, showing the results of PCA on scaled first (PC1) and second (PC2) ordination axes. Open circles represent individual 1 cm resolution down-core samples (n = 250), distinguishing between units using different colours. Samples from minerogenic intervals 1, 2 and 3 are plotted using symbols. Vectors reflect the PCA scores of selected environmental variables.*

# Discussion

## Detection of glacier activity

### *Sources of error*

Understanding catchment processes is imperative for an accurate reconstruction of glacier activity using multi proxy analyses of sediments deposited in distal glacier-fed lakes (Rubensdotter and Rosqvist, 2009; Wittmeier et al., 2015). This is particularly pertinent for processes that may leave a similar physical imprint in lacustrine sediments (Ballantyne, 2002; Leonard, 1997; Rubensdotter and Rosqvist, 2009). Based on the laminated sediments of core HAP0212 and the grain size signature of selected sediments ("grain size"), we suggest that mass wasting events had a limited influence on the Hajeren record. Moreover, a scarcity of mapped fine-grained glacigenic deposits in the catchment indicates that the impact of paraglacial modification is limited (Van der Bilt et al., 2015) . This is supported by minimal minerogenic input in unit 2, also suggesting a high sensitivity of the record to the signature of glacial flour.

A site-specific source of error may stem from the presence of two glaciers in the Hajeren catchment (Fig.1), potentially responding differently to the same climate forcing. However, based on their mapped extent (NPI, 2015), both glaciers show a uniform post-LIA retreat pattern as anticipated based on a corresponding aspect and elevation range. To further assess their individual climate sensitivity, we applied the Hypsometric Index (HI) proposed by Jiskoot et al. (2009) using aerials, a Digital Elevation Model (DEM) and mapped glacier extent (NPI, 2015). Near-identical HI values of 2.13 for the North- and 2.14 for the South Glacier support the notion that both glaciers respond similarly to climate variability.

### *5.1.2 Multi-proxy approach*

Organic content, approximated by LOI, is often used as an inverse indicator of minerogenic sedimentation in glacier-fed lakes to reconstruct glacier activity (Dahl et al., 2003; Karlén, 1976). However, as will be discussed, LOI values in Lake Hajeren do not appear to be governed by minerogenic sedimentation alone, as suggested by a high correlation with redox sensitive Fe/Ti ratios as well as ARM (Fig. 5). Moreover, low (<5%) values during intervals of generally dense minerogenic sedimentation extinguish the amplitude of variation recorded by the LOI record (Bakke et al., 2005; McKay and Kaufman, 2009).

To overcome these limitations, we use DBD to track variations in minerogenic lacustrine input and relate these to past variations in glacier activity. Apart from the influx of minerogenic matter, DBD is affected by variations in grain size. Highest values are found in fine-grained, relatively poorly sorted sediments of low porosity (Menounos, 1997). Glacigenic suspended load is typically dominated by the fine clay and silt fractions (Leemann and Niessen, 1994b). Therefore, lacustrine sediments with a glacial imprint are characterized by a high density as demonstrated by Bakke et al. (2005).

Following Vasskog et al. (2012) and Wittmeier et al. (2015), we also use PCA to help fingerprint glacigenic sediments. Based on strong loading of DBD and minerogenic indicators Ti, K, Zr and Rb, we argue that PC1 captures the signal of glacier variability in the catchment (Fig. 9). With a loading of -0.945, Ti kcps demonstrate the highest PC1 scores. As such, we validate the physical evidence from DBD variability using concurrent changes in LOI-normalized Ti to detect changes in glacier mass turnover (Bakke et al., 2009) (Fig.10). Also, samples from unit 1, a period of sustained minerogenic sedimentation and historical glacier activity, group in the same sector of the ordination plot as DBD and Ti/LOI (Fig. 9).

Finally, the applied multi-proxy toolbox includes grain size analysis on previously described selected minerogenic intervals (Fig. 4 and 7). Quantification of the fine-

grained fractions allows additional testing and identification of a glacial signature (Leemann and Niessen, 1994a; Matthews and Karlén, 1992; Peach and Perrie, 1975).

## Non-glacial environmental variability

Minimal minerogenic input is prevalent during the Middle to Late Holocene sediments of unit 2 (Fig. 4). Sediments are mostly organic-rich (Fig. 5) and high LOI correlates strongly with redox-sensitive Fe/Ti ratio ($\varrho = 0.68$, $n = 338$), as well as XARM ($\varrho = 0.67$, $n = 256$). We argue that, apart from the inferred advances around 4100, 3300 and 1100 cal BP ("Early Neoglacial advances") glaciers disappeared from the catchment after ≈ 7.4-6.7 ka cal BP. Instead, it seems plausible that shifting redox conditions in the lake catchment or within the lake itself governed the sedimentation throughout most of unit 2, particularly between ≈ 4000 and 1400 cal BP. The transition from minerogenic Early Holocene sediments towards core samples that group with LOI and correlated Fe/Ti and ARM values is expressed in the ordination diagram of figure 9. Evidently, ARM variability does not co-vary with shifts in minerogenic-derived magnetic grain size in Hajeren as in other glacier-fed lakes (Matthews and Karlén, 1992; Snowball and Sandgren, 1996). Based on the congruous positive relationship seen in figure 8, ARM variability in unit 2 appears to be biologically controlled. Though we lack data to detect biogenic magnetite using a Moskowitz diagram (Moskowitz et al., 1993), we tentatively attribute this biological control to Magnetotactic Bacteria (MTB`s), following Paasche et al. (2004). These synthesize Magnetite near the Oxic-Anoxic Transition Zone (OATZ) and also occur in adjacent lake Kløsa (Røthe et al., 2015). Coeval high and correlated Fe/Ti ratios, an indicator of redox diagenesis (Croudace et al., 2006; Cuven et al., 2010), support the prevalence of anoxic conditions.

## Holocene glacier variability

### *Deglaciation*

Distinctly disparate sediment characteristics suggest a different source of the sediments from units 4 and 5 as compared to the rest of the core. This dissimilarity is particularly well expressed by high MS values and captured by the ordination

diagram displayed in figure 9. In general, high DBD and Ti/LOI values indicate high lithogenic influx in a dynamic setting as demonstrated by the course-grained lithology (Fig. 4). The association of the sandy silts of unit 4 with the underlying diamict and gravel of unit 5 is diagnostic for the transition from ice-contact to distal glacier-fed lake during ice retreat (Ballantyne, 2002). In keeping with this interpretation, we suggest that the diamict of unit 5 is a till, deposited when ice occupied the lake basin. The overlying open-work gravel facies is indicative of sub-aqueous outwash as suggested by Ashley (1995). In summary, following ice retreat, the depositional environment of Hajeren progressively evolved from an ice-contact delta to a more ice-distal setting. The latter gravels progressively fine up into the silty sands of unit 4, suggesting a gradual transition towards a more ice-distal setting (Ballantyne, 2003). The bulk of unit 4 comprises stratified sediments where alternations between silty and sandy beds are recorded by shifts in Ti/LOI (Fig. 4). Such facies are associated with rapid deposition of reworked glacigenic material during deglaciation (Eyles et al., 1990; Müller, 1999). High sedimentation rates are furthermore supported by the presence of dewatering structures. Based on the observed compacted nature of unit 4 deposits, these may also reflect deformation by stranded ice, following Fulton (1965) and Eyles et al. (1991). Overall, we suggest that the sediments of unit 4 and 5 were rapidly deposited during regional deglaciation. Based on the presented age-depth model (Fig. 6), we argue that the Hajeren watershed deglaciated prior to 11300 cal BP. These findings agree with Landvik et al. (2013), who propose deglaciation of Mitrahalvøya peninsula around 12.2 ka BP.

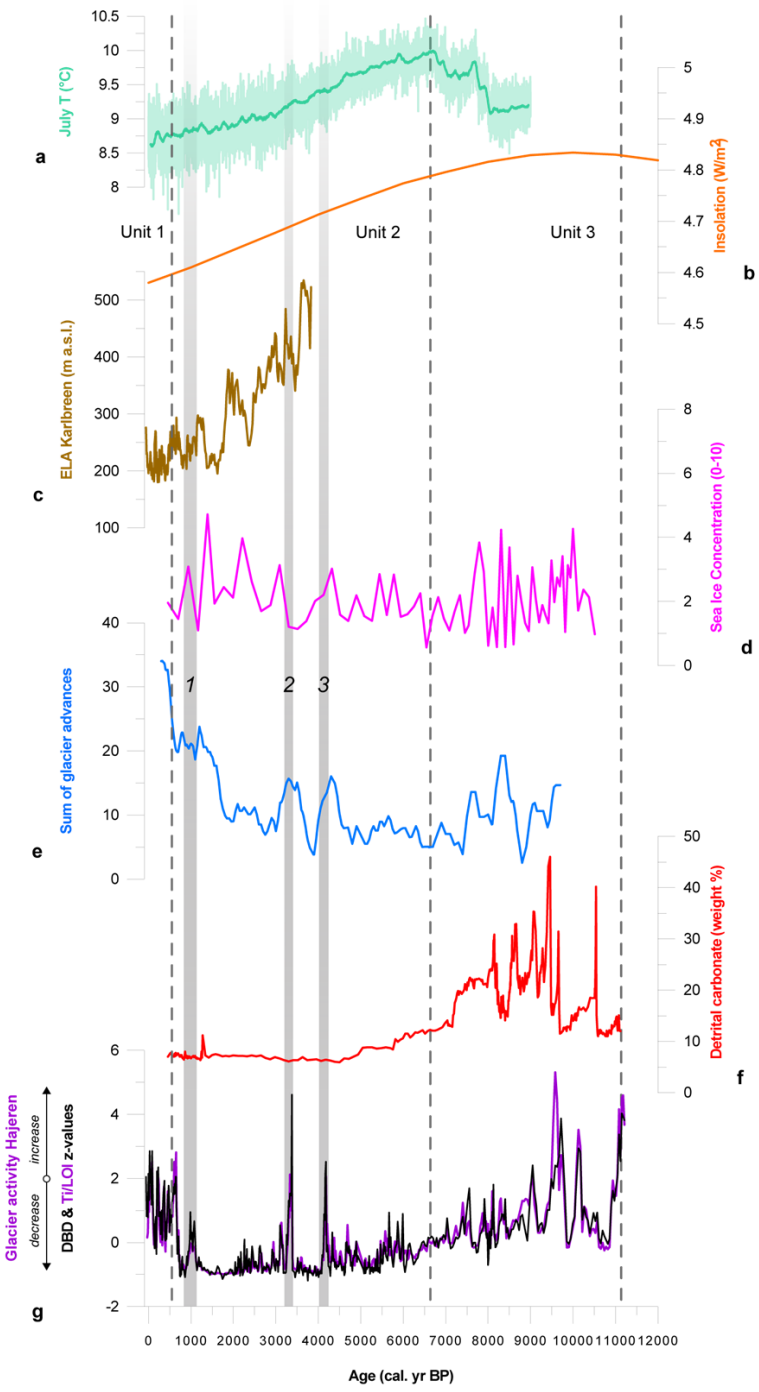


***Fig.10**. Comparison between standardized scores of main indicators glacier activity indicators DBD and Ti/LOI from Hajeren (G) and July temperature*

*modelled by Renssen et al. (2009) (A), summer insolation at 80° North (Huybers, 2006) (B), Equilibrium Altitude Line (ELA) reconstruction for adjacent Karlbreen by Røthe et al. (2015) (C), scaled sea-ice concentration from (de Vernal et al., 2013)(D), the sum of reconstructed glacier advances from Wanner et al. (2008) (E) and Labrador shelf Detrital Carbonate Peaks (DCPs) from Jennings et al. (2015) (F). Neoglacial glacier advances 1, 2 and 3 are emphasized using grey bars.*

### *11270-6700 cal BP: Early Holocene glacier activity*

All proxy records in figure 4 show a steep drop after the transition from unit 4 to 3, indicative of the previously discussed shift in ice proximity and general depositional environment after deglaciation. However, the indicators used to reconstruct glacier activity, DBD and Ti/LOI, show that minerogenic input remains high but variable, with a gradual decrease towards unit 2 (≈ 6700 cal BP). Moreover, samples from unit 3 have similar ordination scores as those from unit 1 (Fig. 9), deposited during a period of documented glacier activity in the catchment ("setting"). Notwithstanding frequent high-amplitude variability, visual inspection of unit 3 reveals a continuous sequence of regularly laminated sediments, suggesting of a low-energy depositional environment.

We therefore argue that glaciers were active in the Hajeren catchment during the Early Holocene. Modification of older glacigenic sediments cannot be excluded (Rubensdotter and Rosqvist, 2009). However, the small catchment size (Fig. 1) (Harbor and Warburton, 1993) and rapid exhaustion of fine-grained deposits (Van der Bilt et al., 2015) argue against prolonged paraglacial activity.

Both indicators of glacier activity as well as sea ice concentration variations in the Fram Strait by de Vernal et al. (2013) indicate a dynamic Early Holocene towards ≈ 9000 cal BP (Fig. 10f and 10g). This period was characterized by a series of well-expressed high amplitude peaks in glacier activity at 10130, between 9500-9700 and around 9050 cal BP. Timing of these events fall within the uncertainty margin of a 10Be dated moraine at nearby Kongsfjordhallet (Henriksen et al., 2014). Moreover, the most pronounced peak between 9500-9700 cal BP coincides with an established Scandinavian glacier advance, known as the Erdalen event (Nesje, 2009). Based on its amplitude and a gradual build-up, we argue this event reflects a Holocene glacier

maximum. The mentioned Stage 1 moraines provide geomorphological evidence for a pre-LIA maximum in the Hajeren catchment (Van der Bilt et al., 2015). Strong visual correspondence between the inferred peaks in Early Holocene glacier activity and Labrador shelf Ice Rafted Debris (IRD) spikes (Fig. 10f) (Jennings et al., 2015) hints at forcing by meltwater pulses from the retreating Laurentide Ice Sheet (LIS). This is supported by a maximum cross correlation of 0.42 at a 20 year time lag for the discussed interval. It has been argued that such discharge cooled the North Atlantic by inhibiting meridional overturning circulation (Kaplan and Wolfe, 2006; Thornalley et al., 2009). Figure 10f illustrates that two of these IRD peaks coincide with the inferred 9500-9700 cal BP glacier maximum in the Hajeren record. Correlation with IRD peaks found at North Atlantic sites more distal to the LIS further underlines the regional climatic significance of this event (Bond et al., 2001).

Following the inferred 9500-9700 cal BP Holocene glacier maximum, the amplitude of inferred events decreased markedly (Fig. 10g). This shift marks the arrival of Atlantic surface waters in the adjacent Kongsfjorden (Rasmussen et al., 2014; Ślubowska-Woldengen et al., 2007), which ameliorated local climate. Subsequent periods of increased glacier activity are less pronounced and minerogenic lacustrine input gradually declines towards unit 2 (Fig. 10g). However, this pattern is notably interrupted by three successive spikes in minerogenic input between ± 7900 and 8300 cal BP, simultaneous with an increase in sedimentation rates (Fig. 6). These events fall within the time frame of the well-known 8.2 ka BP event, another climatic perturbation driven by catastrophic meltwater pulses from the melting LIS (Alley and Ágústsdóttir, 2005; Daley et al., 2011; Kleiven et al., 2008). In contrast to other regional records (Wanner et al., 2011), the 8.2 ka BP event does not stand out as a prominent early Holocene climate event in the Hajeren record (Fig. 10g), as previously shown by (Hormes et al., 2009). However, it is argued that the 8.2 ka BP event was characterized by both cold and dry conditions (Rohling and Pälike, 2005; Spurk et al., 2002), and glacier mass balance depends on both temperature and precipitation (Oerlemans, 2005). We argue that arid conditions during the 8.2 ka BP event may have restricted glacier growth in the Hajeren catchment. We theorize that the concurrent reconstructed sea ice maximum (Fig. 10d) may have cut-off marine

moisture sources, in keeping with (Müller et al., 2012). Additionally, Greenland ice-core data revealed significant decadal-scale variability during the 8.2 ka BP, with a main event lasting less than 70 years (Thomas et al., 2007), constraining ice accumulation in the Hajeren catchment.

After spiking around 7400 cal BP, minerogenic input steadily decreases towards the transition to unit 2 (Fig. 10g). We therefore argue that glaciers disappeared from the catchment between ≈ 7400-6700 cal BP. This decline is concurrent with a sharp increase in modelled July temperatures towards mid-Holocene peak values (Fig. 10a) by Renssen et al. (2009). This simulation takes the cooling effect of melting LIS remnants into account, which may have helped sustain glacier activity in the Hajeren catchment by delaying and retarding the response to the Holocene summer insolation maximum (Fig. 10a and 10b). Our claim is supported by the onset of undisturbed sedimentation alongside an ice-cored moraine in adjacent Lake Kløsa after 6700 cal BP (Røthe et al., 2015). Moreover, this minimum age estimate of the termination of Early Holocene glacier activity concurs with the transition towards the organic-rich sediments of unit 2 in our record (Fig. 5).

### *4250-4050 and 3380-3230 cal BP: Early Neoglacial advances*

Mid-Holocene (unit 2) sediments are mostly organic-rich and appear to be governed by redox processes (Fig. 5 and 8). Generally, minerogenic input is minimal as reflected by low DBD and Ti/LOI values (Fig. 4). This pattern is interrupted by the previously discussed minerogenic intervals 3 and 2 (Fig. 4 and 5). Based on multiple lines of proxy evidence, we here argue these represent centennial-scale glacier advances between 4250-4050 and 3380-3230 cal BP, respectively.

During inferred events, henceforth referred to as advances 3 and 2 (Fig. 10g), the main indicators of glacier activity, Ti/LOI and DBD, peak at values similar to those seen in the Early Holocene (Fig. 10g). This analogy is supported by the grouping of advances 1 and 2 samples with those from units 3 and 1 in the ordination diagram of figure 8. Concurrently, declining LOI, (X)ARM and Fe/Ti values (Fig. 5) suggest a waning influence of biological (redox) processes on lake conditions during the

discussed intervals. This is also demonstrated by the deviation of LOI/XARM combinations from the inferred biologically driven trend for other Mid-Holocene samples (Fig. 8). Instead, samples from the discussed intervals plot near those from minerogenic unit 1, which comprises sediments from a period of documented historical glacier activity. Though the onset of these advances appears abrupt (Fig. 10g), both lithostratigraphy and radiograph grayscale imagery suggest gradual change, as indicated by the laminated nature of the sediments (Fig. 4 and 5). Also, underrepresentation of coarser fractions suggests these intervals were not deposited by rapid mass-wasting events (Karlén, 1981; Rubensdotter and Rosqvist, 2009) (Fig. 7). Instead, the observed bimodal grain size distribution, with modes in the fine and medium silt fractions, is diagnostic for glacigenic suspended load (Leemann and Niessen, 1994a; Støren et al., 2008; Vasskog et al., 2012).

The proposed centennial-scale cycles of glacier growth and decay are rapid, though not unprecedented. Jóhannesson et al. (1989) infer a response time of decades for small glaciers such as those of the Hajeren catchment. Moreover, reconstructed glacier activity at the comparably-sized Kråkenes cirque system shows a similarly fast sequence of formation and disappearance during the Younger Dryas (Bakke et al., 2009; Paasche, 2011). Also, evidence from modelling studies suggests that small and steep glaciers, like those in the Hajeren catchment, generally show a sensitive response to climate shifts (Jiskoot, 2011). Finally, short response time is also supported by photographic evidence of a rapid historical post-LIA retreat of both glaciers in the catchment (NPI, 2015).

Based on marine proxy evidence from the Fram Strait and adjacent Kongsfjorden (Rasmussen et al., 2014; Werner et al., 2013), declining sea-surface temperatures and increased ice-rafting mark the end of the Holocene Hypsithermal on Svalbard after 5000 cal BP. This is corroborated by terrestrial evidence from macrofossil analysis (Birks, 1991), suggesting cooler summers after 4000 cal BP. First evidence of glacier reformation comes from Linnébreen on southwest Spitsbergen, which reformed after 4600 ± 0.2 cal BP (Reusche et al., 2014; Svendsen and Mangerud, 1997). Røthe et al. (2015) suggest that neighbouring Karlbreen reformed around 3800 cal BP. As such,

the discussed glacier advances in the Hajeren catchment occurred after the onset of Neoglaciation on Svalbard. Moreover, reviews of Holocene glacier variability in the (sub)-Arctic shows that timing of both events is consistent with established advances in Scandinavia (Nesje, 2009), Iceland (Geirsdóttir et al., 2009) as well as Alaska (Barclay et al., 2009) and Canada (Menounos et al., 2009). This is also reflected by a correlation with maxima in reconstructed glacier advances from mostly mid-high latitude sites on the Northern Hemisphere by Wanner et al. (2011), shown in figure 10e.

We propose that the interplay between long- and short-term regional forcings created suitable conditions for the discussed centennial-scale glacier advances. The onset of Neoglacial cooling occurred against a background of gradual orbital forced summer cooling as shown in figure 10b (Huybers, 2006) . Stronger advection of Arctic water, linked to increased sea-ice export through the Fram Strait (Funder et al., 2011; Werner et al., 2013), led to a further deterioration of climate conditions after 5000 cal BP. We argue that this cooling trend progressively lowered the glaciation threshold in the Hajeren catchment, enabling super-imposed shorter-term forcings to create suitable conditions for the discussed advances. Based on their duration and correspondence with regional records of glacier variability (Wanner et al., 2011) (Fig. 10e), we infer a short-term forcing with a North Atlantic signature. This claim is also supported by correlation of the discussed events with peaks in North Atlantic iceberg-derived debris (Bond et al., 1997). Though initially solely attributed to low solar activity (Bond et al., 2001), recent studies highlight the contribution of internal dynamics of the North Atlantic in driving these quasi-cyclic peaks (Debret et al., 2007; Debret et al., 2009; Renssen et al., 2007; Solomina et al., 2015; Wanner et al., 2011).

### *3230-700 cal BP: unfavorable conditions for glacier growth*

Following the previously discussed short-lived Early Neoglacial glacier advances, minerogenic input drops to a Holocene minimum (Fig. 10g). Based on this evidence, we suggest that glaciers were absent from the catchment between ≈ 3230-1100 cal BP. Though Humlum et al. (2005) also infer ice-free conditions for Longyearbreen

glacier before 1100 cal BP, our record differs from other glacier reconstructions from western Svalbard (Reusche et al., 2014; Røthe et al., 2015). These studies propose a glacier maximum around 1700 cal BP. We argue that glacier growth at that time was driven by increased winter precipitation and suppressed in the lower-lying Hajeren catchment cirques by concurrent warm summers.

After 3000 cal BP, marine records from the Fram strait suggest a generally stronger influence of cold Arctic surface waters and increased sea-ice cover (de Vernal et al., 2013; Rasmussen et al., 2014; Werner et al., 2013) (Fig. 10d). Forwick and Vorren (2009) infer shore-fast ice conditions in Isfjorden in South Spitsbergen. Such conditions would have cut off the main moisture source from the maritime glaciers of West Spitsbergen, creating unfavourable conditions for ice growth (Müller et al., 2012). Apart from a short-lived lowering around 2300 cal BP, this is also reflected by a fairly constant reconstructed Equilibrium Line Altitude (ELA) of adjacent Karlbreen (Fig. 10c). However, particularly after 2000 cal BP (Rasmussen et al., 2014), unstable conditions drove episodic, rapid sea-ice fluctuations that increased moisture availability (de Vernal et al., 2013; Liu et al., 2012; Müller et al., 2012) (Fig. 10d). Werner et al. (2013) attribute this shift to episodic strengthening of warmer Atlantic water inflow, ameliorating climate. This is supported by Sarnthein et al. (2003), who infer SST peaks concurrent with the mentioned 2200 cal BP ELA lowering and 1700 cal BP glacier maximum at adjacent Karlbreen. Moreover, D'Andrea et al. (2012) and Kaufman (2009) show relatively high coeval summer air temperatures. Based on the outlined evidence, we concur with Røthe et al. (2015) that increased winter precipitation drove glacier growth at the time. We argue that warm summers offset any gains in accumulation through increased ablation in the low-lying Hajeren catchment cirques. In short, we suggest that between ≈ 3230-1100 cal BP, conditions in the Hajeren catchment were either too dry or too warm to sustain glacier growth.

Around 1100 cal BP, a sustained peak in Ti/LOI and DBD values during interval 1 marks a shift towards predominantly minerogenic lacustrine sedimentation (Fig. 10g). Though peak values of this interval are subdued compared to the discussed

minerogenic intervals, ordination and grain size data suggest a similar signature (Fig. 7 and 9). We therefore argue that interval 1 reflects a period of glacier activity, henceforth referred to as advance 1 (Fig. 10). Timing corresponds to the re-growth of Longyearbreen glacier on southern Svalbard documented by Humlum et al. (2005). Also, figure 10c shows a synchronous 100m lowering of the reconstructed ELA at adjacent Karlbreen. The temperature record of D'Andrea et al. (2012) indicate that the period around 1100 cal BP was characterized by the coolest summers of the past 1800 years. This signals that the discussed advance was temperature-driven as previously suggested by Humlum et al. (2005).

Shortly after 1000 cal BP, minerogenic input drops to background levels (Fig. 10g). This decline coincides with a period marked by high summer temperatures (D'Andrea et al., 2012). We propose that this warming ended the previously discussed advance, represented by interval 1. Subsequently, organic-rich sediments become prevalent (Fig. 5). We argue that this epoch, which lasted until ≈ 750 cal BP (Fig. 10g), marks the Medieval Climate Anomaly (MCA) (Bradley et al., 2003). These findings agree with Spielhagen et al. (2011) and Grinsted et al. (2006), who reconstruct concurrent summer warming of sub-surface waters and increased ice core melt, respectively.

### *700 cal BP-present: Little Ice Age*

Unit 1 marks the first prolonged episode of minerogenic sedimentation in Lake Hajeren since ≈ 7400-6700 cal BP as shown in figures 4 and 10g. We propose that the transition into unit 1 marks the onset of the Little Ice Age (LIA) in the Hajeren catchment. Based on sustained high minerogenic input, we argue that glaciers were continuously present after ≈ 700 cal BP. Coincident minimum ELA`s at Karlbreen suggest this time interval was marked by the most favourable local conditions for glacier growth in at least 3800 years (Fig. 10e and 10c). Also, Dylmer et al. (2013) demonstrate that this transition is concurrent with a sudden reduction in Atlantic water flow off Svalbard. Timing of LIA glacier growth around 700 cal BP also agrees with the findings of Svendsen and Mangerud (1997) for Linnébreen glacier and Furrer (1991) for Adolfbreen glacier on northwest Spitsbergen. Following with

Werner (1993) and Røthe et al. (2015), we observe a two-step LIA in our record with glacier activity peaking around 650 cal BP and again at the close of the 19th century (Fig. 10c and 10g).

While available records all present evidence for widespread glacier growth on Svalbard during the LIA, its signature remains ambiguous. Müller et al. (2012) infer extensive sea-ice cover for the past 600 years, based on high IP25 flux rates. Additionally, Fauria et al. (2010) suggest maximum winter sea-ice extent between the 17th and 19th centuries using ice-core d18O data from Lomonosovfonna. This evidence is supported by low concentrations of marine-derived salt ions from the same site (Grinsted et al., 2006). Furthermore, Spielhagen et al. (2011) reconstructed increasing summer SST`s in the Eastern Fram Strait during this period. In line with these findings, D'Andrea et al. (2012) demonstrate a concurrent increase in summer air temperatures. The outlined combination of extensive sea-ice and warm summers would starve glaciers from moisture in winter (Liu et al., 2012; Müller et al., 2012) whilst increasing summer ablation, creating conditions unfavourable for glacier growth (Oerlemans, 2005). Hence, the climatic driver of LIA glacier growth on Svalbard remains elusive and deserves future investigation.

## Conclusions

This study presents a continuous reconstruction of Holocene glacier variability on Svalbard at centennial timescales, combining physical, geochemical and magnetic proxies with multivariate statistics. Integrating our findings from Lake Hajeren in a regional paleoclimatic context, we observe a three-staged Holocene climate history. Following deglaciation around 11300 cal BP, glaciers remained present in the catchment throughout the Early Holocene, culminating in a glacier maximum around 9.5 cal BP. During this period, glacier activity appears to be affected by meltwater pulses from the melting LIS (Jennings et al., 2015). Following a late onset of the HTM around 6.7 ka cal BP, in line with modelled cooling effects from the melting LIS (Renssen et al., 2009), glaciers disappear from the catchment. Instead, changing redox conditions driven by stratification of the water column governed lacustrine

sedimentation during most of the Middle and Late Holocene. Two advances between 4205-4050 and 3380-3220 cal BP mark the onset of the Neoglacial and coincide with brief episodes of North Atlantic cooling (Bond et al., 2001; Debret et al., 2007; Renssen et al., 2007). A gradual decline in summer insolation progressively lowered the glaciation threshold towards the Late Holocene, resulting in prolonged glacier activity around 700 cal BP. This local onset of the LIA is in line with advances reported at nearby sites (Furrer, 1991; Røthe et al., 2015; Svendsen and Mangerud, 1997; Werner, 1993). The rapid response of the small Hajeren glaciers improves our understanding of climate variability on Svalbard, suggesting that the Holocene was punctuated by major centennial-scale perturbations. As such, this study underlines the value of glacier-fed lake sediments in contextualizing Arctic climate dynamics.

### Acknowledgements

This study has received funding from the Norwegian Research Council through the project «Shifting Climate States of the Polar Regions» (210004). This work was also supported by the Norwegian Research Council funded Arctic Field Grant program as well as the Norwegian Research School in Climate Dynamics. We would like to acknowledge Rob D`Anjou, Nicholas Balascio, Marthe Gjerde and Torgeir Røthe for retrieving the studied sediment cores. Finally, we thank our reviewers, Ólafur Ingólfsson and Anne Hormes, for improving this manuscript with their comments.

## References

Aagaard-Sørensen, S., Husum, K., Hald, M., Marchitto, T., Godtliebsen, F., 2014. Sub sea surface temperatures in the Polar North Atlantic during the Holocene: Planktic foraminiferal Mg/Ca temperature reconstructions. The Holocene 24, 93-103.
Alley, R.B., Ágústsdóttir, A.M., 2005. The 8k event: cause and consequences of a major Holocene abrupt climate change. Quaternary Science Reviews 24, 1123-1149.
Ashley, G., 1995. Glaciolacustrine environments. Glacial Environments 1, 417-444.
Bakke, J., Dahl, S.O., Paasche, Ø., Riis Simonsen, J., Kvisvik, B., Bakke, K., Nesje, A., 2010. A complete record of Holocene glacier variability at Austre Okstindbreen, northern Norway: an integrated approach. Quaternary Science Reviews 29, 1246-1262.
Bakke, J., Lie, Ø., Heegaard, E., Dokken, T., Haug, G.H., Birks, H.H., Dulski, P., Nilsen, T., 2009. Rapid oceanic and atmospheric changes during the Younger Dryas cold period. Nature Geoscience 2, 202-205.

Bakke, J., Nesje, A., Dahl, S.O., 2005. Utilizing physical sediment variability in glacier-fed lakes for continuous glacier reconstructions during the Holocene, northern Folgefonna, western Norway. The Holocene 15, 161-176.
Bakke, J., Trachsel, M., Kvisvik, B.C., Nesje, A., Lyså, A., 2013. Numerical analyses of a multi-proxy data set from a distal glacier-fed lake, Sørsendalsvatn, western Norway. Quaternary Science Reviews 73, 182-195.
Ballantyne, C., 2003. Paraglacial landsystems. Glacial Landsystems. Arnold, London, 432-461.
Ballantyne, C.K., 2002. Paraglacial geomorphology. Quaternary Science Reviews 21, 1935-2017.
Barclay, D.J., Wiles, G.C., Calkin, P.E., 2009. Holocene glacier fluctuations in Alaska. Quaternary Science Reviews 28, 2034-2048.
Benestad, R., Hanssen-Bauer, I., Skaugen, T., Førland, E., 2002. Associations between sea-ice and the local climate on Svalbard. Oslo: Norwegian Meteorological Institute Report, 1-7.
Birks, H., 1998. DG Frey and ES Deevey Review 1: Numerical tools in palaeolimnology–Progress, potentialities, and problems. Journal of Paleolimnology 20, 307-332.
Birks, H.H., 1991. Holocene vegetational history and climatic change in west Spitsbergen-plant macrofossils from Skardtjørna, an Arctic lake. The Holocene 1, 209-218.
Blaauw, M., 2010. Methods and code for 'classical' age-modelling of radiocarbon sequences. Quaternary Geochronology 5, 512-518.
Blott, S.J., Pye, K., 2001. GRADISTAT: a grain size distribution and statistics package for the analysis of unconsolidated sediments. Earth surface processes and Landforms 26, 1237-1248.
Boës, X., Rydberg, J., Martinez-Cortizas, A., Bindler, R., Renberg, I., 2011. Evaluation of conservative lithogenic elements (Ti, Zr, Al, and Rb) to study anthropogenic element enrichments in lake sediments. Journal of Paleolimnology 46, 75-87.
Bond, G., Kromer, B., Beer, J., Muscheler, R., Evans, M.N., Showers, W., Hoffmann, S., Lotti-Bond, R., Hajdas, I., Bonani, G., 2001. Persistent solar influence on North Atlantic climate during the Holocene. Science 294, 2130-2136.
Bond, G., Showers, W., Cheseby, M., Lotti, R., Almasi, P., Priore, P., Cullen, H., Hajdas, I., Bonani, G., 1997. A pervasive millennial-scale cycle in North Atlantic Holocene and glacial climates. science 278, 1257-1266.
Bradley, R.S., Hughes, M.K., Diaz, H.F., 2003. Climate in medieval time. Science 302, 404-405.
Carrivick, J.L., Tweed, F.S., 2013. Proglacial lakes: character, behaviour and geological importance. Quaternary Science Reviews 78, 34-52.
Croudace, I.W., Rindby, A., Rothwell, R.G., 2006. ITRAX: description and evaluation of a new multi-function X-ray core scanner. SPECIAL PUBLICATION-GEOLOGICAL SOCIETY OF LONDON 267, 51.
Cuven, S., Francus, P., Lamoureux, S.F., 2010. Estimation of grain size variability with micro X-ray fluorescence in laminated lacustrine sediments, Cape Bounty, Canadian High Arctic. Journal of Paleolimnology 44, 803-817.
D'Andrea, W.J., Vaillencourt, D.A., Balascio, N.L., Werner, A., Roof, S.R., Retelle, M., Bradley, R.S., 2012. Mild Little Ice Age and unprecedented recent warmth in an 1800 year lake sediment record from Svalbard. Geology 40, 1007-1010.
Dahl, S.O., Bakke, J., Lie, Ø., Nesje, A., 2003. Reconstruction of former glacier equilibrium-line altitudes based on proglacial sites: an evaluation of approaches and selection of sites. Quaternary Science Reviews 22, 275-287.
Daley, T.J., Thomas, E.R., Holmes, J.A., Street-Perrott, F.A., Chapman, M.R., Tindall, J.C., Valdes, P.J., Loader, N.J., Marshall, J.D., Wolff, E.W., Hopley, P.J., Atkinson, T., Barber,

K.E., Fisher, E.H., Robertson, I., Hughes, P.D.M., Roberts, C.N., 2011. The 8200 yr BP cold event in stable isotope records from the North Atlantic region. Global and Planetary Change 79, 288-302.
Dallmann, W.K.E., 2015. Geoscience Atlas of Svalbard. Norwegian Polar Institute Tromsø.
de Vernal, A., Hillaire-Marcel, C., Rochon, A., Frechette, B., Henry, M., Solignac, S., Bonnet, S., 2013. Dinocyst-based reconstructions of sea ice cover concentration during the Holocene in the Arctic Ocean, the northern North Atlantic Ocean and its adjacent seas. Quaternary Science Reviews 79, 111-121.
Debret, M., Bout-Roumazeilles, V., Grousset, F., Desmet, M., McManus, J.F., Massei, N., Sebag, D., Petit, J.-R., Copard, Y., Trentesaux, A., 2007. The origin of the 1500-year climate cycles in Holocene North-Atlantic records. Climate of the Past Discussions 3, 679-692.
Debret, M., Sebag, D., Crosta, X., Massei, N., Petit, J.-R., Chapron, E., Bout-Roumazeilles, V., 2009. Evidence from wavelet analysis for a mid-Holocene transition in global climate forcing. Quaternary Science Reviews 28, 2675-2688.
Dylmer, C., Giraudeau, J., Eynaud, F., Husum, K., Vernal, A.D., 2013. Northward advection of Atlantic water in the eastern Nordic Seas over the last 3000 yr. Climate of the Past 9, 1505-1518.
Eyles, N., Mullins, H.T., Hine, A.C., 1990. Thick and fast: Sedimentation in a Pleistocene fiord lake of British Columbia, Canada. Geology 18, 1153-1157.
Eyles, N., Mullins, H.T., Hine, A.C., 1991. The seismic stratigraphy of Okanagan Lake, British Columbia; a record of rapid deglaciation in a deep 'fiord-lake'basin. Sedimentary Geology 73, 13-41.
Fauria, M.M., Grinsted, A., Helama, S., Moore, J., Timonen, M., Martma, T., Isaksson, E., Eronen, M., 2010. Unprecedented low twentieth century winter sea ice extent in the Western Nordic Seas since AD 1200. Climate Dynamics 34, 781-795.
Folk, R.L., Ward, W.C., 1957. Brazos River bar: a study in the significance of grain size parameters. Journal of Sedimentary Research 27.
Forwick, M., Vorren, T.O., 2009. Late Weichselian and Holocene sedimentary environments and ice rafting in Isfjorden, Spitsbergen. Palaeogeography, Palaeoclimatology, Palaeoecology 280, 258-274.
Fulton, R.J., 1965. Silt deposition in late-glacial lakes of southern British Columbia. American Journal of Science 263, 553-570.
Funder, S., Goosse, H., Jepsen, H., Kaas, E., Kjær, K.H., Korsgaard, N.J., Larsen, N.K., Linderson, H., Lysså, A., Möller, P., 2011. A 10,000-year record of Arctic Ocean sea-ice variability—view from the beach. Science 333, 747-750.
Furrer, G., 1991. Zum Alter Waamoränen um das Vorfeld des Erikbreen und auf der westlichsten Lernerinsel - ein Beitrag zur Gletchergeschichte des Liefdesfjords. Sonderveröffentlichungen, Geologisches Institut der Universität zu Köln 21.
Førland, E.J., Benestad, R., Hanssen-Bauer, I., Haugen, J.E., Skaugen, T.E., 2012. Temperature and precipitation development at Svalbard 1900–2100. Advances in Meteorology 2011.
Geirsdóttir, Á., Miller, G.H., Axford, Y., Sædís, Ó., 2009. Holocene and latest Pleistocene climate and glacier fluctuations in Iceland. Quaternary Science Reviews 28, 2107-2118.
Grimm, E., 2011. Tilia software v. 1.7. 16. Illinois State Museum, Springfield.
Grimm, E.C., 1987. CONISS: a FORTRAN 77 program for stratigraphically constrained cluster analysis by the method of incremental sum of squares. Computers & Geosciences 13, 13-35.
Grinsted, A., Moore, J.C., Pohjola, V., Martma, T., Isaksson, E., 2006. Svalbard summer melting, continentality, and sea ice extent from the Lomonosovfonna ice core. Journal of Geophysical Research: Atmospheres (1984–2012) 111.

Guyard, H., Chapron, E., St-Onge, G., Labrie, J., 2013. Late-Holocene NAO and ocean forcing on high-altitude proglacial sedimentation (Lake Bramant, Western French Alps). The Holocene.
Harbor, J., Warburton, J., 1993. Relative rates of glacial and nonglacial erosion in alpine environments. Arctic and Alpine Research, 1-7.
Heiri, O., Lotter, A.F., Lemcke, G., 2001. Loss on ignition as a method for estimating organic and carbonate content in sediments: reproducibility and comparability of results. Journal of paleolimnology 25, 101-110.
Henriksen, M., Alexanderson, H., Landvik, J.Y., Linge, H., Peterson, G., 2014. Dynamics and retreat of the Late Weichselian Kongsfjorden ice stream, NW Svalbard. Quaternary Science Reviews 92, 235-245.
Hormes, A., Blaauw, M., Dahl, S.O., Nesje, A., Possnert, G., 2009. Radiocarbon wiggle-match dating of proglacial lake sediments–Implications for the 8.2 ka event. Quaternary geochronology 4, 267-277.
Hotelling, H., 1933. Analysis of a complex of statistical variables into principal components. Journal of educational psychology 24, 417.
Humlum, O., Elberling, B., Hormes, A., Fjordheim, K., Hansen, O.H., Heinemeier, J., 2005. Late-Holocene glacier growth in Svalbard, documented by subglacial relict vegetation and living soil microbes. The Holocene 15, 396-407.
Huybers, P., 2006. Early Pleistocene glacial cycles and the integrated summer insolation forcing. Science 313, 508-511.
Jennings, A., Andrews, J., Pearce, C., Wilson, L., Ólafsdóttir, S., 2015. Detrital carbonate peaks on the Labrador shelf, a 13–7 ka template for freshwater forcing from the Hudson Strait outlet of the Laurentide Ice Sheet into the subpolar gyre. Quaternary Science Reviews 107, 62-80.
Jiskoot, H., 2011. Dynamics of Glaciers, Encyclopedia of snow, ice and glaciers. Springer, pp. 245-256.
Jiskoot, H., Curran, C.J., Tessler, D.L., Shenton, L.R., 2009. Changes in Clemenceau Icefield and Chaba Group glaciers, Canada, related to hypsometry, tributary detachment, length–slope and area–aspect relations. Annals of Glaciology 50, 133-143.
Jóhannesson, T., Raymond, C.F., Waddington, E.D., 1989. A Simple Method for Determining the Response Time of Glaciers, in: Oerlemans, J. (Ed.), Glacier Fluctuations and Climatic Change. Springer Netherlands, pp. 343-352.
Jones, K.P.N., McCave, I.N., Patel, D., 1988. A computer-interfaced sedigraph for modal size analysis of fine-grained sediment. Sedimentology 35, 163-172.
Kaplan, M.R., Wolfe, A.P., 2006. Spatial and temporal variability of Holocene temperature in the North Atlantic region. Quaternary Research 65, 223-231.
Karlén, W., 1976. Lacustrine sediments and tree-limit variations as indicators of Holocene climatic fluctuations in Lappland, northern Sweden. Geografiska Annaler. Series A. Physical Geography, 1-34.
Karlén, W., 1981. Lacustrine Sediment Studies. A Technique to Obtain a Continous Record of Holocene Glacier Variations. Geografiska Annaler. Series A. Physical Geography, 273-281.
Kaufman, D.S., 2009. An overview of late Holocene climate and environmental change inferred from Arctic lake sediment. Journal of Paleolimnology 41, 1-6.
Kleiven, H.K.F., Kissel, C., Laj, C., Ninnemann, U.S., Richter, T.O., Cortijo, E., 2008. Reduced North Atlantic deep water coeval with the glacial Lake Agassiz freshwater outburst. Science 319, 60-64.
Koinig, K.A., Shotyk, W., Lotter, A.F., Ohlendorf, C., Sturm, M., 2003. 9000 years of geochemical evolution of lithogenic major and trace elements in the sediment of an alpine

lake–the role of climate, vegetation, and land-use history. Journal of Paleolimnology 30, 307-320.
Krasilščikov, A., 1975. Stratigraphy and tectonics of the Precambrian of Svalbard, The geological development of Svalbard during the Precambrian, Lower Palaeozoic, and Devonian. Symposium on Svalbard's geology. Oslo, pp. 2-5.
Kylander, M.E., Ampel, L., Wohlfarth, B., Veres, D., 2011. High-resolution X-ray fluorescence core scanning analysis of Les Echets (France) sedimentary sequence: new insights from chemical proxies. Journal of Quaternary Science 26, 109-117.
Lamoureux, S., Gilbert, R., 2004. Physical and chemical properties and proxies of high latitude lake sediments, in: Smol, J., Pienitz, R., Douglas, M.V. (Eds.), Long-term Environmental Change in Arctic and Antarctic Lakes. Springer Netherlands, pp. 53-87.
Landvik, J.Y., Brook, E.J., Gualtieri, L., Linge, H., Raisbeck, G., Salvigsen, O., Yiou, F., 2013. 10Be exposure age constraints on the Late Weichselian ice-sheet geometry and dynamics in inter-ice-stream areas, western Svalbard. Boreas 42, 43-56.
Larsen, D.J., Miller, G.H., Geirsdóttir, Á., Ólafsdóttir, S., 2012. Non-linear Holocene climate evolution in the North Atlantic: a high-resolution, multi-proxy record of glacier activity and environmental change from Hvítárvatn, central Iceland. Quaternary science reviews 39, 14-25.
Leemann, A., Niessen, F., 1994a. Holocene glacial activity and climatic variations in the Swiss Alps: reconstructing a continuous record from proglacial lake sediments. The Holocene 4, 259-268.
Leemann, A., Niessen, F., 1994b. Varve formation and the climatic record in an Alpine proglacial lake: calibrating annually-laminated sediments against hydrological and meteorological data. The Holocene 4, 1-8.
Legendre, P., Birks, H.J.B., 2012. From classical to canonical ordination, Tracking environmental change using lake sediments. Springer, pp. 201-248.
Leonard, E.M., 1985. Glaciological and climatic controls on lake sedimentation, Canadian Rocky Mountains. Zeitschrift für Gletscherkunde und Glazialgeologie 21, 35-42.
Leonard, E.M., 1997. The relationship between glacial activity and sediment production: evidence from a 4450-year varve record of neoglacial sedimentation in Hector Lake, Alberta, Canada. Journal of Paleolimnology 17, 319-330.
Liermann, S., Beylich, A.A., van Welden, A., 2012. Contemporary suspended sediment transfer and accumulation processes in the small proglacial Sætrevatnet sub-catchment, Bødalen, western Norway. Geomorphology 167–168, 91-101.
Liu, J., Curry, J.A., Wang, H., Song, M., Horton, R.M., 2012. Impact of declining Arctic sea ice on winter snowfall. Proceedings of the National Academy of Sciences 109, 4074-4079.
Loeng, H., 1991. Features of the physical oceanographic conditions of the Barents Sea. Polar research 10, 5-18.
Löwemark, L., Chen, H.-F., Yang, T.-N., Kylander, M., Yu, E.-F., Hsu, Y.-W., Lee, T.-Q., Song, S.-R., Jarvis, S., 2011. Normalizing XRF-scanner data: A cautionary note on the interpretation of high-resolution records from organic-rich lakes. Journal of Asian Earth Sciences 40, 1250-1256.
Matthews, J.A., Karlén, W., 1992. Asynchronous neoglaciation and Holocene climatic change reconstructed from Norwegian glaciolacustrine sedimentary sequences. Geology 20, 991-994.
McGuire, A.D., Chapin, F.S., Walsh, J.E., Wirth, C., 2006. Integrated Regional Changes in Arctic Climate Feedbacks: Implications for the Global Climate System. Annual Review of Environment and Resources 31, 61-91.

McKay, N.P., Kaufman, D.S., 2009. Holocene climate and glacier variability at Hallet and Greyling Lakes, Chugach Mountains, south-central Alaska. Journal of Paleolimnology 41, 143-159.
McKay, N.P., Kaufman, D.S., 2014. An extended Arctic proxy temperature database for the past 2,000 years. Scientific Data 1.
Menounos, B., 1997. The water content of lake sediments and its relationship to other physical parameters: an alpine case study. The Holocene 7, 207-212.
Menounos, B., Osborn, G., Clague, J.J., Luckman, B.H., 2009. Latest Pleistocene and Holocene glacier fluctuations in western Canada. Quaternary Science Reviews 28, 2049-2074.
Miller, G.H., Alley, R.B., Brigham-Grette, J., Fitzpatrick, J.J., Polyak, L., Serreze, M.C., White, J.W.C., 2010. Arctic amplification: can the past constrain the future? Quaternary Science Reviews 29, 1779-1790.
Montgomery, D.C., 2008. Design and analysis of experiments. John Wiley & Sons.
Moskowitz, B.M., Frankel, R.B., Bazylinski, D.A., 1993. Rock magnetic criteria for the detection of biogenic magnetite. Earth and Planetary Science Letters 120, 283-300.
Munsell, A.H., Color, M., 2000. Munsell soil color charts. Munsell Color.
Müller, B.U., 1999. Paraglacial sedimentation and denudation processes in an Alpine valley of Switzerland. An approach to the quantification of sediment budgets. Geodinamica Acta 12, 291-301.
Müller, J., Werner, K., Stein, R., Fahl, K., Moros, M., Jansen, E., 2012. Holocene cooling culminates in sea ice oscillations in Fram Strait. Quaternary Science Reviews 47, 1-14.
Nesje, A., 1992. A piston corer for lacustrine and marine sediments. Arctic and Alpine Research, 257-259.
Nesje, A., 2009. Latest Pleistocene and Holocene alpine glacier fluctuations in Scandinavia. Quaternary Science Reviews 28, 2119-2136.
Nordli, Ø., 2010. The Svalbard airport temperature series. Bulletin of Geography. Physical Geography Series, 5-25.
Nordli, Ø., Przybylak, R., Ogilvie, A.E., Isaksen, K., 2014. Long-term temperature trends and variability on Spitsbergen: the extended Svalbard Airport temperature series, 1898-2012. Polar research 33.
NPI, 1936. s36_2066, in: dpi, s. (Ed.). NPI, Svalbard.
NPI, 2009. 2009, in: 13822 (Ed.). Norwegian Polar Institute
NPI, 2015. Svalbardkartet.
Oerlemans, J., 2005. Extracting a Climate Signal from 169 Glacier Records. Science 308, 675-677.
Ohta, Y., Larionov, A.N., Tebenkov, A.M., Lepvrier, C., Maluski, H., Lange, M., Hellebrandt, B., 2002. Single-zircon Pb-evaporation and 40Ar/39Ar dating of the metamorphic and granitic rocks in north-west Spitsbergen. Polar research 21, 73-89.
Ólafsdóttir, S., Geirsdóttir, Á., Miller, G.H., Stoner, J.S., Channell, J.E., 2013. Synchronizing Holocene lacustrine and marine sediment records using paleomagnetic secular variation. Geology 41, 535-538.
Overpeck, J., Hughen, K., Hardy, D., Bradley, R., Case, R., Douglas, M., Finney, B., Gajewski, K., Jacoby, G., Jennings, A., 1997. Arctic environmental change of the last four centuries. Science 278, 1251-1256.
Paasche, Ø., 2011. Cirque Glaciers, in: Singh, V.P., Singh, P., Haritashya, U.K. (Eds.), Encyclopedia of Snow, Ice and Glaciers. Springer, pp. 141-144.
Paasche, Ø., Løvlie, R., Dahl, S.O., Bakke, J., Nesje, A., 2004. Bacterial magnetite in lake sediments: late glacial to Holocene climate and sedimentary changes in northern Norway. Earth and Planetary Science Letters 223, 319-333.

Paasche, Ø., Olaf Dahl, S., Bakke, J., Løvlie, R., Nesje, A., 2007. Cirque glacier activity in arctic Norway during the last deglaciation. Quaternary Research 68, 387-399.
Peach, P.A., Perrie, L.A., 1975. Grain-size distribution within glacial varves. Geology 3, 43-46.
Pithan, F., Mauritsen, T., 2014. Arctic amplification dominated by temperature feedbacks in contemporary climate models. Nature Geosci 7, 181-184.
Rasmussen, T.L., Thomsen, E., Skirbekk, K., Ślubowska-Woldengen, M., Klitgaard Kristensen, D., Koç, N., 2014. Spatial and temporal distribution of Holocene temperature maxima in the northern Nordic seas: interplay of Atlantic-, Arctic-and polar water masses. Quaternary Science Reviews 92, 280-291.
RCoreTeam, 2014. R: a language and environment for statistical computing. Vienna, Austria: R Foundation for Statistical Computing; 2012. Open access available at: http://cran. r-project. org.
Reimer, P.J., Bard, E., Bayliss, A., Beck, J.W., Blackwell, P.G., Ramsey, C.B., Buck, C.E., Cheng, H., Edwards, R.L., Friedrich, M., 2013. IntCal13 and Marine13 radiocarbon age calibration curves 0–50,000 years cal BP. Radiocarbon 55, 1869-1887.
Renssen, H., Goosse, H., Fichefet, T., 2007. Simulation of Holocene cooling events in a coupled climate model. Quaternary Science Reviews 26, 2019-2029.
Renssen, H., Seppä, H., Heiri, O., Roche, D., Goosse, H., Fichefet, T., 2009. The spatial and temporal complexity of the Holocene thermal maximum. Nature Geoscience 2, 411-414.
Reusche, M., Winsor, K., Carlson, A.E., Marcott, S.A., Rood, D.H., Novak, A., Roof, S., Retelle, M., Werner, A., Caffee, M., 2014. < sup> 10</sup> Be surface exposure ages on the late-Pleistocene and Holocene history of Linnébreen on Svalbard. Quaternary Science Reviews 89, 5-12.
Richards, J., Moore, R.D., Forrest, A.L., 2012. Late-summer thermal regime of a small proglacial lake. Hydrological Processes 26, 2687-2695.
Rohling, E.J., Pälike, H., 2005. Centennial-scale climate cooling with a sudden cold event around 8,200 years ago. Nature 434, 975-979.
Roland, E., Haakensen, N., 1985. Glasiologiske undersøkelser i Norge 1982. Rapport-Norges Vassdrags-og Elektrisitetsvesen, Hydrologisk Avdeling.
Rollison, H.R., 1993. Using Geochemical Data: Evaluation, Presentation. Interpretation. New York: Longan Scientific and Technical Press.
Rosqvist, G.C., Schuber, P., 2003. Millennial-scale climate changes on south Georgia, southern ocean. Quaternary Research 59, 470-475.
Rubensdotter, L., Rosqvist, G., 2009. Influence of geomorphological setting, fluvial-, glaciofluvial-and mass-movement processes on sedimentation in alpine lakes. The Holocene 19, 665-678.
Røthe, T.O., Bakke, J., Vasskog, K., Gjerde, M., D'Andrea, W.J., Bradley, R.S., 2015. Arctic Holocene glacier fluctuations reconstructed from lake sediments at Mitrahalvøya, Spitsbergen. Quaternary Science Reviews 109, 111-125.
Salvigsen, O., Høgvard, K., 2006. Glacial history, Holocene shoreline displacement and palaeoclimate based on radiocarbon ages in the area of Bockfjorden, north-western Spitsbergen, Svalbard. Polar Research 25, 15-24.
Sarnthein, M., Kreveld, S., Erlenkeuser, H., Grootes, P., Kucera, M., Pflaumann, U., Schulz, M., 2003. Centennial-to-millennial-scale periodicities of Holocene climate and sediment injections off the western Barents shelf, 75 N. Boreas 32, 447-461.
Screen, J.A., Simmonds, I., 2010. The central role of diminishing sea ice in recent Arctic temperature amplification. Nature 464, 1334-1337.

Sergeeva, L., 1983. Trace element associations as indicators of sediment accumulation in lakes, in: Meriläinen, J., Huttunen, P., Battarbee, R.W. (Eds.), Paleolimnology. Springer Netherlands, pp. 81-84.
Serreze, M.C., Barry, R.G., 2011. Processes and impacts of Arctic amplification: A research synthesis. Global and Planetary Change 77, 85-96.
Simonneau, A., Chapron, E., Garçon, M., Winiarski, T., Graz, Y., Chauvel, C., Debret, M., Motelica-Heino, M., Desmet, M., Di Giovanni, C., 2014. Tracking Holocene glacial and high-altitude alpine environments fluctuations from minerogenic and organic markers in proglacial lake sediments (Lake Blanc Huez, Western French Alps). Quaternary Science Reviews 89, 27-43.
Ślubowska-Woldengen, M., Rasmussen, T.L., Koç, N., Klitgaard-Kristensen, D., Nilsen, F., Solheim, A., 2007. Advection of Atlantic Water to the western and northern Svalbard shelf since 17,500 calyr BP. Quaternary Science Reviews 26, 463-478.
Šmilauer, P., Lepš, J., 2014. Multivariate Analysis of Ecological Data Using CANOCO 5. Cambridge university press.
Snowball, I., Sandgren, P., 1996. Lake sediment studies of Holocene glacial activity in the Kårsa valley, northern Sweden: contrasts in interpretation. The Holocene 6, 367-372.
Solomina, O.N., Bradley, R.S., Hodgson, D.A., Ivy-Ochs, S., Jomelli, V., Mackintosh, A.N., Nesje, A., Owen, L.A., Wanner, H., Wiles, G.C., 2015. Holocene glacier fluctuations. Quaternary Science Reviews 111, 9-34.
Solomon, S., 2007. Climate change 2007-the physical science basis: Working group I contribution to the fourth assessment report of the IPCC. Cambridge University Press.
Spielhagen, R.F., Werner, K., Sørensen, S.A., Zamelczyk, K., Kandiano, E., Budeus, G., Husum, K., Marchitto, T.M., Hald, M., 2011. Enhanced modern heat transfer to the Arctic by warm Atlantic water. Science 331, 450-453.
Spurk, M., Leuschner, H.H., Baillie, M.G.L., Briffa, K.R., Friedrich, M., 2002. Depositional frequency of German subfossil oaks: climatically and non-climatically induced fluctuations in the Holocene. The Holocene 12, 707-715.
Stoner, J.S., Jennings, A., Kristjánsdóttir, G.B., Dunhill, G., Andrews, J.T., Hardardóttir, J., 2007. A paleomagnetic approach toward refining Holocene radiocarbon-based chronologies: paleoceanographic records from the north Iceland (MD99-2269) and east Greenland (MD99-2322) margins. Paleoceanography 22, PA1209.
Striberger, J., Björk, S., Ingólfsson, Ó., Kjær, K.H., Snowball, I., Uvo, C.B., 2011. Climate variability and glacial processes in eastern Iceland during the past 700 years based on varved lake sediments. Boreas 40, 28-45.
Støren, E.N., Dahl, S.O., Lie, Ø., 2008. Separation of late-Holocene episodic paraglacial events and glacier fluctuations in eastern Jotunheimen, central southern Norway. The Holocene 18, 1179-1191.
Sundqvist, H., Kaufman, D., McKay, N., Balascio, N., Briner, J., Cwynar, L., Sejrup, H., Seppä, H., Subetto, D., Andrews, J., 2014. Arctic Holocene proxy climate database–new approaches to assessing geochronological accuracy and encoding climate variables. Climate of the Past Discussions 10, 1-63.
Svendsen, J.I., Mangerud, J., 1997. Holocene glacial and climatic variations on Spitsbergen, Svalbard. The Holocene 7, 45-57.
Tanaka, H., Hirabayashi, H., Matsuoka, T., Kaneko, H., 2012. Use of fall cone test as measurement of shear strength for soft clay materials. Soils and Foundations 52, 590-599.
Ter Braak, C., 1988. CANOCO-a FORTRAN Programme for Canonical Community Ordination by [partial][detrended][canonical] Correspondence Analysis, Principal Components Analysis and Redundancy Analysis (version 2.1). Agricultural Mathematics Group.

Thomas, E.R., Wolff, E.W., Mulvaney, R., Steffensen, J.P., Johnsen, S.J., Arrowsmith, C., White, J.W., Vaughn, B., Popp, T., 2007. The 8.2 ka event from Greenland ice cores. Quaternary Science Reviews 26, 70-81.
Thompson, R., Turner, G., 1979. British geomagnetic master curve 10,000-0 yr BP for dating European sediments. Geophysical Research Letters 6, 249-252.
Thomson, J., Croudace, I.W., Rothwell, R.G., 2006. A geochemical application of the ITRAX scanner to a sediment core containing eastern Mediterranean sapropel units. Geological Society, London, Special Publications 267, 65-77.
Thornalley, D.J.R., Elderfield, H., McCave, I.N., 2009. Holocene oscillations in temperature and salinity of the surface subpolar North Atlantic. Nature 457, 711-714.
Tjallingii, R., Röhl, U., Kölling, M., Bickert, T., 2007. Influence of the water content on X-ray fluorescence core-scanning measurements in soft marine sediments. Geochemistry, Geophysics, Geosystems 8.
Van der Bilt, W.G., Bakke, J., Balascio, N.L., 2015. Mapping sediment-landform assemblages to constrain the impact of paraglacial modification on sedimentation in a glacier-fed lake on northwest Spitsbergen Submitted.
Vasskog, K., Nesje, A., Støren, E.N., Waldmann, N., Chapron, E., Ariztegui, D., 2011. A Holocene record of snow-avalanche and flood activity reconstructed from a lacustrine sedimentary sequence in Oldevatnet, western Norway. The Holocene, 0959683610391316.
Vasskog, K., Paasche, Ø., Nesje, A., Boyle, J.F., Birks, H.J.B., 2012. A new approach for reconstructing glacier variability based on lake sediments recording input from more than one glacier. Quaternary Research 77, 192-204.
Wanner, H., Beer, J., Bütikofer, J., Crowley, T.J., Cubasch, U., Flückiger, J., Goosse, H., Grosjean, M., Joos, F., Kaplan, J.O., 2008. Mid-to Late Holocene climate change: an overview. Quaternary Science Reviews 27, 1791-1828.
Wanner, H., Solomina, O., Grosjean, M., Ritz, S.P., Jetel, M., 2011. Structure and origin of Holocene cold events. Quaternary Science Reviews 30, 3109-3123.
Werner, A., 1993. Holocene moraine chronology, Spitsbergen, Svalbard: lichenometric evidence for multiple Neoglacial advances in the Arctic. The Holocene 3, 128-137.
Werner, K., Spielhagen, R.F., Bauch, D., Hass, H.C., Kandiano, E., 2013. Atlantic Water advection versus sea-ice advances in the eastern Fram Strait during the last 9 ka: Multiproxy evidence for a two-phase Holocene. Paleoceanography 28, 283-295.
Wittmeier, H.E., Bakke, J., Vasskog, K., Trachsel, M., 2015. Reconstructing Holocene glacier activity at Langfjordjøkelen, Arctic Norway, using multi-proxy fingerprinting of distal glacier-fed lake sediments. Quaternary Science Reviews 114, 78-99.
Østrem, G., Liestøl, O., 1964. Glaciological investigations in Norway 1963. Norsk Geografisk Tidsskrift 18, 281-340.

# Conclusions

This thesis set out to generate high-resolution Arctic and Antarctic Holocene paleoclimate proxy timeseries, a key step in improving our limited understanding of polar climate dynamics to contextualize ongoing amplified change. For this purpose, glacier-fed lake sediments, prime targets for high-resolution paleoclimate studies, were investigated, employing a toolbox of physical, geochemical, magnetic and biological proxies to reconstruct change. To enhance the potential of this approach, special emphasis was placed on exploring the potential of numerical techniques, constraining the impact of non-glacial processes, up-scaling site-specific findings and constraining the climatic signature of glacier shifts.

The presented work advances our knowledge of Holocene polar climate variability by presenting the first full Holocene record of glacier variability from Svalbard (paper 3), the first two quantitative full Holocene temperature reconstructions from the Arctic (paper 4) as well as the first continuous reconstruction of Holocene glacier ELA from sub-Antarctic South Georgia (paper 5). Other contributions include constraining the imprint of non-glacial processes on the signature of glacier-fed lake sediments (papers 2, 3 and 5), as well as quantifying and propagating analytical and chronological uncertainty (papers 3, 4 and 5).

In the following paragraphs, the main empirical and methodological findings of this thesis will be synthesized, while also addressing limitations and identifying promising future research avenues.

## Main findings

*Pervasive Early Holocene freshwater input weakened poleward heat transport in the Arctic Atlantic between ± 10-8 ka BP, suppressing summer temperatures and stimulating glacier growth*

Following a brief temperature spike around 10 ka BP (paper 4), linked to post-glacial AMOC rejuvenation (Risebrobakken et al., 2011), reconstructed cooling and glacier growth indicates climate deterioration on Svalbard between ± 10-8 ka BP (papers 3 and 4). Even more so, paper 3 demonstrates that Hajeren glacier activity reached a Holocene maximum around 9.5 ka BP, in line with local and regional evidence (Henriksen et al., 2014; Nesje, 2009). This evidence of a pre-LIA Holocene glacier maximum is also supported by the findings of paper 2, reporting on weathered moraines outboard LIA limits. Assessing the cause(s) of this climate deterioration, coincident with the insolation maximum associated with the Hypsithermal (Renssen et al., 2005), both papers 2 and 4 indicate forcing by the melting LIS. Peaks in reconstructed glacier activity mimic LIS-sourced glacial freshwater pulses into the Labrador Sea (paper 3)(Jennings et al., 2015). Paleotemperature estimates correspond with a decline in Atlantic overturning circulation (Mjell et al., 2015), a major contributor to the Arctic`s heat budget (paper 4)(Eldevik and Nilsen, 2013). In line with a growing body of work (Blaschek et al., 2015; Came et al., 2007; Elmore et al., 2015; Thornalley et al., 2009), these findings indicate the pervasive influence of freshwater input from the melting LIS during the Early Holocene, perturbing the AMOC and cooling the North Atlantic Arctic. This conclusion contrasts with the (still) widely held view that catastrophic meltwater outbursts are required to perturb regional climate (Alley and Ágústsdóttir, 2005; Broecker et al., 1989).

*Step-wise inception of Neoglacial on Svalbard between 7-5 ka BP driven by strengthening influence of polar water and sea-ice against background of orbital cooling*

After the last significant LIS vestiges melted (Dyke et al., 2003), a rapid decrease in glacigenic minerogenic input and peaking summer temperatures mark the

Hypsithermal on Svalbard around 7 ka BP (papers 3 and 4). Following this late optimum (Darby et al., 2012; Kaplan and Wolfe, 2006; Kaufman et al., 2004), the evolution of summer temperatures on Svalbard reveal a millennial-scale cooling trend (paper 4), a defining characteristic of Holocene climate (Bradley, 1999; Wanner et al., 2011). This gradual inception of the Neoglacial period is, however, interspersed by two cooling steps between ± 7-5 ka BP and ± 4-3.5 ka BP. Occurring against a background of orbital cooling (Huybers, 2006), the findings of paper 4 demonstrate that these shifts were driven by the strengthening influence of Arctic sea-ice and water, in line with Müller et al. (2009), Müller et al. (2012) and Werner et al. (2013). This trend reflects a local expression of a pan-Arctic phenomenon: progressive post-glacial flooding of the Siberian shelfs, completed by 5.2 ka BP (Bauch et al., 2001), transformed these areas into `*sea-ice factories*` (Werner et al., 2013), exporting cold Arctic water and ice into the North Atlantic (Blaschek and Renssen, 2013).

*Svalbard Neoglacial characterized by centennial-scale glacial cycles and persistent summer temperature variations coeval with shifts in Atlantic overturning circulation*

Outlined step-wise cooling ushered in the Neoglacial on Svalbard (paper 4), lowering the glaciation threshold so that glaciers could reform (Reusche et al., 2014; Røthe et al., 2015; Svendsen and Mangerud, 1997). However, the small cirque glaciers of the studied Hajeren catchment only intermittently reformed during three centennial-scale cycles of glacier growth and decay (paper 3).The first two of these events, centred around 4200 and 3300 cal BP, are coeval with maxima in a compilation of reconstructed glacier advances (Wanner et al., 2011). The significance of these events in an Arctic-Atlantic context is reflected by their coincidence with advances in Canada, Iceland and Scandinavia (Geirsdóttir et al., 2009; Menounos et al., 2009; Nesje, 2009). Correspondence of these events with `Bond cycles` 3 and 2 suggest these events were driven by a reorganization North Atlantic circulation (Bond et al., 1997; Debret et al., 2007; Debret et al., 2009). Paper 4 shows that Svalbard summer temperature responded sensitively to shifts in Atlantic circulation during the last 4 ka (Mjell et al., 2015). However, reconstructed temperatures reveal that cool, but not particularly cold conditions prevailed in the Hajeren catchment at the time of the

discussed glacier events. The discussed advances may therefore have been precipitation-driven. The climatic signature of subsequent prolonged LIA glacier activity from 700 cal BP onwards is even more elusive as available paleoclimate records indicate a conjunction of high summer temperatures and extensive winter sea-ice extent (D'Andrea et al., 2012; Müller et al., 2012; Spielhagen et al., 2011), both detrimental to glacier mass balance.

*Late Holocene glacier history of South Georgia reveals ± 1250 cal BP stationary maximum, inter-hemispheric MCO and LIA, retreat behind current limits around 500 cal BP and recent retreat at unprecedented rates*

Paper 5 presents the first continuous reconstruction of glacier activity from the sub-Antarctic that covers the past millennium, complementing moraine chronologies and observational studies (Hall, 2009b; Solomina et al., 2015). Supporting the findings of (Masiokas et al., 2009; Schaefer et al., 2009), the presented Hamberg glacier ELA reconstruction reveal that the amplitude of Neoglacial advances diminished towards the present, in contrast with Northern Hemisphere evidence (paper 3)(Solomina et al., 2015). Advances include a stationary maximum around 1250 BP, when glaciers deposited moraines in the Middle Hamberg lake (Clapperton et al., 1989b), as well as a two-step LIA, with advances around 300 and 120 cal BP (paper 5). Notably, the presented evidence suggests a concurrent bi-polar onset of the latter event, in support of mounting evidence (Bertler et al., 2011). More tentatively, the Hamberg record also indicates an inter-hemispheric MCO after Villalba (1994), revealing reduced glacier coverage during an episode of widespread regional warmth and drought (Chambers et al., 2014; Hall et al., 2010; Moreno et al., 2014; Moy et al., 2008; Mulvaney et al., 2012; Noon et al., 2003). In contrast with moraine chronologies, the presented lake sediment-based reconstruction from South Georgia in paper 5 also reveals information on retreat phases. Considering the present decline of (sub)-Antarctic glaciers (Cook et al., 2005; Glasser et al., 2011; Gordon et al., 2008; Masiokas et al., 2008), such events may serve as analogues for the future. In addition to recent retreat, two particularly distinct retreat phases have been identified on South Georgia in paper 5 around 500 and 200 cal BP. While the former events attest to the

range of natural sub-Antarctic climate variability, indicating retreat behind present-day limits, recent retreat progresses at rates not seen during the past millennium.

*Late Holocene glacier mass balance on South Georgia driven by transient phase-dependent interactions between regional circulation patterns and global forcing*

In general, the findings of paper 5 underscore the strong control of regional circulation patterns on centennial-scale Holocene climate variability in high southern latitudes (background). Contextualizing the Hamberg ELA reconstruction in a regional paleoclimate framework, strong correspondence between glacier variability and SWW, SAM and ENSO indices become apparent (Abram et al., 2014; Moy et al., 2008; Yan et al., 2011), driving intricate (wind-driven) precipitation and temperature feedbacks. For example, the onset of the outlined MCO on South Georgia concurs with a reconstructed SWW minimum (Moy et al., 2008), driving glacier retreat through a reduction in wind-driven orographic (winter) precipitation (Gordon et al., 2008; Moreno et al., 2010). In addition, paper 5 also highlights the transient imprint of phase-dependent relationships between the outlined regional circulation patterns and the associated modulation of lower-latitude teleconnections after e.g. Fogt et al. (2011) and Ding et al. (2012). For example, retreat to a smaller-than-present minimum around 500 cal BP is explained through strengthening of equatorial Pacific teleconnections, associated with concurrent weakening of the SAM (Abram et al., 2014; Carvalho et al., 2005), driving a marked increase in regional SSTs (Shevenell et al., 2011). Finally, paper 5 also suggests that Late Holocene Southern Ocean climate also responded to change with a global signature, though impacts were compounded by regional feedbacks. Examples include recent retreat in response to ongoing global warming as well as the inferred synchronous bi-polar expression of the LIA. While both events seem temperature-driven (paper 5), SAM-driven shifts in SWW intensity exacerbated the glacier response through (wind-driven) precipitation changes (Moreno et al., 2010; Moy et al., 2008).

*The application of novel numerical techniques permits resolving past glacier change at centennial-scale timescales whilst appraising uncertainty and representing non-linear responses*

From a methodological perspective, this thesis has focused on exploring the potential of numerical techniques to help assess and improve the robustness of sediment-based paleoclimate reconstructions from glacier-fed lakes. This pursuit can be deconstructed into two main strategies: assessing (dis)similarity and appraising (un)certainty. The former has principally been tackled through the calibration of sediment-based findings against physical evidence of past glacier size, using moraines, maps and photographs. The non-linear approach presented in paper 5 marks an improvement beyond the present state-of-the-art, which is characterized by the use of (over)simplified linear models (Bakke and Nesje, 2011). The employed part-quadratic model accommodates non-linear glacier behaviour allows the study of glaciers with a complex hypsometry like the Hamberg glacier (Clapperton et al., 1989a; Osmaston, 2005). Additionally, ordination (PCA) and cluster (CONISS) techniques were applied to assess (dis)similarity between different sediments (Grimm, 1987; Hotelling, 1933), categorizing them into units, produced or deposited by the same process or in a similar environment. Following e.g. Vasskog et al. (2012) and Bakke et al. (2013), these tools aided accurate detection of sediments with a glacigenic imprint (papers 3 and 5). In appraising (un)certainty, this thesis primarily focused on its chronological dimensions. Foremost, instead of selecting the `best` fit, all iterations of ran age-depth models were considered for papers 4 and 5 to encompass the full range of prescribed chronological uncertainty. This approach enables a more encompassing discussion about the correspondence between records, including the detection of leads and lags, while up-scaling and contextualizing site-specific findings. Also, by investigating the co-variance between age-depth iterations of two timeseries that capture the same environmental process (i.e. glacier activity) over the same time interval (paper 5)(Werner and Tingley, 2015), their chronological spread could be narrowed, reducing uncertainty. In addition, the limits of analytical (un)certainty were also quantified, for example through calculation of pooled

standard deviations on sparsely replicated alkenone measurements (paper 4), sensitivity analysis within the 1σ range on parameters of the discussed ELA model using Monte Carlo simulation (paper 5) and calculation of the Signal to Noise ratio on scanning XRF data (paper 3)(Montgomery, 2008; Polissar and D'Andrea, 2014).

*Geomorphological mapping and sediment source fingerprinting are useful tools to constrain in-lake and surface processes in glacier-fed lake catchments*

Paper 2 demonstrates the worth of geomorphological mapping to assess the impact of catchment processes on glacier-fed lake sediment archives, in part validating paper 3. For example, as previously outlined, surveyed weathered Stage 1 moraines (implicitly) support the hypothesis of an Early Holocene glacier maximum, postulated in paper 3. Moreover, by inferring a cold-based regime for the South Glacier, it is argued that the North Glacier is the main contributor of glacigenic sediments to Lake Hajeren. Also, and arguable most crucial for validation of the lake Hajeren sediments as an archive of past glacier change, is constraining the impact of paraglacial modification (Jansson et al., 2005; Rubensdotter and Rosqvist, 2009). The geomorphological map of paper 1 demonstrates an absence of older glacigenic deposits in the Hajeren catchment and favours their rapid exhaustion, restricting the paraglacial period. In addition to glacigenic processes, mapping also helped constraining the impact of non-glacial input on the lake sediment record. In particular, paper 2 limits the impact of mass-wasting processes as the accompanying map shows that Lake Hajeren is surrounded by gently sloping expanses of weathered material. Complementing this exercise, papers 3 and 5 fingerprint the imprint of non-glacial processes on the investigated lake sediment cores, employing multiple independently measured parameters for validation purposes. For example, grain size analysis allowed identification of the discussed Neoglacial minerogenic events as centennial-scale glacier advances in paper 3. Also, investigation of ARM, LOI and mobile geochemical elements constrained dilution of a (glacigenic) minerogenic signature by biological processes in paper 3 (McKay and Kaufman, 2009). In paper 5, magnetic proxies χbulk 77K/293K and MS were employed after (Dearing et al., 2001) and (Thompson et al., 1975) to detect the abrupt input of catchment-derived

minerogenic input. Identification of these events as abrupt slumps enabled filtering out non-glacial noise and strengthened chronological control.

## Limitations

Following from the above, this thesis has reached its main goal, expanding our knowledge of Holocene climate variability in Earth`s high latitude regions by addressing the specified objectives. Yet, a series of limitations can be identified, related to **1**) mapping quality, **2**) source-to-sink analysis, **3**) closed-sum effects, 4) validation, **5**) alkenone calibration and **6**) our understanding of Southern Ocean climate dynamics.

- The accuracy of the geomorphological map in paper 2 is hampered by two constraints. First, the aerial photographs used for remote-sensing could not be orthorectified due to a lack of Rational Polynomial Coefficients (RPCs), particularly affecting the projection of high-relief surfaces. Secondly, field mapping was performed using a handheld GPS with 5m accuracy as the studied Svalbard field site falls outside the range of differential GPS networks. Both instances represent forces majeure that can only be resolved through the improvement of existing spatial data infrastructure.

- Now attempted through a combination of geomorphological mapping and fingerprinting of lake sediments (papers 2 and 3), a full process-based understanding of a catchment`s glacier-to-lake sediment cascade requires more comprehensive source-to-sink analysis (Allen, 2008). After Wittmeier et al. (2015), the analysis of catchment sediment samples could help close this knowledge gap, fingerprinting sediment genesis. Employing tools like X-Ray Diffraction (XRD), morphometry and analysis of particle size distribution would enable the identification of erosion and transport pathways.

- As previously outlined by e.g. McKay and Kaufman (2009) and Löwemark et al. (2011), paper 3 underscores that the concentrations of detrital and biogenic

sediment components are interrelated. Ensuing closed-sum effects may dilute the imprint of a glacigenic signature in glacier-fed lake sediments through an increase in biological production or preservation potential, hampering paleoenvironmental interpretations. As shown in paper 3, normalizing minerogenic against biogenic parameters offers solace. However, this simple approach requires that the processes governing either minerogenic or biogenic input act independently. This is unlikely the case: a more thorough understanding of bio-geochemical lacustrine processes is therefore desirable.

- Following e.g. (Røthe et al., 2015) and Wittmeier et al. (2015), this thesis demonstrates that sediment density shows consistent strong co-variance with detrital geochemical elements. Though highly likely in glacier-fed settings, this persistent relationship does not per se prove nor validate glacigenic input, as argued in papers 3 and 5. Instead, it merely reveals the presence of a source of minerogenic input. More emphasis should be placed on advanced grain size analysis for validation purposes, because is the unsorted, silt-clay dominated signature that distinguishes glacial flour from other minerogenic sediments (Bakke et al., 2005; Leemann and Niessen, 1994). New tools like laser diffraction and morphometry of particles could fill this gap.

- The temperature sensitivity of the alkenone-based reconstruction presented in paper 4 has not been determined with site-specific pairings of UK37 concentrations and measured water or air temperature. Also, the used calibration is based on two datasets, thousands of kilometres away from the studied sites (D'Andrea et al., 2016). Although the spread of inter-site variance is modest, we cannot exclude that site-specific differences growth factors affected alkenone temperature sensitivity. Moreover, the applied calibration is taxon-specific: while C37 isomer concentrations indicate a Group I signature (D'Andrea et al., 2016), DNA analyses are required to ascertain this.

- Contextualizing reconstructed Late Holocene glacier variability on South Georgia in paper 5, the incongruence and scarcity of available literature on Southern Ocean climate dynamics became apparent. For example, discussing the intensity of the SWW, Lamy et al. (2010) infer a Late Holocene weakening, while Moreno et al. (2010) find evidence for strengthening. Moreover, there is only a handful of published terrestrial paleoclimate records from the Southern Ocean island between more frequently studied Patagonia and New Zealand (Hall, 2007; Hall, 2009a; Mulvaney et al., 2012; Noon et al., 2003; Strother et al., 2015). There is also a strong Pacific bias in Southern Ocean paleoclimate research, while recent studies propose a more active role for the Atlantic ocean (King, 2014; Li et al., 2014). Finally, the impact of sea-ice feedbacks is generally overlooked due to an absence of reconstructions (Collins et al., 2013). Together, these limitations restrict efforts aimed at contextualizing Holocene Southern Ocean climate variability.

## Outlook

Following the prior overview of the major findings and limitations, this thesis concludes with an outlook for the future. In the following paragraph, promising research avenues that may harness and enhance the potential of glacier-fed lake sediments as paleoclimate archives is outlined.

- Geomorphological catchment mapping should become an intrinsic component of glacier-fed lake sediment studies: ensuing maps help constrain the impact of catchment processes on lacustrine sedimentation. New digital surveying tools such as LIDAR, differential GPS and GIS have made such exercises cheaper, less time consuming and far more accurate over the past decades.

- Following from the outlined significant relationship between summer temperature and winter precipitation at the ELA (Østrem and Liestøl, 1964), all parameters of this closed system may be inferred throughout the Holocene when integrating ELA reconstructions with quantitative paleothermometry.

The presented full Holocene glacier and temperature reconstructions from Lake Hajeren on Svalbard underscore the potential of this approach in the High Arctic. Particularly when carried out in tandem with hydrogen isotope analyses e.g. Balascio et al. (2013), this strategy may constrain both key components of climate variability: temperature as well as hydrological changes. The latter is expected to have a significant impact on future mass balance and ocean circulation, but remain under-investigated (Allen and Ingram, 2002; Krinner et al., 2007; Min et al., 2008). Also, as glacier-fed lake sediments represent terrestrial paleoclimate archives, such exercises could provide us with a rare window on past atmospheric change.

- Dealing with uncertainty has taken centre stage in the (academic) discourse on climate change (Allen et al., 2000; Forest et al., 2002; Rowlands et al., 2012; Stainforth et al., 2005; Webster et al.). The ensuing shift towards more quantitative paleoclimate assessments has been driven by the incorporation of novel numerical techniques (Birks et al., 2012). This is also reflected by the contents of this thesis, prioritizing the quantification and propagation of chronological and analytical uncertainty. These, however, represent mere first forays into a new inter-disciplinary research niche, where Quaternary geologists, paleoecologists, mathematicians and modellers meet. Stronger synergies between these communities may well spark the next leap forward in the field of paleoclimatology.

- The impact of biological processes on the signature of glacial sediments has consistently been highlighted throughout this thesis. The outlined dilution of a minerogenic signature through closed-sum-effects and the biogenic control on mineral magnetic properties are prominent examples of how biogenic processes may compromise interpretations if undetected (paper 3). More emphasis should be placed on constraining the impact of in-lake biogeochemical processes. Especially in glacier-fed settings, stratification-driven changes in redox state, forced by underflows of cold dense water or

variations in ice cover (Anderson et al., 2008; Brown and Duguay, 2010; Leemann and Niessen, 1994; Richards et al., 2012), can leave a strong sedimentological imprint. Interestingly, recent studies suggest that microbial community structure co-varies with glacier activity (Gutiérrez et al., 2015; Sheik et al., 2015), opening possibilities to employ microbes as proxies for past glacier change.

- From a paleoclimate perspective, both conclusion and limitations paragraphs identified a number of promising future focal points. Foremost, there is a lack of spatio-temporal data coverage in the Southern Ocean, characterized by the underrepresentation of Atlantic sites as well as records that cover centennial-scale and fill the gap between prevalent observational meteorological studies and millennial-scale proxy-based reconstructions. In the Arctic, the reported pervasive meltwater-driven cooling in the North Atlantic during the Early Holocene deserves future investigation. This period may serve as an analogue for the future as projected melting of the Greenland Ice Sheet (GIS) and hydrological intensification will increase freshwater fluxes (Church et al., 2013; Min et al., 2008). From a bi-polar perspective, the operation of inter-hemispheric climate linkages, notably the bi-polar seesaw (Broecker, 1998), remains a major unresolved paleoclimate conundrum. A critical first step in addressing these knowledge gaps is the recovery and integration of high-resolution proxy archives, e.g. glacier-fed lake sediments, providing a robust empirical basis for future high latitude paleoclimate work.

# References cited in conclusions section

Abram, N.J., Mulvaney, R., Vimeux, F., Phipps, S.J., Turner, J., England, M.H., 2014. Evolution of the Southern Annular Mode during the past millennium. Nature Clim. Change 4, 564-569.
Allen, M.R., Ingram, W.J., 2002. Constraints on future changes in climate and the hydrologic cycle. Nature 419, 224-232.
Allen, M.R., Stott, P.A., Mitchell, J.F.B., Schnur, R., Delworth, T.L., 2000. Quantifying the uncertainty in forecasts of anthropogenic climate change. Nature 407, 617-620.
Allen, P.A., 2008. From landscapes into geological history. Nature 451, 274-276.
Alley, R.B., Ágústsdóttir, A.M., 2005. The 8k event: cause and consequences of a major Holocene abrupt climate change. Quaternary Science Reviews 24, 1123-1149.
Anderson, N.J., Brodersen, K.P., Ryves, D.B., McGowan, S., Johansson, L.S., Jeppesen, E., Leng, M.J., 2008. Climate versus in-lake processes as controls on the development of community structure in a low-arctic lake (South-West Greenland). Ecosystems 11, 307-324.
Bakke, J., Nesje, A., 2011. Equilibrium-line altitude (ELA), Encyclopedia of Snow, Ice and Glaciers. Springer, pp. 268-277.
Bakke, J., Nesje, A., Dahl, S.O., 2005. Utilizing physical sediment variability in glacier-fed lakes for continuous glacier reconstructions during the Holocene, northern Folgefonna, western Norway. The Holocene 15, 161-176.
Bakke, J., Trachsel, M., Kvisvik, B.C., Nesje, A., Lyså, A., 2013. Numerical analyses of a multi-proxy data set from a distal glacier-fed lake, Sørsendalsvatn, western Norway. Quaternary Science Reviews 73, 182-195.
Balascio, N.L., D'Andrea, W.J., Bradley, R.S., Perren, B.B., 2013. Biogeochemical evidence for hydrologic changes during the Holocene in a lake sediment record from southeast Greenland. The Holocene.
Bauch, H.A., Mueller-Lupp, T., Taldenkova, E., Spielhagen, R.F., Kassens, H., Grootes, P.M., Thiede, J., Heinemeier, J., Petryashov, V., 2001. Chronology of the Holocene transgression at the North Siberian margin. Global and Planetary Change 31, 125-139.
Bertler, N.A.N., Mayewski, P.A., Carter, L., 2011. Cold conditions in Antarctica during the Little Ice Age — Implications for abrupt climate change mechanisms. Earth and Planetary Science Letters 308, 41-51.
Birks, H.J.B., Lotter, A.F., Juggins, S., Smol, J.P., 2012. Tracking environmental change using lake sediments: data handling and numerical techniques. Springer Science & Business Media.
Blaschek, M., Renssen, H., 2013. The impact of early Holocene Arctic shelf flooding on climate in an atmosphere–ocean–sea–ice model. Climate of the Past 9, 2651-2667.
Blaschek, M., Renssen, H., Kissel, C., Thornalley, D., 2015. Holocene North Atlantic Overturning in an atmosphere-ocean-sea ice model compared to proxy-based reconstructions. Paleoceanography 30, 1503-1524.
Bond, G., Showers, W., Cheseby, M., Lotti, R., Almasi, P., Priore, P., Cullen, H., Hajdas, I., Bonani, G., 1997. A pervasive millennial-scale cycle in North Atlantic Holocene and glacial climates. science 278, 1257-1266.
Bradley, R.S., 1999. Paleoclimatology: reconstructing climates of the Quaternary. Academic Press.
Broecker, W.S., 1998. Paleocean circulation during the last deglaciation: a bipolar seesaw? Paleoceanography 13, 119-121.

Broecker, W.S., Kennett, J.P., Flower, B.P., Teller, J.T., Trumbore, S., Bonani, G., Wolfli, W., 1989. Routing of meltwater from the Laurentide Ice Sheet during the Younger Dryas cold episode.
Brown, L.C., Duguay, C.R., 2010. The response and role of ice cover in lake-climate interactions. Progress in physical geography 34, 671-704.
Came, R.E., Oppo, D.W., McManus, J.F., 2007. Amplitude and timing of temperature and salinity variability in the subpolar North Atlantic over the past 10 ky. Geology 35, 315-318.
Carvalho, L.M.V., Jones, C., Ambrizzi, T., 2005. Opposite Phases of the Antarctic Oscillation and Relationships with Intraseasonal to Interannual Activity in the Tropics during the Austral Summer. Journal of Climate 18, 702-718.
Chambers, F.M., Brain, S.A., Mauquoy, D., McCarroll, J., Daley, T., 2014. The 'Little Ice Age' in the Southern Hemisphere in the context of the last 3000 years: Peat-based proxy-climate data from Tierra del Fuego. The Holocene 24, 1649-1656.
Church, J.A., Clark, P.U., Cazenave, A., Gregory, J.M., Jevrejeva, S., Levermann, A., Merrifield, M., Milne, G., Nerem, R., Nunn, P., 2013. Sea level change. Climate change, 1137-1216.
Clapperton, C., Sugden, D., Pelto, M., 1989a. Relationship of land terminating and fjord glaciers to Holocene climatic change, South Georgia, Antarctica, Glacier Fluctuations and Climatic Change. Springer, pp. 57-75.
Clapperton, C.M., Sugden, D.E., Birnie, J., Wilson, M.J., 1989b. Late-glacial and Holocene glacier fluctuations and environmental change on South Georgia, Southern Ocean. Quaternary Research 31, 210-228.
Collins, L.G., Allen, C.S., Pike, J., Hodgson, D.A., Weckström, K., Massé, G., 2013. Evaluating highly branched isoprenoid (HBI) biomarkers as a novel Antarctic sea-ice proxy in deep ocean glacial age sediments. Quaternary Science Reviews 79, 87-98.
Cook, A., Fox, A., Vaughan, D., Ferrigno, J., 2005. Retreating glacier fronts on the Antarctic Peninsula over the past half-century. Science 308, 541-544.
D'Andrea, W.J., Theroux, S., Bradley, R.S., Huang, X., 2016. Does phylogeny control-temperature sensitivity? Implications for lacustrine alkenone paleothermometry. Geochimica et Cosmochimica Acta 175, 168-180.
D'Andrea, W.J., Vaillencourt, D.A., Balascio, N.L., Werner, A., Roof, S.R., Retelle, M., Bradley, R.S., 2012. Mild Little Ice Age and unprecedented recent warmth in an 1800 year lake sediment record from Svalbard. Geology 40, 1007-1010.
Darby, D.A., Ortiz, J.D., Grosch, C.E., Lund, S.P., 2012. 1,500-year cycle in the Arctic Oscillation identified in Holocene Arctic sea-ice drift. Nature geoscience 5, 897-900.
Dearing, J., Hu, Y., Doody, P., James, P.A., Brauer, A., 2001. Preliminary reconstruction of sediment-source linkages for the past 6000 yr at the Petit Lac d'Annecy, France, based on mineral magnetic data. Journal of Paleolimnology 25, 245-258.
Debret, M., Bout-Roumazeilles, V., Grousset, F., Desmet, M., McManus, J.F., Massei, N., Sebag, D., Petit, J.-R., Copard, Y., Trentesaux, A., 2007. The origin of the 1500-year climate cycles in Holocene North-Atlantic records. Climate of the Past Discussions 3, 679-692.
Debret, M., Sebag, D., Crosta, X., Massei, N., Petit, J.-R., Chapron, E., Bout-Roumazeilles, V., 2009. Evidence from wavelet analysis for a mid-Holocene transition in global climate forcing. Quaternary Science Reviews 28, 2675-2688.
Ding, Q., Steig, E.J., Battisti, D.S., Wallace, J.M., 2012. Influence of the tropics on the Southern Annular Mode. Journal of Climate 25, 6330-6348.
Dyke, A.S., Moore, A., Robertson, L., 2003. Deglaciation of North America. Geological Survey of Canada Ottawa, Ontario, Canada.
Eldevik, T., Nilsen, J.E.Ø., 2013. The Arctic–Atlantic Thermohaline Circulation*. Journal of Climate 26, 8698-8705.

Elmore, A.C., Wright, J.D., Southon, J., 2015. Continued meltwater influence on North Atlantic Deep Water instabilities during the early Holocene. Marine Geology 360, 17-24.
Fogt, R., Bromwich, D., Hines, K., 2011. Understanding the SAM influence on the South Pacific ENSO teleconnection. Climate Dynamics 36, 1555-1576.
Forest, C.E., Stone, P.H., Sokolov, A.P., Allen, M.R., Webster, M.D., 2002. Quantifying Uncertainties in Climate System Properties with the Use of Recent Climate Observations. Science 295, 113-117.
Geirsdóttir, Á., Miller, G.H., Axford, Y., Sædís, Ó., 2009. Holocene and latest Pleistocene climate and glacier fluctuations in Iceland. Quaternary Science Reviews 28, 2107-2118.
Glasser, N.F., Harrison, S., Jansson, K.N., Anderson, K., Cowley, A., 2011. Global sea-level contribution from the Patagonian Icefields since the Little Ice Age maximum. Nature Geosci 4, 303-307.
Gordon, J.E., Haynes, V.M., Hubbard, A., 2008. Recent glacier changes and climate trends on South Georgia. Global and Planetary Change 60, 72-84.
Grimm, E.C., 1987. CONISS: a FORTRAN 77 program for stratigraphically constrained cluster analysis by the method of incremental sum of squares. Computers & Geosciences 13, 13-35.
Gutiérrez, M.H., Galand, P.E., Moffat, C., Pantoja, S., 2015. Melting glacier impacts community structure of Bacteria, Archaea and Fungi in a Chilean Patagonia fjord. Environmental microbiology 17, 3882-3897.
Hall, B., Koffman, T., Denton, G., 2010. Reduced ice extent on the western Antarctic Peninsula at 700–970 cal. yr BP. Geology 38, 635-638.
Hall, B.L., 2007. Late-Holocene advance of the Collins Ice Cap, King George Island, South Shetland Islands. The Holocene 17, 1253-1258.
Hall, B.L., 2009a. Holocene glacial history of Antarctica and the sub-Antarctic islands. Quaternary Science Reviews 28, 2213-2230.
Hall, B.L., 2009b. Holocene glacial history of Antarctica and the sub-Antarctic islands (e.g. South Georgia). Quaternary Science Reviews 28, 2213-2230.
Henriksen, M., Alexanderson, H., Landvik, J.Y., Linge, H., Peterson, G., 2014. Dynamics and retreat of the Late Weichselian Kongsfjorden ice stream, NW Svalbard. Quaternary Science Reviews 92, 235-245.
Hotelling, H., 1933. Analysis of a complex of statistical variables into principal components. Journal of educational psychology 24, 417.
Huybers, P., 2006. Early Pleistocene glacial cycles and the integrated summer insolation forcing. Science 313, 508-511.
Jansson, P., Rosqvist, G., Schneider, T., 2005. Glacier fluctuations, suspended sediment flux and glacio-lacustrine sediments. Geografiska Annaler: Series A, Physical Geography 87, 37-50.
Jennings, A., Andrews, J., Pearce, C., Wilson, L., Ólafsdóttir, S., 2015. Detrital carbonate peaks on the Labrador shelf, a 13–7 ka template for freshwater forcing from the Hudson Strait outlet of the Laurentide Ice Sheet into the subpolar gyre. Quaternary Science Reviews 107, 62-80.
Kaplan, M.R., Wolfe, A.P., 2006. Spatial and temporal variability of Holocene temperature in the North Atlantic region. Quaternary Research 65, 223-231.
Kaufman, D.S., Ager, T.A., Anderson, N.J., Anderson, P.M., Andrews, J.T., Bartlein, P.J., Brubaker, L.B., Coats, L.L., Cwynar, L.C., Duvall, M.L., Dyke, A.S., Edwards, M.E., Eisner, W.R., Gajewski, K., Geirsdóttir, A., Hu, F.S., Jennings, A.E., Kaplan, M.R., Kerwin, M.W., Lozhkin, A.V., MacDonald, G.M., Miller, G.H., Mock, C.J., Oswald, W.W., Otto-Bliesner, B.L., Porinchu, D.F., Rühland, K., Smol, J.P., Steig, E.J., Wolfe, B.B., 2004.

Holocene thermal maximum in the western Arctic (0–180°W). Quaternary Science Reviews 23, 529-560.
King, J., 2014. Climate science: A resolution of the Antarctic paradox. Nature 505, 491-492.
Krinner, G., Magand, O., Simmonds, I., Genthon, C., Dufresne, J.-L., 2007. Simulated Antarctic precipitation and surface mass balance at the end of the twentieth and twenty-first centuries. Climate Dynamics 28, 215-230.
Lamy, F., Kilian, R., Arz, H.W., Francois, J.-P., Kaiser, J., Prange, M., Steinke, T., 2010. Holocene changes in the position and intensity of the southern westerly wind belt. Nature Geoscience 3, 695-699.
Leemann, A., Niessen, F., 1994. Varve formation and the climatic record in an Alpine proglacial lake: calibrating annually-laminated sediments against hydrological and meteorological data. The Holocene 4, 1-8.
Li, X., Holland, D.M., Gerber, E.P., Yoo, C., 2014. Impacts of the north and tropical Atlantic Ocean on the Antarctic Peninsula and sea ice. Nature 505, 538-542.
Löwemark, L., Chen, H.-F., Yang, T.-N., Kylander, M., Yu, E.-F., Hsu, Y.-W., Lee, T.-Q., Song, S.-R., Jarvis, S., 2011. Normalizing XRF-scanner data: A cautionary note on the interpretation of high-resolution records from organic-rich lakes. Journal of Asian Earth Sciences 40, 1250-1256.
Masiokas, M.H., Luckman, B.H., Villalba, R., Delgado, S., Skvarca, P., Ripalta, A., 2009. Little Ice Age fluctuations of small glaciers in the Monte Fitz Roy and Lago del Desierto areas, south Patagonian Andes, Argentina. Palaeogeography, Palaeoclimatology, Palaeoecology 281, 351-362.
Masiokas, M.H., Villalba, R., Luckman, B.H., Lascano, M.E., Delgado, S., Stepanek, P., 2008. 20th-century glacier recession and regional hydroclimatic changes in northwestern Patagonia. Global and Planetary Change 60, 85-100.
McKay, N.P., Kaufman, D.S., 2009. Holocene climate and glacier variability at Hallet and Greyling Lakes, Chugach Mountains, south-central Alaska. Journal of Paleolimnology 41, 143-159.
Menounos, B., Osborn, G., Clague, J.J., Luckman, B.H., 2009. Latest Pleistocene and Holocene glacier fluctuations in western Canada. Quaternary Science Reviews 28, 2049-2074.
Min, S.-K., Zhang, X., Zwiers, F., 2008. Human-Induced Arctic Moistening. Science 320, 518-520.
Mjell, T.L., Ninnemann, U.S., Eldevik, T., Kleiven, H.K.F., 2015. Holocene Multidecadal-to-Millennial Scale Variations in Iceland-Scotland Overflow and Their Relationship to Climate. Paleoceanography.
Montgomery, D.C., 2008. Design and analysis of experiments. John Wiley & Sons.
Moreno, P., Francois, J., Moy, C., Villa-Martínez, R., 2010. Covariability of the Southern Westerlies and atmospheric CO2 during the Holocene. Geology 38, 727-730.
Moreno, P.I., Vilanova, I., Villa-Martínez, R., Garreaud, R., Rojas, M., De Pol-Holz, R., 2014. Southern Annular Mode-like changes in southwestern Patagonia at centennial timescales over the last three millennia. Nature communications 5.
Moy, C.M., Dunbar, R.B., Moreno, P.I., Francois, J.-P., Villa-Martínez, R., Mucciarone, D.M., Guilderson, T.P., Garreaud, R.D., 2008. Isotopic evidence for hydrologic change related to the westerlies in SW Patagonia, Chile, during the last millennium. Quaternary Science Reviews 27, 1335-1349.
Mulvaney, R., Abram, N.J., Hindmarsh, R.C., Arrowsmith, C., Fleet, L., Triest, J., Sime, L.C., Alemany, O., Foord, S., 2012. Recent Antarctic Peninsula warming relative to Holocene climate and ice-shelf history. Nature 489, 141-144.

Müller, J., Massé, G., Stein, R., Belt, S.T., 2009. Variability of sea-ice conditions in the Fram Strait over the past 30,000 years. Nature Geoscience 2, 772-776.
Müller, J., Werner, K., Stein, R., Fahl, K., Moros, M., Jansen, E., 2012. Holocene cooling culminates in sea ice oscillations in Fram Strait. Quaternary Science Reviews 47, 1-14.
Nesje, A., 2009. Latest Pleistocene and Holocene alpine glacier fluctuations in Scandinavia. Quaternary Science Reviews 28, 2119-2136.
Noon, P., Leng, M., Jones, V., 2003. Oxygen-isotope (δ18O) evidence of Holocene hydrological changes at Signy Island, maritime Antarctica. The Holocene 13, 251-263.
Osmaston, H., 2005. Estimates of glacier equilibrium line altitudes by the Area× Altitude, the Area× Altitude Balance Ratio and the Area× Altitude Balance Index methods and their validation. Quaternary International 138, 22-31.
Polissar, P.J., D'Andrea, W.J., 2014. Uncertainty in paleohydrologic reconstructions from molecular δD values. Geochimica et Cosmochimica Acta 129, 146-156.
Renssen, H., Goosse, H., Fichefet, T., Brovkin, V., Driesschaert, E., Wolk, F., 2005. Simulating the Holocene climate evolution at northern high latitudes using a coupled atmosphere-sea ice-ocean-vegetation model. Climate Dynamics 24, 23-43.
Reusche, M., Winsor, K., Carlson, A.E., Marcott, S.A., Rood, D.H., Novak, A., Roof, S., Retelle, M., Werner, A., Caffee, M., 2014. < sup> 10</sup> Be surface exposure ages on the late-Pleistocene and Holocene history of Linnébreen on Svalbard. Quaternary Science Reviews 89, 5-12.
Richards, J., Moore, R.D., Forrest, A.L., 2012. Late-summer thermal regime of a small proglacial lake. Hydrological Processes 26, 2687-2695.
Risebrobakken, B., Dokken, T., Smedsrud, L.H., Andersson, C., Jansen, E., Moros, M., Ivanova, E.V., 2011. Early Holocene temperature variability in the Nordic Seas: The role of oceanic heat advection versus changes in orbital forcing. Paleoceanography 26.
Risebrobakken, B., Moros, M., Ivanova, E.V., Chistyakova, N., Rosenberg, R., 2010. Climate and oceanographic variability in the SW Barents Sea during the Holocene. The Holocene.
Rowlands, D.J., Frame, D.J., Ackerley, D., Aina, T., Booth, B.B.B., Christensen, C., Collins, M., Faull, N., Forest, C.E., Grandey, B.S., Gryspeerdt, E., Highwood, E.J., Ingram, W.J., Knight, S., Lopez, A., Massey, N., McNamara, F., Meinshausen, N., Piani, C., Rosier, S.M., Sanderson, B.M., Smith, L.A., Stone, D.A., Thurston, M., Yamazaki, K., Hiro Yamazaki, Y., Allen, M.R., 2012. Broad range of 2050 warming from an observationally constrained large climate model ensemble. Nature Geosci 5, 256-260.
Rubensdotter, L., Rosqvist, G., 2009. Influence of geomorphological setting, fluvial-, glaciofluvial-and mass-movement processes on sedimentation in alpine lakes. The Holocene 19, 665-678.
Røthe, T.O., Bakke, J., Vasskog, K., Gjerde, M., D'Andrea, W.J., Bradley, R.S., 2015. Arctic Holocene glacier fluctuations reconstructed from lake sediments at Mitrahalvøya, Spitsbergen. Quaternary Science Reviews 109, 111-125.
Schaefer, J.M., Denton, G.H., Kaplan, M., Putnam, A., Finkel, R.C., Barrell, D.J., Andersen, B.G., Schwartz, R., Mackintosh, A., Chinn, T., 2009. High-frequency Holocene glacier fluctuations in New Zealand differ from the northern signature. science 324, 622-625.
Sheik, C.S., Stevenson, E.I., Den Uyl, P.A., Arendt, C.A., Aciego, S.M., Dick, G.J., 2015. Microbial communities of the Lemon Creek Glacier show subtle structural variation yet stable phylogenetic composition over space and time. Frontiers in microbiology 6.
Shevenell, A., Ingalls, A., Domack, E., Kelly, C., 2011. Holocene Southern Ocean surface temperature variability west of the Antarctic Peninsula. Nature 470, 250-254.

Solomina, O.N., Bradley, R.S., Hodgson, D.A., Ivy-Ochs, S., Jomelli, V., Mackintosh, A.N., Nesje, A., Owen, L.A., Wanner, H., Wiles, G.C., 2015. Holocene glacier fluctuations. Quaternary Science Reviews 111, 9-34.
Spielhagen, R.F., Werner, K., Sørensen, S.A., Zamelczyk, K., Kandiano, E., Budeus, G., Husum, K., Marchitto, T.M., Hald, M., 2011. Enhanced modern heat transfer to the Arctic by warm Atlantic water. Science 331, 450-453.
Stainforth, D.A., Aina, T., Christensen, C., Collins, M., Faull, N., Frame, D.J., Kettleborough, J.A., Knight, S., Martin, A., Murphy, J.M., Piani, C., Sexton, D., Smith, L.A., Spicer, R.A., Thorpe, A.J., Allen, M.R., 2005. Uncertainty in predictions of the climate response to rising levels of greenhouse gases. Nature 433, 403-406.
Strother, S.L., Salzmann, U., Roberts, S.J., Hodgson, D.A., Woodward, J., Van Nieuwenhuyze, W., Verleyen, E., Vyverman, W., Moreton, S.G., 2015. Changes in Holocene climate and the intensity of Southern Hemisphere Westerly Winds based on a high-resolution palynological record from sub-Antarctic South Georgia. The Holocene 25, 263-279.
Svendsen, J.I., Mangerud, J., 1997. Holocene glacial and climatic variations on Spitsbergen, Svalbard. The Holocene 7, 45-57.
Thompson, R., Battarbee, R.W., O'Sullivan, P.E., Oldfield, F., 1975. Magnetic susceptibility of lake sediments. Limnology and Oceanography 20, 687-698.
Thornalley, D.J.R., Elderfield, H., McCave, I.N., 2009. Holocene oscillations in temperature and salinity of the surface subpolar North Atlantic. Nature 457, 711-714.
Vasskog, K., Paasche, Ø., Nesje, A., Boyle, J.F., Birks, H.J.B., 2012. A new approach for reconstructing glacier variability based on lake sediments recording input from more than one glacier. Quaternary Research 77, 192-204.
Villalba, R., 1994. Tree-ring and glacial evidence for the Medieval Warm Epoch and the Little Ice Age in southern South America, The Medieval Warm Period. Springer, pp. 183-197.
Wanner, H., Solomina, O., Grosjean, M., Ritz, S.P., Jetel, M., 2011. Structure and origin of Holocene cold events. Quaternary Science Reviews 30, 3109-3123.
Webster, M., Forest, C., Reilly, J., Babiker, M., Kicklighter, D., Mayer, M., Prinn, R., Sarofim, M., Sokolov, A., Stone, P., Wang, C., Uncertainty Analysis of Climate Change and Policy Response. Climatic Change 61, 295-320.
Werner, J.P., Tingley, M.P., 2015. Technical Note: Probabilistically constraining proxy age–depth models within a Bayesian hierarchical reconstruction model. Climate of the Past 11, 533-545.
Werner, K., Spielhagen, R.F., Bauch, D., Hass, H.C., Kandiano, E., 2013. Atlantic Water advection versus sea-ice advances in the eastern Fram Strait during the last 9 ka: Multiproxy evidence for a two-phase Holocene. Paleoceanography 28, 283-295.
Wittmeier, H.E., Bakke, J., Vasskog, K., Trachsel, M., 2015. Reconstructing Holocene glacier activity at Langfjordjøkelen, Arctic Norway, using multi-proxy fingerprinting of distal glacier-fed lake sediments. Quaternary Science Reviews 114, 78-99.
Yan, H., Sun, L., Wang, Y., Huang, W., Qiu, S., Yang, C., 2011. A record of the Southern Oscillation Index for the past 2,000 years from precipitation proxies. Nature Geosci 4, 611-614.
Østrem, G., Liestøl, O., 1964. Glaciological investigations in Norway 1963. Norsk Geografisk Tidsskrift 18, 281-340.

# Supplementary Material

# Paper 2

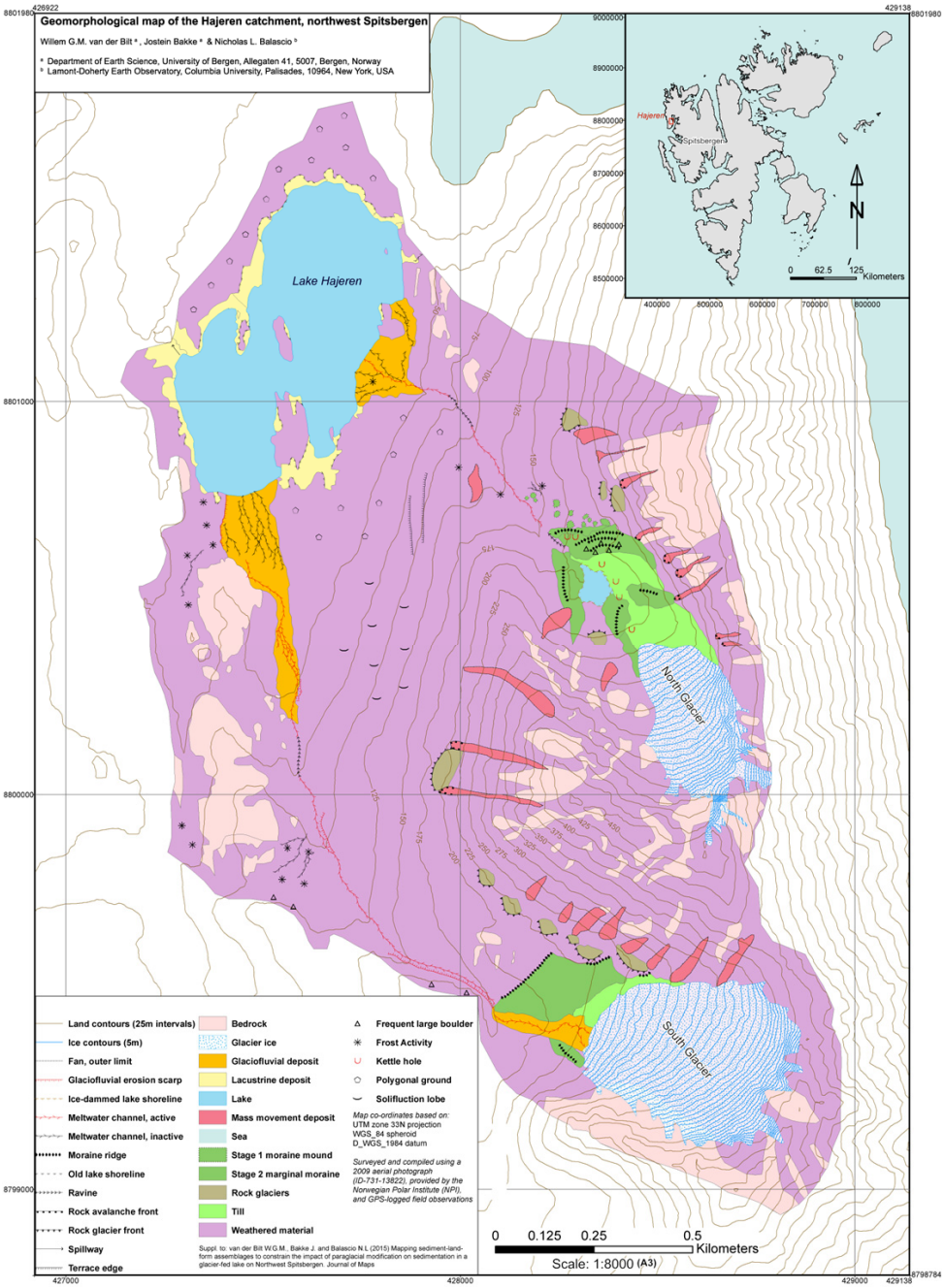


*Geomorphological map of the Hajeren catchment, accompanying paper 2.*

# Paper 5

| Sample | Depth (cm) | Very fine silt (%) | Zr/Rb |
|---|---|---|---|
| *1* | 2 | 26.5 | 1.005 |
| *2* | 5 | 38.8 | 1.073 |
| *3* | 8 | 1.0 | 1.124 |
| *4* | 11 | 23.9 | 1.057 |
| *5* | 14 | 25.1 | 0.994 |
| *6* | 17 | 16.4 | 1.149 |
| *7* | 20 | 23.6 | 0.961 |
| *8* | 23 | 30.5 | 0.811 |
| *9* | 26 | 23.7 | 0.996 |
| *10* | 29 | 21.8 | 1.079 |
| *11* | 32 | 24.2 | 1.033 |
| *12* | 35 | 23.2 | 1.040 |
| *13* | 38 | 22.1 | 0.985 |
| *14* | 41 | 20.5 | 1.070 |
| *15* | 44 | 21.3 | 1.133 |
| *16* | 47 | 3.7 | 1.063 |

***Fig I**. Very fine silt content for selected grain size samples (n=16) from core RVP2. For this purpose, 10 grams of wet sediment were extracted, dried and analysed in a Micromeritics Sedigraph 5100, suspending samples in a 0.005% Calgon solution after Jones et al. (1988). Variations in very silt content, characteristic for suspended glacigenic input (Leemann and Niessen, 1994), was then correlated against Zr/Rb to test this proxies` purported sensitivity to variations in grain size distributions (Kylander et al., 2011).*

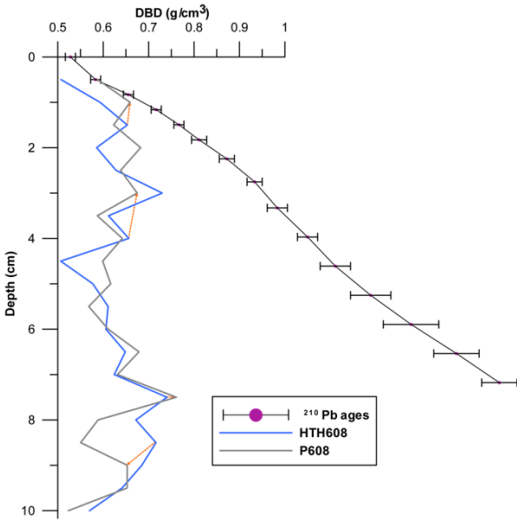

| ID | Age (Yr BP) | Error (Yr) | Depth HTH608 (cm) | Depth MHLP608 (cm) |
|---|---|---|---|---|
| *Pb1* | -55 | 2 | 0.25 | 0.00 |
| *Pb2* | -45 | 2 | 0.75 | 0.50 |
| *Pb3* | -32 | 2 | 1.25 | 0.83 |
| *Pb4* | -21 | 2 | 1.75 | 1.16 |
| *Pb5* | -12 | 2 | 2.25 | 1.49 |
| *Pb6* | -4 | 3 | 2.75 | 1.83 |
| *Pb7* | 7 | 3 | 3.25 | 2.25 |
| *Pb8* | 18 | 3 | 3.75 | 2.75 |
| *Pb9* | 27 | 4 | 4.25 | 3.33 |
| *Pb10* | 39 | 4 | 4.75 | 3.97 |
| *Pb11* | 50 | 6 | 5.25 | 4.61 |
| *Pb12* | 64 | 8 | 5.75 | 5.25 |
| *Pb13* | 80 | 11 | 6.25 | 5.89 |
| *Pb14* | 98 | 9 | 6.75 | 6.54 |
| *Pb15* | 115 | 7 | 7.25 | 7.18 |

***Fig II**. A: 210Pb ages in purple with listed uncertainty range reported by (Vatle, 2012), transferred from the depth-scale of Middle Hamberg Lake (MHL) sampled gravity core HTH608 to that of piston core P608. To this end, we selected alignment points between the DBD stratigraphy of both cores (orange), employing the Analyseries software package (Paillard et al., 1996). B: an overview table, listing all 210Pb samples and both HTH608 as well as P608 depth-scales.*

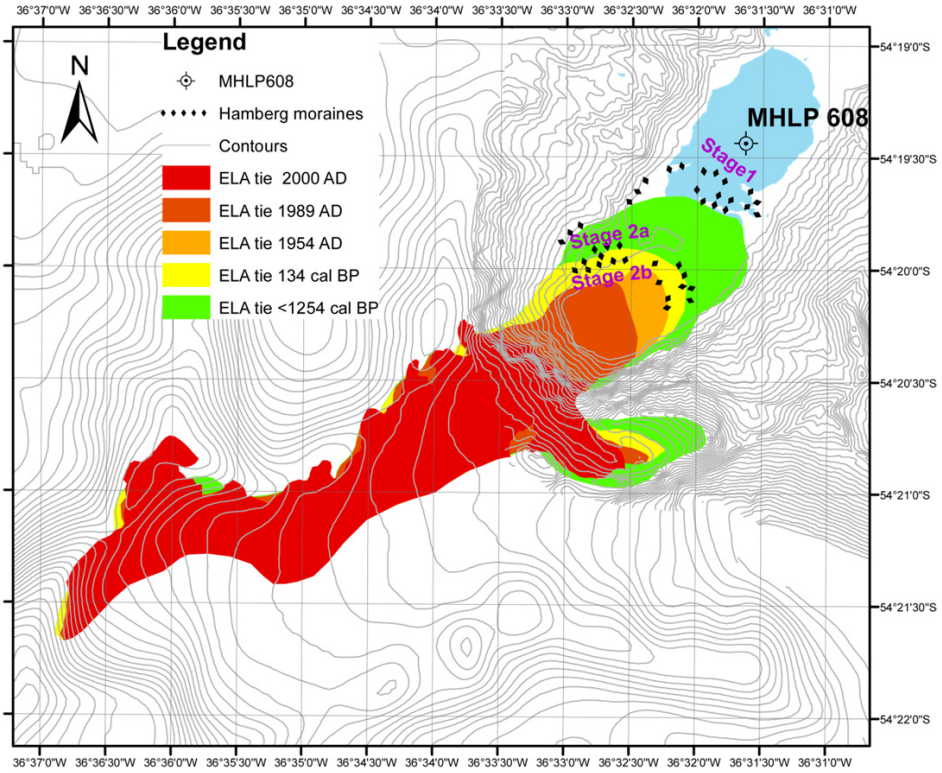


***Fig III**. Mapped glacier extent for each of the ELA tie-points listed in Table 4 in the main text ("ELA estimates"), mapping outlines in ArcMap 10.2. As outlined in the main text, we used a combination of moraine evidence (depicted Stage 1 and 2 moraines) as well as photographs and maps to constrain past glacier size. The divide between the studied Hamberg overspill glacier and the Moraine fjord tributary system is based on Pfeffer et al. (2014). To calculate the employed Area Altitude Balance Ratio ("ELA estimates") (Osmaston, 2005), we calculated glacier surface area (m2) between 50m contours for each time-slice.*

**f(x):**

**f1(x) = a1 + b1 * x**

**for x > x0**

**f2(x) = a2 + b2 *x + c2 * x2**

**for x <= x0**

**f1(x0) = f2(x0) and f'1(x0) = f'2(x0)**

**for x = x0**

***Fig IV***. *The full model that describes the ELA regression model described in the main text under the "ELA reconstruction" paragraph. Here, x denotes Ti, the employed sedimentary recorder of glacial erosion, used to approximate ELA f(x), whereas x_0 represents the Ti value for the outlined 1.5-2 cm core depth cliff change-point. The final line describes the continuity and smoothness constraints that piece f1(x) and f2(x) together to avoid jumps in the Ti-ELA dependence and its slope.*

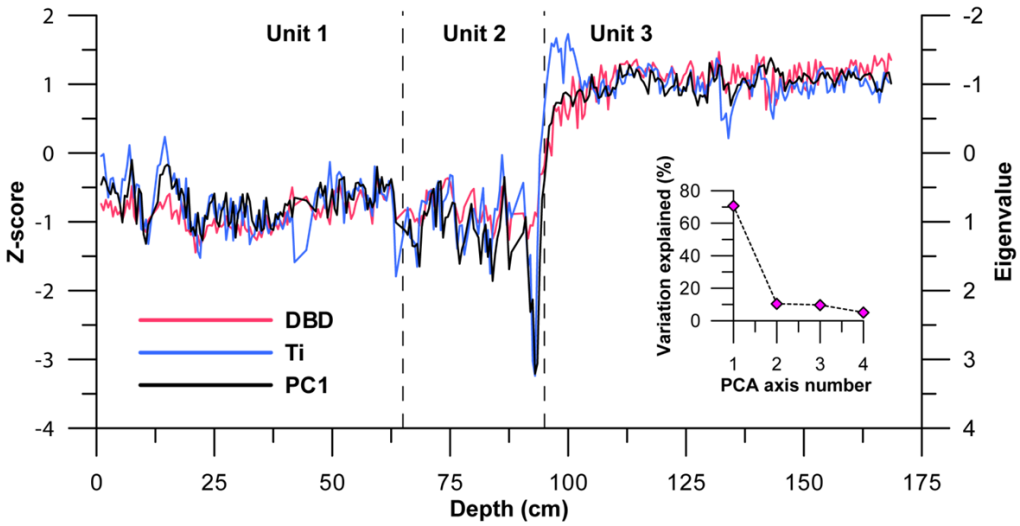

| Parameter | PC1 | PC2 |
|---|---|---|
| *DBD* | -0.9454 | 0.261 |
| *LOI* | 0.9074 | -0.3563 |
| *Si* | -0.9596 | 0.2162 |
| *K* | -0.8842 | -0.1679 |
| *Ca* | -0.9652 | 0.1941 |
| *Ti* | -0.966 | 0.071 |
| *Mn* | -0.6362 | -0.4145 |
| *Fe* | 0.6275 | 0.4078 |
| *Rb* | -0.8461 | -0.0165 |
| *Sr* | -0.9253 | 0.1941 |
| *Zr* | -0.8185 | -0.3121 |
| *MS* | 0.402 | 0.6855 |

***Fig V**. A: Standardized (z-score) values of investigated minerogenic (glacigenic) indicators DBD and Ti in core MHLP608, plotted with eigenvalue scores of the first PCA axis (PC1), reflecting variations in all parameters listed in B. A scree plot in the lower-right panel of the graph shows the significance of PC1 (70.7%) versus other three axes. C: Table with PC1 eigenvalues for all incorporated sediment parameters discussed under the "ELA reconstruction" paragraph of the main text. As can be seen, physical minerogenic indicator DBD has strong scores, like measured detrital elements like Ti.*